Thesis for the degree of Doctor of Philosophy

Parameter estimation in heterogeneous catalysis

Jonas Sjöblom

CHALMERS

Chemical Reaction Engineering
Department of Chemical and Biological Engineering
Chalmers University of Technology
Göteborg, Sweden 2009

Parameter estimation in heterogeneous catalysis

Jonas Sjöblom

ISBN 978-91-7385-271-5

Doktorsavhandlingar vid Chalmers tekniska högskola
Ny serie nr 2952
ISSN 0346-718X

Chemical Reaction Engineering
Department of Chemical and Biological Engineering
Chalmers University of Technology
SE-412 96 Göteborg
Sweden
Telephone: +46 (0)31-772 1000

Chalmers Reproservice
Göteborg, Sweden 2009

Cover: A scores scatter plot displaying the most important experiments (Blue and Green) out of a huge amount of possible experiments in order to estimate kinetic parameters as accurately as possible.

Parameter estimation in heterogeneous catalysis

Jonas Sjöblom
Chemical Reaction Engineering, Department of Chemical and Biological Engineering
Chalmers University of Technology

Abstract

The detailed modelling of heterogeneous catalytic systems is challenging due to the unknown nature of new catalytic materials as well as the often required transient nature of the resulting models. Thus, this thesis deals with the methodologies involved in the kinetic modelling of heterogeneous catalysis and in particular NO_X reduction systems. The methods presented increase the understanding of the interplay between model parameters and also decrease the number of necessary laboratory experiments. The effect of more efficient parameter estimation methods should result in faster model development which is required in any process development but especially for catalytic emission control.

In the first paper, injection parameters for an engine rig with a NO_X Storage and Reduction (NSR) system were optimised using different experimental designs at different load points. The optimised settings were used as a map for a control strategy complying with a European Transient Cycle (ETC).

In the second paper, we developed a method that copes with the large number of unknown model parameters by applying a Latent Variable (LV) model to the Jacobian matrix in the fitting procedure. The LV model results in a low-dimensional approximation of the Jacobian with reduced parameter correlation and enables improved efficiency in parameter estimation. In the third paper, Experimental design for precise parameter estimation was performed in a batch-sequential way using D-optimality as the objective function. A screening methodology similar to that used for drug discovery in the pharmaceutical industry was applied for a large number of simulated candidate experiments. By applying an LV model to the Jacobian of all these experiments, a reduced parameter correlation was obtained and the number of necessary experiments was reduced. The results from the second and third paper pinpoint a number of benefits of using LV models including:

1) the determination of the effective rank, *i.e.* the number of independent phenomena present in the data at hand,
2) the analysis of the correlation structure which is useful in the parameter assessment and
3) the linear approximation in few dimensions enables more efficient computations.

In the fourth paper, a detailed model for the Selective Catalytic Reduction of NO_X using Hydrocarbon as a reducing agent (HC-SCR) over silver alumina ($Ag\text{-}Al_2O_3$) was developed. By applying an experimental design to the steady state levels and also selecting the run order, improved fitting properties were obtained due to the increased parameter sensitivity enabled by the transient experiments.

This thesis also contains a description of the modelling techniques and challenges encountered during this thesis project. An assessment of the importance as well as the parameter correlation is given. This demonstrates the intimate interplay between model assumptions and the stipulated model parameters and exemplifies a thorough assessment of the whole modelling chain from initial experiments to model validation.

Keywords: Parameter estimation, Jacobian, Latent Variable models, Experimental design, Design of experiments, microkinetic modelling, heterogeneous catalysis, sensitivity analysis

LIST OF PAPERS

This thesis is based on the work contained in the following papers

I. Use of experimental design in development of a catalyst system
Jonas Sjöblom, Klaus Papadakis, Derek Creaser, C. U. Ingemar Odenbrand
Catalysis Today 100 (2005) 243-248.

II. New Approach for Microkinetic Mean-Field Modelling using Latent Variables
Jonas Sjöblom and Derek Creaser
Computers & Chemical Engineering, 31 (2007) 4, 307-317.

III. Latent variable projections of sensitivity data for experimental screening and kinetic modelling, Jonas Sjöblom and Derek Creaser,
Computers & Chemical Engineering, 32 (2008) 12, 3121-3129.

IV. Kinetic modeling of selective catalytic reduction of NOx with octane over Ag-Al_2O_3, Derek Creaser, Hannes Kannisto, Jonas Sjöblom and Hanna Härelind Ingelsten, Applied Catalysis B: Environmental 90 2009, 18-28.

CONTRIBUTION REPORT

Paper I: Responsible for designing the experiments, evaluation and all writing.
Paper II: Responsible for the idea, planning, performance, evaluation and all writing.
Paper III: Responsible for the idea, planning, performance, evaluation and all writing.
Paper IV: Responsible for design evaluation (Steady State), development of the matlab code and writing some parts of the paper.

The following papers have not been included in this thesis:

An evaluation of orthogonal signal correction applied to calibration transfer of near infrared spectra
Sjöblom, Jonas; Svensson, Olof; Josefson, Mats; Kullberg, Hans; Wold, Svante Chemometrics and Intelligent Laboratory Systems, 44 (1998) 229-244.

Development of a Dosing Strategy for a Heavy-Duty Diesel Exhaust Cleaning System Based on NO_X Storage and Reduction Technology by Design of Experiments
K. Papadakis, C.U. I. Odenbrand, J. Sjöblom, D. Creaser
Applied Catalysis B: Environmental, 70 (2007) 215-225.

Modeling mass transport with microkinetics in monolithic NOx storage and reduction catalyst
Björn Wickman, Andreas Lundström, Jonas Sjöblom and Derek Creaser
Topics in Catalysis, 42-43 (2007) 1-4, p123-127.

PREFACE

Having wandered around in both professions as well as in nature it is amazing how important pictures are to mankind. Pictures are used to efficiently send messages and "One picture says more than a thousand words" (Chinese proverb) goes without saying. But pictures are still just projections of the complex reality down to a more manageable format. Nevertheless I also feel the need for an illustration of this thesis.

The search for a perfect fit is like reaching 1500 meter above sea level[1] somewhere in Sarek, Laponia, Sweden. The way to get there is to draw a map[2] and find your way through. How to reach the peak of the mountain is of secondary interest as long as you get there. There are helicopters[3] even though they are not allowed at all places in Sarek. If you run in the terrain you can cover a large area in your search but if you do not watch out you may slip and fall badly. If you walk slowly you will not slip but the food may run out for you.
Parameter fitting (using gradient methods) is like searching for that peak of the mountain provided with a map that you made yourself or bought really cheap at the gas station and an altitude indicator[4]. You are also instructed to only walk uphill; downhill will only take you farther away from the goal. But this time the weather is completely foggy! You cannot see more than a few meters away. You start to walk and climb and soon you find yourself on a pile of moraine. You realize that you are far from the goal and move down from the rock pile, jump around a bit and restart again, just to find yourself on another pile a few moments later.
Sometimes the climbing goes through cold mountain streams and sometimes through boulder terrain, drawing on your reserves. All of a sudden the sun breaks through and you realize where you have been and you can also perceive the peak far away. You even find a small path! You feel much better even if the path goes downhill, because soon you will be able to climb higher than ever before. Hoping that the peak you see is the good one…

Sarek national park, a wonderful place to be if you are well prepared and have nice weather. (photo: Hans Molin)

[1] This altitude is the ultimate fit of a simulated run and experimental data
[2] The map is the model that we decide upon
[3] Helicopters take you from one point to another, this is referred to as "manual tuning"
[4] A look at the altitude indicator is the function call, *i.e.* residual calculation

TABLE OF CONTENTS

1. INTRODUCTION

This thesis is about parameter estimation in heterogeneous catalysis and specifically applied to NO_X reduction for vehicle emissions. The internationally strong interest in NO_X reduction makes this research area very intense, but on the other hand, the fundamental understanding enabled by mathematical modelling is unfortunately often not as frequent. This introduction presents some issues in mathematical modelling in heterogeneous catalysis and hopefully justifies modelling efforts in general and this PhD project in particular.

1.1. Global warming and NO_X reduction

Reduction of carbon dioxide (CO_2) emissions from vehicles is an important factor in the abatement of global warming [Hansen 2004]. Since CO_2 formation is a natural consequence of fuel combustion, the natural way to reduce CO_2 emissions is to decrease fuel consumption. The most efficient way to reduce CO_2 emissions is of course to decrease transportation or to use renewable fuels. Yet, for transportation that nevertheless will exist, fuel consumption can be reduced by running the engine "lean" (oxygen excess) and the most common type of lean burn engine is the diesel engine.

In a traditional gasoline engine, which utilises stoichiometric combustion (neither oxygen excess nor deficiency), the harmful exhausts are reduced using a three-way catalyst which simultaneously oxidises carbon monoxide (CO), hydrocarbons (HC) and reduces nitrogen oxides (NO_X). The diesel engine, on the other hand, produces lean emissions and cannot use this technology because the NO_X reduction process is inhibited by the oxygen rich atmosphere. NO_X emissions are also a pollutant since they contribute to *e.g.* acid rain and ground level ozone (which causes urban smog). For a long time this was not an issue since diesel engines produce relatively low NO_X emissions. However, as the legislation for diesel vehicles has become more stringent for NO_X emissions, new catalysts, especially for heavy duty diesel engines need to be developed.

Even though there is technology available to meet the current emission legislation, compliance to future legislation will be even harder to attain. Furthermore, there are issues regarding the ageing of the catalyst, cold-start problems as well as the reduction of particulate matter (soot) to deal with. Additionally, future alternative fuels will bring significant challenges to the research community within heterogeneous catalysis. Nevertheless, whatever advanced technique that will be used to solve future emission problems, heterogeneous catalysis will be indispensable and thus, a profound understanding of the catalytic processes will be crucial.

1.2. Mathematical modelling and heterogeneous catalysis

To achieve a profound understanding of heterogeneous catalytic systems, mathematical modelling is a key technique [Berger 2008, Franceschini 2008a, Guthenke 2007, Koci 2007]. Models can be used for many different objectives, *e.g.* prediction to improve on-board control and aftertreatment design but most importantly (and exclusively in this thesis) models can be used to increase the understanding of heterogeneous catalysis. For example, by analysing a complex model (that contains different phenomena), the different phenomena can be evaluated for a specific situation. Also, in the case of aftertreatment development, appropriate actions can be taken. A typical example would be to assess whether the limiting factor for

NO_X reduction is governed by mass transfer resistance or the amount of active material. Furthermore, the models need to be detailed enough to enable the assessment of different phenomena (different dominating reactions depending on the exhaust gas composition). Additionally, due to the highly dynamic nature of an aftertreatment system (changing flow conditions and temperatures depending on the vehicle operation as well as the reducing agent that is injected dynamically), the models also need to capture transient phenomena. Thus, this thesis contributes to the long term objective of increased understanding of heterogeneous catalysis by improvement in modelling methodology.

When assessing a model applied to practical (non-theoretical) situations, the use of experiments is very important. In order to draw high quality conclusions, the model and model analysis as well as the experiments need to be of high quality[5]. These parts are performed iteratively in order to improve understanding of the catalytic process [Box 1965a], see Figure 1.

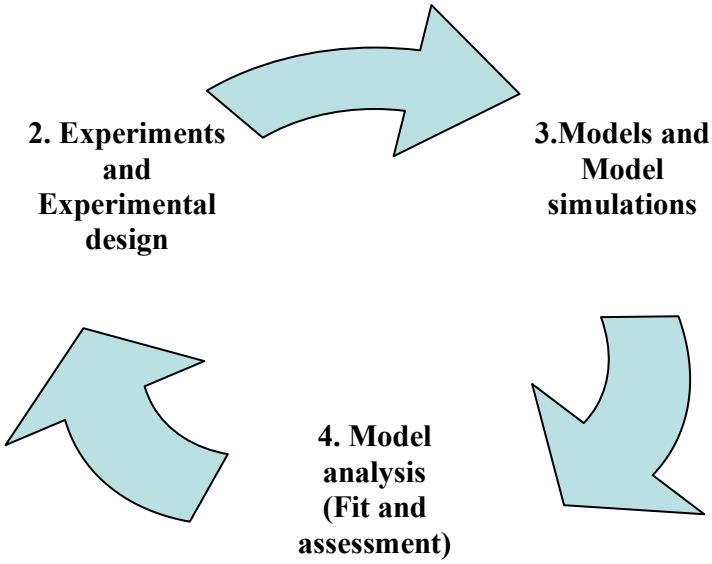

Figure 1. A schematic picture of the machinery involved in the modelling cycle. The numbers indicate the chapters in the thesis where these parts are further described. The applications of these different parts (including papers I-IV) are given in chapter 5.

There are two major obstacles in achieving the goals of improved understanding. The first is associated with the vast amount of information available (catalyst characterisation, similarities to other systems, extrapolation of information from other experimental conditions etc) which results in complex reaction mechanisms and thus many model parameters. Secondly, an even greater obstacle is the fact that all these numerous parameters, as well as the model structure itself, may turn out to be inappropriate. This can result from incorrect assumptions or erroneous simplifications and more details will be given in the rest of this thesis. In short, one could say that the modelling of processes that take place at a molecular level is inherently difficult using only macroscopic observations. Consequently, the modelling effort can be difficult and time consuming. However, even if the models are erroneous, they are often proven useful and the need to improve at any stage in the modelling cycle constitutes the motivation for this PhD project.

[5] High quality does not necessarily mean low noise levels. With the notion high quality means that the experiments can be well characterised, *i.e.* the noise levels as well as any other uncertainties are investigated and quantified.

1.2.1. Challenges with parameter fitting

One basic assumption during parameter fitting is that the model is correct. Furthermore, the most common fitting procedures are based on gradient search methods, which work best with parameter values in the vicinity of the true values. However, when the model is potentially unsuitable, the parameters are far from the true values and/or the experimental design is not well adapted for the objective, correlation between parameters occurs. Normal gradient calculations are not well suited to deal with this correlation and consequently, the objective of paper II is to show how latent variable models can be used for more efficient parameter fitting. The analysis of the correlation structure gives valuable information about how many parameters that can be adequately fitted. Moreover, a better choice of parameters subject to fitting can thus be obtained.

1.2.2. Challenges with experimental design for precise parameter estimation

Experimental design is a methodology that aims at maximising the information content given by a limited number of observations (experiments). For linear models, the methodology is quite straight forward, see *e.g.* [Montgomery 2001]. For nonlinear models, the situation becomes more complicated, but manageable since the pioneering work by Box [Box 1959] and when there are multiple responses the complexity increases by one dimension [Box 1973]. There are many other aspects that come into play, such as

- whether the modelling objective is precise parameter estimation or model discrimination [Buzzi-Ferraris 2009, Hunter 1967]
- the choice of the objective function [Bardow 2008, Box 1970, Franceschini 2008b, Pritchard 1978, Walter 1990] where D-optimality is the one used in this thesis
- The number of experiments in each modelling iteration, *i.e.* the sequential design *e.g.* [Box 1965b, Hosten 1975] where batch-sequential experimental design [Walter 1990] has been applied in this thesis.

However no literature could be identified that simultaneously deals with nonlinear, multi-response models, time-dependent experiments (using many observations) regarding the aim to plan a series of experiments (batch sequential approach). A feasible way to deal with these many aspects is to approximate the Fisher information matrix using a Latent variable model. In paper III it is shown that by using this approach the information content can be more easily quantified and the experiments become less labour intensive.

1.3. Objective

The objective of this thesis is to demonstrate novel methodologies during the modelling cycle. Furthermore, the main focus is on model fit and model assessment, even if the model structure is less than optimal (as is evident from most of the papers in this thesis). For instance, different methods to handle many parameters that are highly correlated are applied. The main tools are Design of Experiments (DoE) and Multivariate Data Analysis (MVDA) and the results show that these methodologies contribute to a deeper understanding and additionally, they are also more computationally efficient. Finally, this thesis is also intended to describe the different parts and aspects of the modelling cycle, to assess the impact of these different parts and also to give recommendations of how to overcome common issues encountered in practical modelling tasks *e.g.* for PhD students in Chemical Engineering.

2. EXPERIMENTS AND THE DESIGN OF EXPERIMENTS

"Without experiment I am nothing. But still try, for who knows what is possible"
Michael Faraday 1791-1867

Even though this thesis is dealing with modelling, it is important to realize that we base all our understanding either explicitly on observations (measurements) of the system in study or from previous knowledge which in turn was based on observations. Furthermore, the type of modelling that was performed in this thesis is based on the assumption that the model is correct and that the data (from observations) are not. The data are probably a good measure of what we want to observe, but is impaired by errors.

In the following sub-section, various experimental techniques are described just to give an understanding of the important consequences they have on the modelling.

"The chain is never stronger than the weakest link" and the chain starts with the experiment[6].

2.1. Design of Experiments (DoE)

Models are almost always tightly connected with experiments. Experiments are used in different stages for different purposes:

- Initial experiments
  - To verify that the reaction occurs
  - To get reasonable ranges for reaction conditions
  - To propose an initial reaction mechanism
- Structured experiments, preferably a statistical design of experiments
  - To estimate effects of reaction conditions
  - To estimate model parameters[7]
- Verification experiments
  - Validation experiments
  - Robustness testing

As long as one has the objective in mind, it is easy to realize that a systematic approach is beneficial. Apart from the initial experiments (where intuition and imagination are more important), the use of experimental design cannot be over-recommended. The use of experimental designs enables *e.g.*

- Independent analysis of different experimental factors
- Maximum information from minimum number of experiments

[6] This does not mean that I consider the experiments to be the weakest link. On the contrary, experiments are often the most well defined and characterized part of the modelling chain.
[7] This is the theme of paper III and will be further described in section 4.5 (Design of Experiments for precise parameter estimation).

For the basic concepts underlying DoE, see any textbook on the subject *e.g.* [Montgomery 2001], [Umetri 1988], or a tutorial [Lundstedt 1998].

2.1.1. Single observation experiments

In "classical" experimentation, one performs one experiment (one observation) and evaluates the results. The characteristic feature is that one experiment produces one "row" of data. This row consists of factors (x-variables) and responses (y-variables). The different experiments can be performed independently, which means that there is no correlation between different experiments (rows). Examples of un-wanted experimental correlations are:

- Experiments performed in the same order as the variation of one of the factors, *i.e.* first all "low-level" experiments followed by all "high-level" experiments.
- Replicates performed in sequence
- Experiments performed so that correlations between different factors occur, *i.e.* a non-orthogonal experimental design.

For catalytic reactors the classical experiments correspond to some integrated value or perhaps some final state of the reaction. It may also be one selected feature of the reaction event such as catalyst ignition.

2.1.2. Time-dependent experiments

One other type of experiment or more precisely one type of experimental data is time-dependent observations. Time-dependent observations are encountered when we have sampling at several sequential time points during an experiment. The correlation between observations is a natural consequence and hence should be adjusted for accordingly.[8]

The advantage of time-dependent observations is that they enable the study of the dynamics. Dynamics are of interest when we do not have steady state or when accumulation is of importance. The non-steady state experiments are here referred to as "transient" experiments. A transient experiment may simply involve a "step change" in inlet concentration, but transient experiments can be extended to include all observations that aim to study the dynamics of the system.
For complex non-linear systems (with many coupled reactions), transient experiments are of utmost importance [Berger 2008]and if the system contains unobservable variables (such as coverage of the catalytic material in a catalytic converter) it becomes even more important. Due to the model non-linearity, one difficulty is the model parameter evaluation in terms of "design factors". However, by using transient experiments one drastically increases the parameter space and enables estimation of kinetic parameters not achievable using steady-state techniques.

[8] Note: All too often one can encounter the determination of degrees of freedom (*e.g.* for calculation of confidence intervals) based on time-dependent observations but still (implicitly or unconsciously) assuming independence of observations. This is all very unfortunate, but on the other hand it is difficult to get any better alternatives accepted by the statistical community.

2.1.3. Orthogonality and correlation

Design of Experiments aims to maximize orthogonality and minimize correlations. There are different types of orthogonality and correlations:

1. Among observations: a classical experimental design is performed with every observation independent of each other. This means that there should be no other correlation between the observations other than specified by the adherent factors.
2. Among factors: adjustable factors should always be made orthogonal while for un-controlled factors the correlation may be difficult to avoid. (Different sampling methods could be considered here.) [9]
3. Among responses: The responses are typically non-adjustable (at least in a direct sense). However during optimization of different responses one may seek orthogonality.

The discussion about orthogonality and mitigation of correlation will be further discussed *e.g.* in section 3.2.

2.1.4. Application of DoE to heterogeneous catalysis

As in every experimental activity, DoE is of utmost importance in order to retrieve maximum information and avoid costly misinterpretations. It is therefore distressing to observe the relative lack of DoE in the field of catalysis compared to, for example, the field of analytical chemistry. However there are publications using DoE and the demonstration of the benefits is as usual very clear. Examples include:

- Optimization of catalyst preparation [Dawson 1992]
- Combinatorial chemistry approach for screening of different catalytic materials [Bricker 2004, Kirsten 2004]
- Spanning the experimental space for improved parameter fitting [Barsan 2003] (however Steady State) [Zamostny 2002] , (papers III & IV)
- Optimization of catalytic processes such as within fuel cells [Dante 2002]
- Use of DoE in kinetic modelling has been studied by the group of Vlachos [Aghalayam 2000, Davis 2004] (papers III & IV)
- Optimization of injection parameters for an NSR system on an engine rig (paper I)

[9] DoE deals with linear models. Note that for non-linear models, the correlation among the factors is actually built-in by definition. One solution often used is then to approximate the nonlinear function with a linearized one. This will be discussed more in section 4.2.

2.2. Experimental Reactor design

The reactor design includes all physical parts of the system. Figures 2 and 3 show two reactor set-ups used in this thesis.

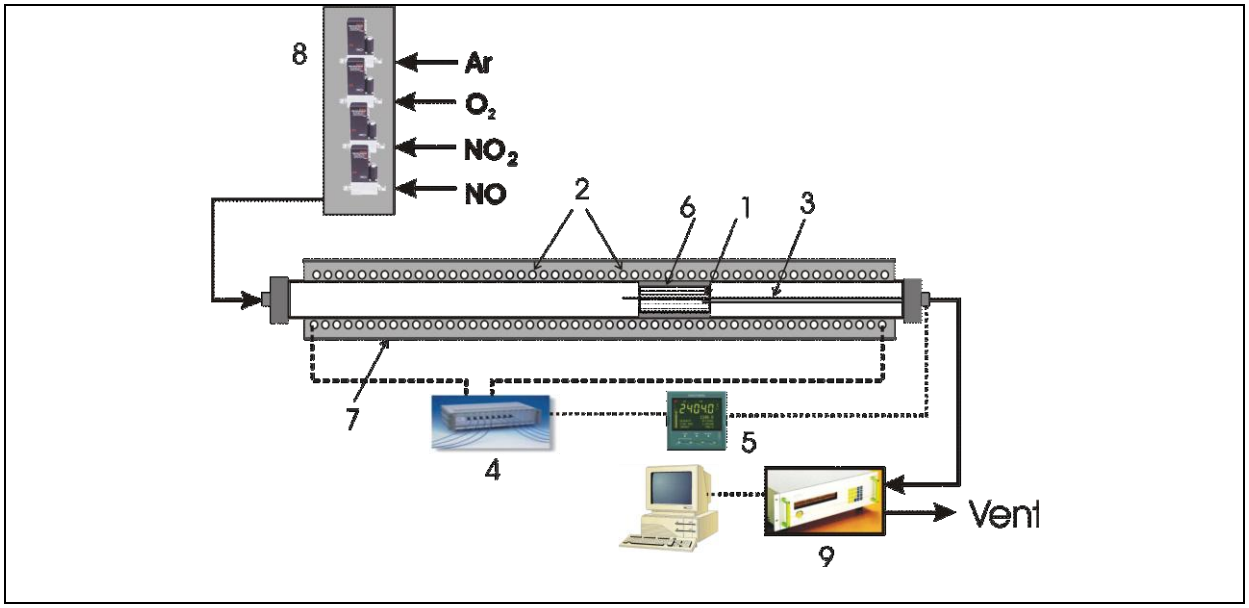

Figure 2 Monolith reactor setup. The monolith (1) is inserted into a quartz glass tube. The tube is heated from outside using a heating coil (2). Two thermocouples (3) measure the temperature inside the monolith (use for simulations) and in front of the monolith (for temperature control). The heating coil is powered by a power supply (4) and controlled by a Eurotherm controller (5). The monolith is fixed in the quartz glass tube (and partially isolated from the heating coil) by quartz wool (6). The quartz glass tube and heating coil is further isolated by quartz wool (7). A gas mixture is fed to the reactor using a set of mass flow controllers (MFC) (8) and the reactor outlet stream goes to various detectors (9) before being vented.

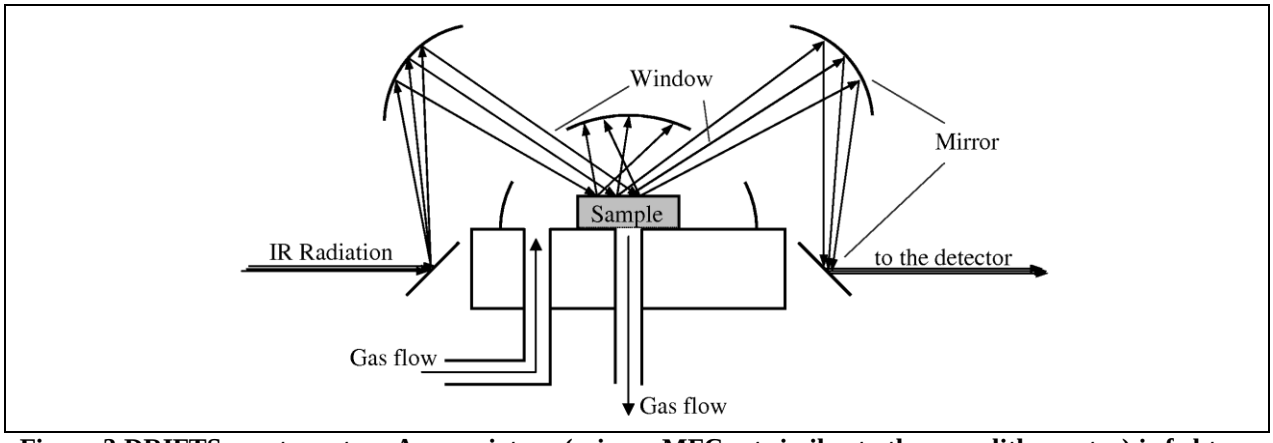

Figure 3 DRIFTS reactor setup. A gas mixture (using a MFC set similar to the monolith reactor) is fed to the "dome" (hemispheric chamber) and passes through a packed bed of catalyst (sample). The bed temperature is controlled by a Eurotherm and the outlet stream goes to a mass spectrometer detector. Infrared radiation strikes the surface where it diffuses into the bed, becomes reflected and collected via an integrating sphere and finally passed to the IR detector.

The reactor design is a very important step that is often neglected due to practical reasons (*e.g.* the reactor already exists, ready to be used). However, the design will define/restrict the experimental limits both in terms of ranges (such as flow, concentration, and temperature

limits) as well as phenomena (such as temperature gradients, velocity profiles). Below is a list of typical examples encountered[10]:

- Velocity profile for the flow entering the monolith: assumed to be plug flow but is probably fully developed laminar flow.
- Concentration profile entering the reactor: When a step change in concentration is performed, the real concentration profile will be "smoothed out" due to dispersion effects, see section 3.4.
- Temperature gradients in gas flow, due to heating coil heating from outside in combination with the absence of mixing in front of the reactor.
- Channelling and stagnant zones in the packed bed.
- Absence of heating of pipes creates longer time lags for some gases due to re-adsorption effects (such as NO_2, H_2O and NH_3).

2.3. Catalyst characterisation

In order to understand the morphology and structure of the catalyst sample a relevant characterisation is needed. This information can then be used to apply a relevant transport model. It also indicates the relevance of a mean field kinetic model, see also section 3.6.1 and 6.2.

2.3.1. N_2 physisorption

By performing N_2 adsorption and desorption at low pressures, the specific surface area and the pore size distribution can be determined. For further reading, see [Barrett 1951, Brunauer 1938, Kannisto 2009a]. For example, in paper IV, the specific surface area (BET area) was $197 m^2/g$ and the pore size distribution was 20-77 Å (80% of the pores) with an average pore diameter of 30 Å (3 nm).

2.3.2. Electron microscopy

By using electron microscopy, *e.g.* Scanning electron microscopy (SEM) or transmission electron microscopy (TEM) one obtains images of the catalyst. In Figure 4, a monolith channel is displayed with a 20 wt% washcoat loading of Ag-Al_2O_3 catalyst. The washcoat is of varying thickness, at approximately 40 µm on the channel walls and thicker in the corners. Figure 5 shows a close up of the monolith wall (cordierite) and a thin layer of Ag-Al_2O_3. From this picture it is clear that the washcoat is not a uniform porous layer, but consist of primary particles of about 1µm which in turn contain even smaller pores, as indicated by BET analysis.

In the TEM image (Figure 6) of an Ag-alumina sample, large silver particles of about 10 nm in diameter can be observed. There are also smaller particles not visible in the TEM image (because they are too small) but evidenced by other methods indicating small nanoclusters of a few atoms which are suggested to be the main reactive sites for the SCR mechanism [Kannisto 2009b].

[10] Most of these effect as well as many other effects will be numerically evaluated in section 5.5

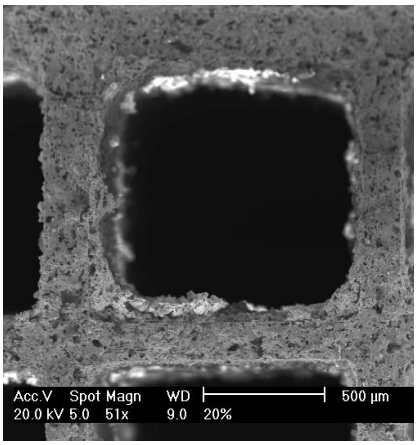

Figure 4. A SEM picture of a monolith channel coated with Ag-Al_2O_3

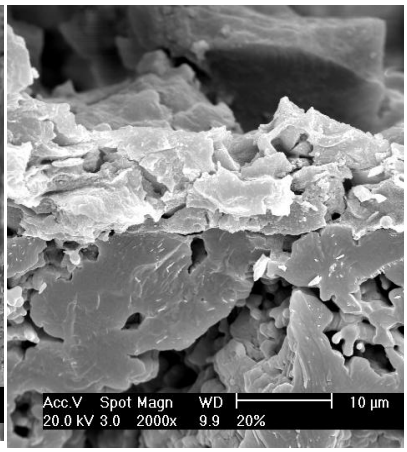

Figure 5. A SEM picture of the cordierite wall and the Ag-Al_2O_3 washcoat.

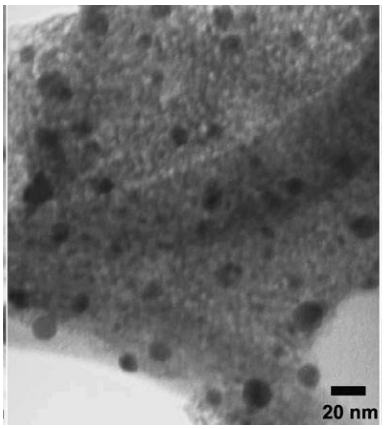

Figure 6. A TEM image from a silver-alumina (SG5) sample, as was used in paper IV. From [Kannisto 2009b]

2.4. Detectors

As indicated in the introduction, experiments, model simulations and analysis are tightly connected. The research heavily relies on experiments and the experimental data is collected by detectors. In a way, one could say that detectors are the foundation on which parameter estimation is based upon, since it is the comparison between the simulated data and the detector signals (*i.e.* the residual) that defines the goodness of fit[11]. During the optimisation of the detector signal there is always a trade-off between *sensitivity* (*i.e.* how much signal) and *selectivity* (*i.e.* how sensible the signal is to interfering signals, interfering species etc).

2.4.1. Mass spectroscopy

Mass spectroscopy (MS) is a technique to separate (and thus quantify) different molecules depending on their mass. The main advantages are that the technique is fast (time resolution about 1/10s) and requires only small amounts of the sample gas (2-10 ml/min). The greatest challenge for quantification is that the calibration procedure is sometimes highly responsive as will be shown below. There are many different types of MS systems, but here only the quadropole type of MS using a SEM detector is described, see Figure 7.

[11] At least under the assumption that the model is correct.

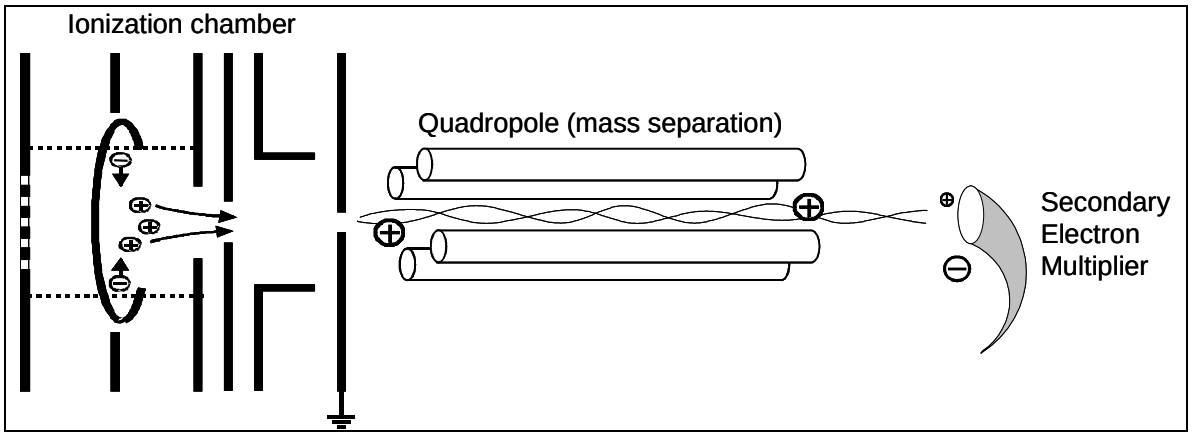

Figure 7 Schematic picture of a Mass Spectrometer instrument setup. Adopted with permission from Dr Norbert Müller, INFICON Limited.

The gases are sampled downstream the reactor by a glass capillary that samples about 2-10 ml/min driven by the very low pressure in the MS system (about 1×10^{-6} mbar). The gas reaches the ionization chamber where electrons with high energy hit the molecules and create positive ions/fragments. The incoming electrons repel the molecular electrons so that they leave the molecule. However, the incoming electrons may also break the bonds between the atoms in the molecule and thus create fragments[12]. Then, the ions are accelerated into the quadropole, where the gases are separated according to their mass (mass over charge). The ions that passed through the quadropole then enter the Secondary Electron Multiplier (SEM) detector where the number of molecules is transformed into a signal. This detector enables a linear response within a very wide range (9 orders of magnitude or more).

The MS signal represents a ratio of mass over charge (m/e) and is not exclusively linked to the concentration in the gas phase. There are different sources of a certain m/e ratio[13]:

1. the molecule of interest itself, charged by +1
2. fragments/molecules of double the mass but with double charge (+2)
3. bigger molecules fragmentized into smaller fragments
4. smaller molecules/fragments that re-combine with other fragments/molecules (present at high concentrations)
5. other molecules with different isotopic composition.

These effects become a "selectivity" problem and it is important to properly handle these issues when quantifying MS data. It is important to note that just because there might be selectivity issues, the MS technique can be made very accurate with high selectivity and furthermore it has the benefits of small and fast sampling.[14]

More details and guidelines on measurement methodology as well as handling of the selectivity issue are given in Appendix A.

[12] The terms fragments and ions are used interchangingly in this chapter.
[13] There are other sources as well, but only the sources relevant to heterogeneous catalysis are listed here.
[14] Another way to solve the selectivity issue is to use a separation technique, such as gas chromatography (GC), however the time resolution is lost unless it is used in combination with on-line measurements and data can be interpolated with sufficient accuracy

2.4.2. Infrared Spectroscopy

Infrared (IR) spectroscopy is a technique where electromagnetic radiation in the range[15] of approx. 4000-1000 cm^{-1} excites vibrational energy levels of molecules. There are different types of spectrometers, but the Fourier Transform spectrometer is the most common type.

2.2.3.1. Gas phase Infrared Spectroscopy

The reactor outlet gas stream enters the IR flow cell and is quantified using a calibration procedure. Since the concentrations are low (ppm levels) the sensitivity issue is partly solved by designing the flow chamber to be long and to let the beam cross the gas flow many times. Also the number of scans can be increased to increase the signal to noise level, *i.e.* sensitivity. The sensitivity issue then becomes a time resolution issue.
Furthermore, the different gas molecules may have overlapping peaks generating a selectivity issue. This can be solved by using multivariate calibration procedures [Martens 1989] or by multiple selection of the spectral domain as implemented in the instrument at the Competence Centre of Catalysis, Chalmers (KCK) (MKS MG2000) [MKS Instruments 2006]

2.2.3.2. Diffuse reflectance Infrared Spectroscopy

In the gas phase there are only 3N-6 normal modes of vibrations for a non-linear molecule, where N is the number of atoms. When a molecule is adsorbed on a surface the number of vibrational modes increases with different adsorption configurations. This makes spectra much more information rich. However it also requires that one can assign different peaks to different vibrations to make the spectra interpretable. This assignment uses both theory and previous knowledge (from similar systems). Using the information from the peak assignment a more plausible reaction mechanism can be derived.

Aspects of peak assignment
The peak assignment task is sometimes difficult due to a number of reasons:

- Peak positions move depending on co-adsorbed species
- Peak position appears at different frequencies due to different support effects (compared to other published information)
- The peak in study is from an unknown specie
- The peak in study can be hidden by other overlapping peaks

A number of counter-measures and methods are available to partly circumvent these problems, including:

- Targeted experiments (one gas at a time)
- Temperature programmed experiments (*e.g.* Temperature Programmed Desorption, TPD) [Gorte 1996]
- Isotopic experiments, such as Steady-State Isotopic Transient Kinetic Analysis SSITKA [Shannon 1995]

Aspects on the quantification of diffuse reflectance data
The quantification will be further described in Appendix A, which deals with the modelling/numerical part. Concerning the experimental part, there are a number of aspects to take into account [Müller 2008]:

- Penetration depth is small, typically less than 0.4 mm for Pt on γ-alumina. This is due to the large portion of pores for high surface area materials.

[15] This range may differ with different applications. 4000-1000 cm^{-1} corresponds to 2500-10000 nm.

- Particle size dependence: Peak heights (as well as peak areas) may depend on particle size distribution, mostly higher peaks for smaller particles, however not always. A simple calculation (see section 7.7 in [Müller 2008]) shows that the majority of surface is internal pore area and only 0.01% is external area. Thus it is really the pore surface that is manifested in the DRIFT spectra.
- Sample preparation: In the study, there was found to be no dependence on how much sample that was pressed into the reactor. This means that the γ-alumina is rigid compared to the mechanical force due to tapping/pressing more sample into the reactor.
- Baseline variation due to temperature. Either separate backgrounds need to be taken or baseline correction using a low order polynomial or a linear interpolation of background spectra can be used to account for baseline variation.
- Negative peaks due to *e.g.* hydroxyl groups: The support may contain adsorbed species during background acquisition. This may need to be accounted for if the pre-adsorbed species overlap with species of interest during reaction conditions.

2.4.3. General remarks on gas phase analysers

There are of course many other gas analysers that are used for reactor experiments, *e.g.* chemiluminisence detectors for NO_X quantification. However, they are often only reliable when operated and calibrated correctly, so they will not be described further. In almost any analyser there will be a few important issues that really need to be dealt with in order not to ruin any subsequent modelling effort. These issues are

- The sensitivity
- The selectivity
- Gas consumption /Time resolution

2.4.4. Temperature sensors

The temperature inside the reactor where the reactions take place is of outmost importance. The measurement should be accurate and non-invasive. The most common temperature sensors at KCK is a thermocouple of type K, which is a standard sensor giving accurate temperature estimates. However, the precision of the temperature is not as much of an issue as is the issue of representativity.

- By insertion of a thermocouple in a monolith channel, the residence time can be affected, thus the conversion and local temperature.
- The heating coil for the monolith reactor setup will induce a temperature gradient in the inlet flow to the monolith.
- The black-body radiation of the monolith can cause a substantial temperature drop at the end of the monolith.

The accuracy of temperature measurements in relation to kinetic modelling was studied by Hansen [Hansen 2007] who found that in order to be able to discriminate between two simple mechanisms, the precision needed to be better than 2K. The temperature gradients (and thus variation in representativity) in a typical monolith reactor is easily more than 5°C.

3. MODELLING

"All models are wrong but some models are useful!" - George E.P. Box

In order to get some perspective, we need to define what we mean by a "model", since it is a very frequently used term for many different kinds of models.
Below is a "definition" or a specification of models used for heterogeneous catalytic reactors applicable in this thesis:

- A model is something used to explain observable and unobservable phenomena. The model can aim to describe physical phenomena or be more empirical in nature.
- A model consists of a structure/mechanism which describes how different phenomena are related.
- A model also has a set of model parameters and for complex (nonlinear) models there is normally no unique set of parameters[16] but an infinite number of sets that will fulfil the objective function[17].
- These parameters should have any (preferably all) of the following properties:
    - Parameter values give the model good fit to experimental data.
    - For physical models, parameter values should be physically reasonable
        - Values within acceptable limits
        - Reasonable relationship between parameters

Frame 1. Definition of a model as viewed upon in this thesis.

The statements above imply that the model parameters are NOT the model. The activity "modelling" is by this definition the extraction of the mechanism (including identifying the model parameters). In this thesis the focus is therefore NOT on modelling but rather on parameter fitting and model (or model parameter) assessment. This may seem strange to some people, who often assume that parameter fitting is always readily achievable and model assessment gives satisfactory conclusions (*i.e.* the model is trustworthy). However, I would like to argue that this is seldom the case and in particular for detailed kinetic models applied to heterogeneous catalysis.

3.1. Linear models

In order to predict reactor outlet concentrations, one could also use a very simple model:

$$r = \sum k_i x_i \qquad \textbf{(1)}$$

Where x_i can be any variable (*e.g.* concentration, but also temperature, flow rate etc.), eventually transformed (squared, inversed, logarithmic, etc) and k_i is a linear constant. The

[16] Unless a suitable experimental design can be performed.
[17] The objective function will be described in section 4 and is often defined as a minimization of the square of the residual (difference between simulated and experimental data).

response *r* can be any response (*e.g.* reaction rate, conversion, selectivity etc). The expression can also be written in matrix notation:

$$r = \mathbf{bx} \quad \textbf{(2)}$$

These models have the advantage that the model parameters can be analysed using classical statistical analysis if handled properly. One prerequisite is that the experimental data enables independent estimation of **b**, *i.e.* that DoE has been applied (see 2.1).

3.1.1. Linear regression

In linear regression analysis one is concerned about finding a relationship between a response variable, y which is assumed to depend on another independent variable. The observations of y will be approximated by "y-hat", $\hat{y}$:

$$y = \hat{y} + e \quad \textbf{(3)}$$

Where the residual, e, is preferably as small as possible.
The "standard" linear regression model:

$$\hat{\mathbf{y}} = \mathbf{bx} \quad \textbf{(4)}$$

Where **x** is a vector of variables (x_0, x_1, x_2, …) where the first variable x0 is unity "1" and corresponds to the intercept. **b** is a vector of regression coefficients where the first element b_0, is the intercept and the remaining coefficients are the "slope" for each corresponding variable in **x**. In order to estimate the parameters in **b** we need a so called "objective function". In linear regression we almost always apply the "least squares" approach and the objective function is to minimize the square of the residual:

$$\min_{\mathbf{b}} f(\mathbf{x},\mathbf{b})^2 = \min_{\mathbf{b}} (\mathbf{y}_{observed} - \hat{\mathbf{y}})^2 \quad (5)$$

By derivation of the objective function with respect to the parameters and setting the derivative to zero i.e. minimization, the solution becomes:

$$\mathbf{b} = \mathbf{X}'\mathbf{Y}(\mathbf{X}'\mathbf{X})^{-1}$$
$$\mathbf{b} = \begin{bmatrix} b_0 \\ b_1 \end{bmatrix} \quad \textbf{(6)}$$

Where we now have extended the least squares to a multivariate case, where we have many x-variables in an **X** matrix and many y-variables in a **Y** matrix.

3.1.2. Assumptions for linear regression

In order to prove that the estimation of the model parameters are the best un-biased ones, we need a few assumptions:

1. The observations are independent

2. The x-variables are exactly known (they have no error)
3. The residual (in the y-direction) is normally distributed with an expected value of zero
4. The variance of the residual is constant over the entire calibration range

These assumptions are very seldom fulfilled even though they can be sufficiently fulfilled if:

1. The experiments were performed according to an experimental design and performed in randomized order.
2. The errors in x are small, compared to the residuals in y.
3. The data can be transformed so that the residual becomes normally distributed.
4. The calibration range is sufficiently small or the residuals are weighted so that the variance becomes constant.

Very often the above mentioned techniques are not enough and better methods are needed. One method is the method of latent variables.

3.2. Multivariate analysis, Latent variable models

The multivariate methods described below (PCA, PCR, PLS) and similar methods are called "Latent variable" methods, because the nature of the low-dimensional hyper plane can be regarded as "latent variables". These methods are very useful in complex systems with many correlated variables and observations.

3.2.1. Principal Component Analysis, PCA

One of the assumptions for linear regression analysis is that the x-variables are exactly known. This may mostly be true enough (at least compared to the uncertainty in measuring the y-variable). Quite often though there is an interest in handling uncertainties in **X** as well. This was first analysed by Pearson in 1901 [Pearson 1901]. The concept has been developed a lot since then and a model type that corresponds to Pearson's study is called Principal Component Analysis (PCA). The difference between a linear regression situation and a PCA model is that the residual to be minimized is not the "vertical" distance but the distance orthogonal to the line (the model). This is depicted in the figure below:

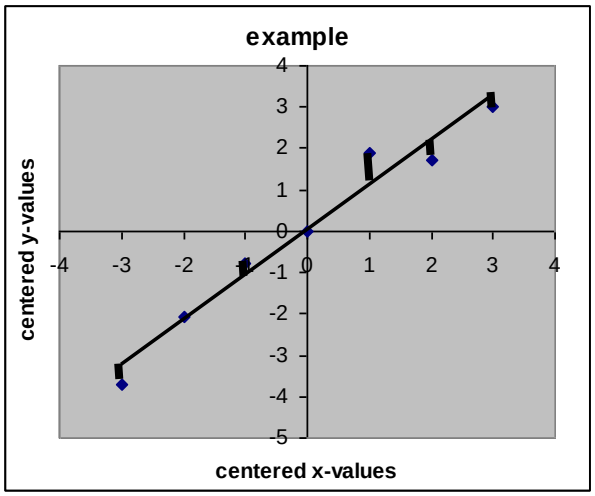

a) "normal" linear regression.: the residual is the vertical distance between the data and the model.

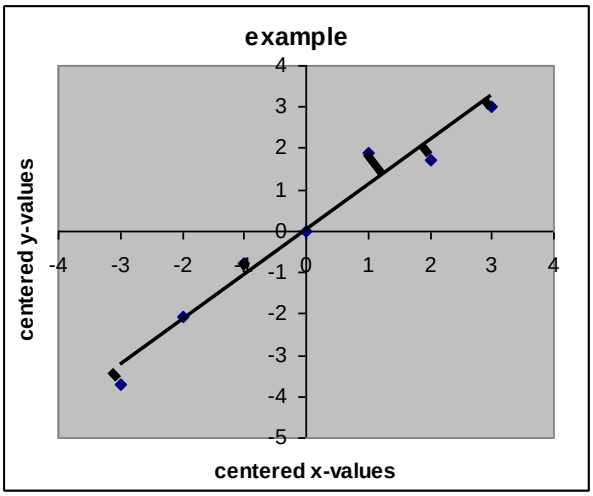

b) PCA: the residual is the distance between the data and the model perpendicular (orthogonal) to the model.

Figure 8. Differences in how the residual is defined between standard linear regression and a PCA model.

In the linear regression case, the model is y=kx and the only parameter is k.
In the PCA case, the model assumes errors in both x and y and the model therefore is

$$\begin{bmatrix} x \\ y \end{bmatrix} = \begin{bmatrix} X \end{bmatrix} = \mathbf{TP'} \qquad (7)$$

T is called the score matrix and consists of the values along the model plane (in the example above, the scores correspond to the values along the line shown in Figure 8b.) The score matrix is the new approximation of the original matrix X, but using fewer dimensions.
P is the "model" and consists of the linear combinations of the original variables that are used to project on to the model plane. Here we have two "parameters" p(1) and p(2) in the vector P. The loading matrix P is orthogonal and normalized to the size of one (orthonormal), *i.e.*;

$$\mathbf{P'P} = \mathbf{I} \qquad (8)$$

The PCA example above can be extended to many more variables and many more observations but works out the same way:
We get a loading matrix P that will be used to project the original matrix X onto a low-dimensional plane, T.
The main advantages of PCA (and other LV methods) are

- It handles errors in x and y.
- It handles co-linear variables.
- It produces models that have components that are orthogonal.

For more details about PCA, see *e.g.* [Eriksson 2001, Martens 1989]

3.2.2. Principal Components Regression, PCR

After making a PCA on a set of x-data, we have the situation where we no longer have correlation between the variables. One way to proceed then is to make a multivariate linear regression but using the scores T instead of the matrix X. the model then becomes:

$$\hat{\mathbf{y}} = \mathbf{Tb} \qquad \textbf{(9)}$$

Where T is the score matrix from a PCA model of X, T=XP. This method will not be further discussed but serves as a "bridge" to the PLS method in the next section.

3.2.3. Partial Least Squares, PLS

The Partial Least Squares method (PLS) or "Projections to Latent Structures" as it sometimes is called is a regression method very similar to the standard multivariate linear regression and the PCR case described above. It uses two separate models for X and Y and then tries to find the correlation between these two models. The model now becomes:

$$\hat{\mathbf{y}}_i - \bar{\mathbf{y}} = (\mathbf{x}_i - \bar{\mathbf{x}})'\mathbf{b} \qquad \textbf{(10)}$$

Where **b** is the regression vector given by:

$$\mathbf{b} = \mathbf{W}(\mathbf{P}'\mathbf{W})^{-1}\mathbf{c} \qquad \textbf{(11)}$$

W, P, and **c** are loading vectors, *i.e.* linear combinations of the original x and y variables. A geometrical picture is given below:

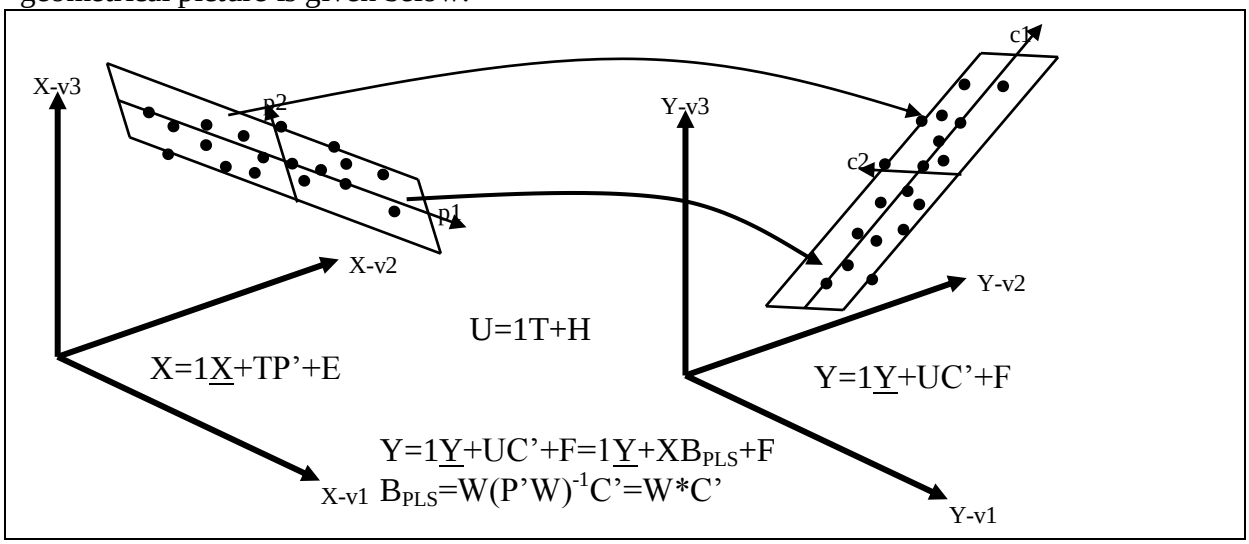

Figure 9. Geometrical description of the PLS model.

Since the **X** and **Y** matrices are "stripped" for every component, the corresponding PLS loadings (**W**) are associated with the corresponding, "stripped" matrix X. In order to make the interpretations more clear, $\mathbf{W}^*$ is used ($\mathbf{W^*}=\mathbf{W}(\mathbf{P'W})^{-1}$). W* can now be compared to the variables in X. Furthermore, this is used in paper II. For further details about calculations and algorithms see [Martens 1989].

3.2.4. Multivariate curve resolution: Alternating least squares (ALS)

Multivariate curve resolution is the process, where a data matrix D[18] is decomposed into different components. One example is the PCA model which decomposes the matrix into scores and loadings using the objective function to maximize the variation in $\hat{\mathbf{D}}$. One "negative" side effect is that the components are calculated in order of explained variance and not as a function of chemical phenomena. The resulting loadings are thus sometimes hard to interpret in terms of "chemical" information, such as an IR spectrum. Similarly the scores possess both positive and negative values, where it would be desirable to have only positive values that could correspond to concentrations. One solution to these objectives is to use Alternating Least Squares (ALS). The ALS is in principle very similar to PCA but by adding non-negativity as constraints, the resulting scores and loadings can be interpreted as concentrations and pure component spectra. The procedure during ALS consists of several steps. First the X matrix, D, is approximated using ordinary PCA. Then by using a rotation matrix R, the final model becomes:

$$\mathbf{D} \approx \hat{\mathbf{D}} = \mathbf{TP}' = \mathbf{TRR}'\mathbf{P}' = \mathbf{CS}' \qquad (12)$$

where C is a matrix of "contributions" and S a matrix of pure "spectra". More details are given in the appendix B. The prerequisite for a successful decomposition is that all species are visible in the spectra and that they vary between different observations. Another prerequisite is that good initial estimates of either concentration or pure spectra (or a combination of both) are available

3.2.5. Comments about latent variable models and projection methods

The phenomenon of projections is not new itself. Plato describes in his book "The republic" how projections of an unobservable reality is taken for the truth and anyone questioning it will be discredited [Lewi 2004]. The same story goes in the novel "Flatland" by E. A. Abbott [Abbott 1884]. In this chapter only the numerical methods of PCA, PCR PLS and ALS are mentioned. There are a large number of similar models and similar algorithms that all produce latent variable types of models. The concept of Latent Variables as a frame work for multivariable modelling have been well described by Burnham [Burnham 1999, Burnham 1996]. Another similar method is Factor Analysis which also is used during ALS.

Multivariate Analysis, MVA (or Latent Variable modelling) has been presented in the literature for many years and is an entire research area in itself. These applications are (by its very nature) often connected to experimental design (see also section 2.1). Applications applied to catalysis include:

- Catalyst synthesis optimization [Tagliabue 2003]
- Sensitivity analysis (see section 4.4.3, paper II and III)
- Catalytic system optimization (paper I)

[18] The reason to use the notation D instead of X is that ALS is typically applied to a spectral matrix, which is a measured matrix D, where as the notation of a matrix X is more general and can be either a measured data matrix but also a sensitivity matrix, *e.g.* the Jacobian matrix.

3.3. Nonlinear models

In kinetic modeling of heterogeneous catalytic systems, nonlinear models are frequent. By nonlinear models we mean models that are nonlinear in the parameters, *i.e.*

$$\frac{\partial y}{\partial \beta} = f(\beta) \qquad \textbf{(13)}$$

This means that the derivative (or sensitivity) of a response with respect to a parameter is dependent of the parameter value itself. In contrast, the model in eq. (4) is linear in the parameters since the derivative with respect to the parameters (b0 and b1) is just a function of x and not of b. One example of a nonlinear model is the Arrhenius expression, eq. (28). The aspect of non-linearity becomes important for parameter estimation, since eq. (13) is heavily used in this process. Parameter estimation will be described in more detail in section 4.
The practical treatment of nonlinear models and nonlinear equation systems (*e.g.* for parameter estimation and for solving ODEs) is approximation by finite differences. Thus, no further description will be given in this thesis.

3.4. Modelling of the reactor system

The main objective is to understand what is occurring in the reactor. However, it is very important to have accurate control of the effects from the rest of the system. A typical reactor system consists of 5 parts with individual properties that influence observations:

1. Mass flow controllers (MFC): Response time and accuracy
2. Pipes upstream: lag time, axial dispersion
3. The reactor (see section 3.5)
4. Pipes downstream: lag time, axial dispersion
5. Detectors: response time and accuracy (selectivity and sensitivity)

The modelling of these parts can be achieved by empty reactor models where simple models can be applied. For dispersion effects, for example, ideal stirred tank reactors can be applied

$$\frac{dc}{dt} = \frac{q}{V_d}(c_f - c) = \frac{1}{\tau}(c_f - c) \qquad \textbf{(14)}$$

Where q is the volumetric flow, V_d is the (probably fictive) dispersion volume and τ is the time constant corresponding to the time it would take for a step in feed concentration to reach 63% of the final level. To model time delay a simple delay model can be applied:

$$c(t) = c_f(t - \tau) \qquad \textbf{(15)}$$

where τ is the time constant corresponding to the time lag of the particular component.

By modelling each part individually, a more accurate estimation of the reactor inlet conditions (which is used as input to the model) as well as detector conditions (which is used for residual calculation) can be obtained. This will be superior to the use of empty reactor data as model input, where all dispersion effects are lumped into upstream effects and downstream effects

(from pipes and detectors) are "moved" upstream. An evaluation of these phenomena is given in section 5.5.

3.5. Modelling of transport phenomena in heterogeneous catalytic reactors

In this section the different models for transport phenomena are presented. The included techniques are not intended to be complete, but rather to describe some common techniques and their properties. In section 5.5, quantifications and deeper analysis of the impact of the different models will be given using the model from paper IV as an example. A good summary of this topic can be found in [Kapteijn 1997].

In this thesis project, the modelling of transport phenomena is of secondary importance since the chemical kinetics is of primary interest. However the transport phenomena must always be considered and therefore a number of options are available. Below is a list of actions in order to enable various approximations for modelling of monolith reactors:

Tuning experimental conditions

By adjusting the experimental conditions appropriately, the transport phenomena can be neglected:

- Use low concentrations:
    - Prerequisites for Fick's law for diffusion (assuming constant diffusion coefficient) is not violated. Also low concentrations leads to low reaction rates, which will decrease the mass transfer resistance.
    - Heat of reaction is low so that the reactor may be assumed to operate isothermally and thus heat transport may be neglected.
- Use low temperatures to make kinetics more limiting than mass transport.
- Use high flow rates to decrease external mass transport resistance.
    - High flow rates will also make the reactor more "differential", making the axial concentration variation over the reactor small and allowing more direct measurement of reaction rates.
- Use a thin washcoat containing the catalytic material so that pore transport resistance becomes negligible.

Dealing with transport phenomena

If the experimental conditions are such that the transport phenomena cannot be neglected, they will need to be treated otherwise the kinetics will be masked by transport limitations and the validity of the kinetic parameters will be reduced. In many cases, the objective may even be to understand the interplay between kinetics and transport phenomena, *e.g.* for automotive catalytic design and process optimisation. There are different options for different phenomena

- Model axial dispersion[19] by "tanks-in-series" (see 3.5.1)
- Approximate radial diffusion by a "film model" (see 3.5.2)

[19] Dispersion is a phenomenon arising from both diffusion and convection.

- Neglect pore transport resistance, or model the pore transport using an effectiveness factor (see 3.5.3)
- Neglect heat transfer, or model the heat flux similar to mass transport (see 3.5.4)

The following sections briefly describe the different methods relevant to this thesis.

3.5.1. Lumping in axial direction: Tanks-in-series

In order to avoid partial differential equations (PDE) for a transient reactor model, the axial dimension may be approximated with a tanks-in-series model.[20] Considering the monolith channel as a tube reactor, this approach approximates the tube reactor with a number of ideal continuously stirred tank reactors (CSTR's) connected in series. This approximation captures the axial dispersion but neglects radial diffusion. When the number of tanks becomes large, the model approaches a plug flow reactor.

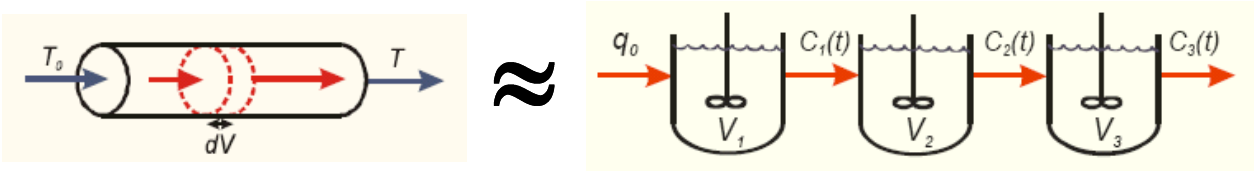

Figure 10. The monolith channel is approximated by a series of continuously stirred tank reactors (CSTR).

It is possible to calculate the number of tanks needed to capture the same phenomena as a tube reactor with dispersion effects, see appendix C, and this number is typically 20-50 for a small lab scale reactor depending on flow rate, temperature and composition. However, due to computational cost of the ode solver, this relatively large number can be reduced if the conversion is low enough, see Figure 11.

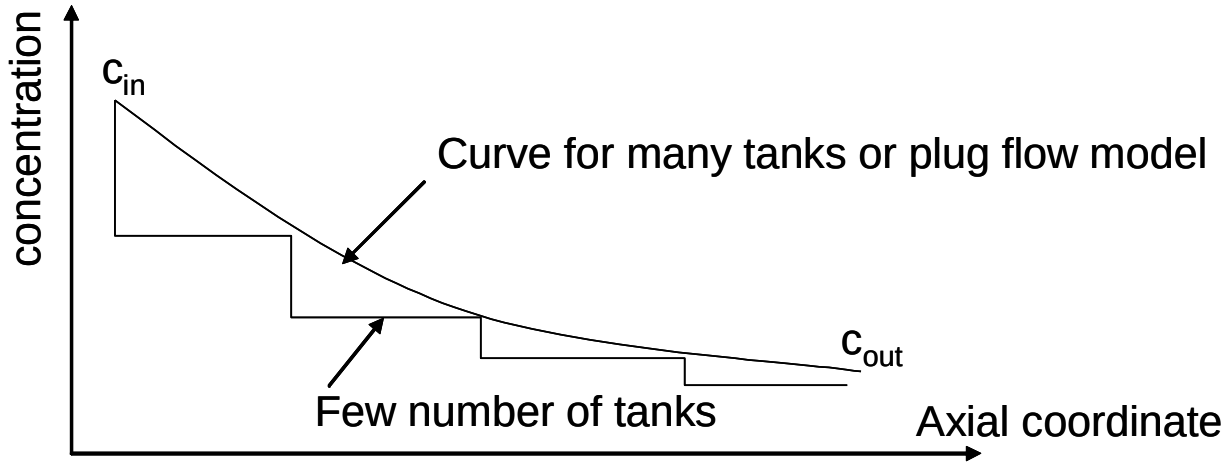

Figure 11 Effect of low number of tanks in the tanks-in-series model. If the conversion (consumption of feed reactants) is low in an overall point of view, the modelling error will be low and computational speed is gained.

[20] As an alternative to tanks in series, the finite elements method (FEM) can be applied. However, tanks-in-series is numerically a more stable/robust model.

3.5.2. Lumping in radial direction: film model for external mass transport

In a fully developed laminar flow (which is the case in a monolith reactor except for a small entrance region) there is no radial velocity component. The transport of molecules to and from the washcoat occurs by diffusion. The diffusion in the bulk gas phase is governed by Ficks law of diffusion: $\mathbf{j}^*_A = D_A \nabla y_A$, where $\mathbf{j}^*_A$ is the radial flux[21], D_A is the diffusivity and ∇y_A is the concentration gradient (driving force). Because we do not want to solve dc/dr (*i.e.* ∇y_A or resolve the true concentration gradient in the gas phase) we can approximate the overall gradient by a film of thickness delta δ with a transport resistance related to the diffusivity. The film model is often defined as:

$$N_A = k_{cA}(c_{A,b} - c_{A,s}) \quad \textbf{(16)}$$

where $c_{A,b}$ is the bulk concentration, $c_{A,s}$ is the gas phase concentration just at the surface and $k_{c,A}$ is a mass transport coefficient. $k_{c,A}$ can be derived from

$$k_{cA} = \frac{Sh \cdot D_A}{d_h} \quad \textbf{(17)}$$

where Sh is the Sherwood number (dimensionless number that characterizes film transport resistance), D_A is the molecular diffusivity and d_h is the characteristic length, in this case the diameter of the monolith channel.
The Sherwood number for monolith channels at steady state conditions was derived by Tronconi [Tronconi 1992], and in spite of the importance of transient experiments, this correlation is used in this thesis and the potential negative consequences are discussed in [Wickman 2007]. See also the appendix C for further details.

3.5.3. Modelling of pore transport resistance

The diffusion in the washcoat is often neglected by assuming that the diffusion transport resistance is sufficiently low, *i.e.* the rate of surface reaction is slower than the transport in the washcoat. This assumption is reasonable as long as the concentration gradient is low (by low conversion) but may be incorrect during transient conditions. Modelling of pore transport resistance was ignored in all papers in this thesis. The reasons for this are:

- Thin washcoat (50-100µm)
- The alumina washcoat is normally full of cracks, which facilitates the transport into the pores even further

One way to evaluate the influence of pore transport resistance is by calculating the Weiss-Prater parameter which is the ratio of observed reaction rate and pore diffusion.

$$\Phi_{Weiss-Prater} = \eta\phi^2 = \frac{L^2 r}{D_{eff} c_s} \quad \textbf{(18)}$$

[21] The flux is normally composed by molecular flux (j*) and bulk flux. The sum of these fluxes are referred to as the combined flux (N). Due to the low concentration levels the bulk flux becomes negligible.

where r is the reaction rate [mole/(s*m^3cat], L is the characteristic length (washcoat thickness, [m]), c_s is the concentration at the surface (which is the same as the bulk concentration if we can neglect the external mass transport resistance) and D_{eff} is the effective diffusivity [m^2/s]. The η is the effectiveness factor and ϕ is the Thiele modulus. More details are given in appendix C.

3.5.4. Heat transfer models

Heat transfer is very similar to mass transfer [Bird 2002] and the tanks-in-series and film models apply equally well to heat transfer. The film model for heat transfer can be written:

$$Q = hA(T_b - T_s)$$
$$h = \frac{Nu \cdot \lambda}{d_h} \quad \textbf{(19)}$$

Where Q is the heat transfer, A is the interfacial area, Tb and Ts are temperatures in the bulk and at the surface respecitively and h is the heat transfer coefficient. Here, the Nusselt number (Nu) is equal to the Sherwood number (Sh) and λ is the thermal conductivity. However, in contrast to molecules, heat can be transferred through the monolith channels and out to the periphery of the reactor. It then becomes a delicate matter whether to model only one channel of the monolith or to take radial heat transfer fully into account. In paper IV the radial heat transfer was lumped into heat transfer to the quartz tube via a lumped heat transport coefficient UA similar to a film model:

$$Q = UA(T_s - T_p) \quad \textbf{(20)}$$

Where Q is the heat transferred from the monolith to the quartz tube, T_s is the catalyst surface temperature and T_p is the temperature of the quartz tube.

3.5.5. Mass and heat balances for a monolith reactor

In addition to the mole balances, the heat balances are included in paper IV as shown in Figure 12.

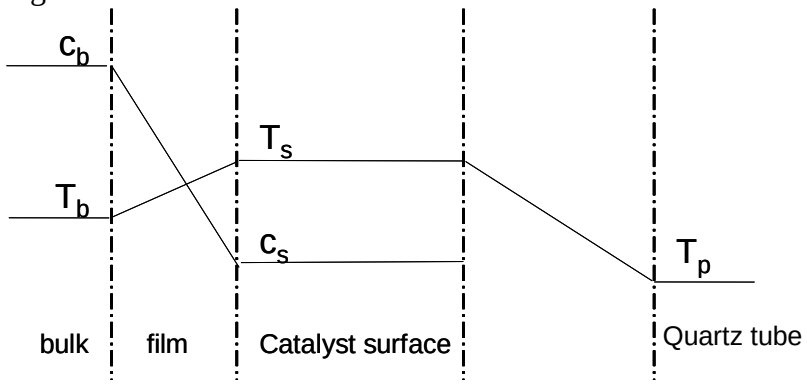

Figure 12. A schematic view of concentrations and temperatures at different radial positions. The straight lines connecting the bulk and the surface is governed by the film model.

The mole and heat balances for the bulk are modelled as tanks-in-series and for each tank the balances are:

$$c_{tot}V_{tenk}\frac{dy_b}{dt} = F_{tot}(y_f - y_b) - k_c a(y_b - y_s)c_{tot} = 0 \quad \textbf{(21)}$$

$$C_{Pgas}c_{tot}V_{\tan k}\frac{dT_b}{dt} = F_{tot}C_{Pgas}(T_f - T_b) + ha(T_s - T_b) = 0 \quad \textbf{(22)}$$

where c_{tot} is the total gas concentration (calculated from the ideal gas law), the accumulation of mass and heat in the bulk (dy_b/dt and dT_b/dt) are set to zero.
The mass balances for the gas at the surface (y_s) and on the surface (θ) are:

$$c_{tot}V_{film}\frac{dy_s}{dt} = \sum_i^{n_{rxn}} \upsilon_i r_i N m_{\tan k} + k_c a(y_b - y_s)c_{tot} = 0 \quad \textbf{(23)}$$

$$\frac{d\theta}{dt} = \sum_i^{n_{rxn}} \chi_i r_i \quad \textbf{(24)}$$

where ν_i and χ_i are the stoichiometric coefficients for the gas phase and surface respectively. The summations are done over all reactions in the mechanism. The accumulation in the gas (*i.e.* in the film closest to the surface) is set to zero, hence the volume of the film closest to the surface never needs to be calculated.

The heat balances for the surface and the quartz tube are:

$$\frac{dT_s}{dt} = \frac{\sum_i^{n_{rxn}} (-\Delta H_{Ri} r_i N m_{\tan k} - ha(T_s - T_g) - UA(T_s - T_p)}{c_{Pmono}m_{mono}} \quad \textbf{(25)}$$

$$\frac{dT_p}{dt} = \frac{\sum_i^{n_{\tan k}} UA(T_{si} - T_p)}{c_{Pp}m_p} \quad \textbf{(26)}$$

Where ΔH_{Ri} is the heat of reaction, h is the heat transfer coefficient, a is the channel area, UA is a lumped expression of the heat transfer coefficient to the outer quartz tube times the external area of the monolith.

3.6. Modelling of kinetics in heterogeneous catalysis

When assuming that a certain set of chemical reactions is occurring in a reactor, the resulting model will be a "kinetic model". The complexity of this set can vary from small sets (see section about lumped expressions 3.6.6) to large sets (see section about microkinetic modelling 3.6.3). These sets will then be used to calculate the reaction rates at every time point and for every reaction in order to solve the mass balance for all reacting species. The set of reactions will implicitly contain a number of kinetic parameters which need to be evaluated. If these parameters are not known, different ways of estimating them exists (see section 3.6.2 below). A number of thermodynamic constraints are also imposed on the kinetic parameters as will be described in section 3.6.4 and an alternative to the Arrhenius expression

is presented in section 3.6.5. The technique of parameter fitting by various methods is described in a later section (4).

3.6.1. Lumping of catalytic surface: The Mean Field approximation

Modern catalytic reactors for NO_X reduction described in *e.g.* paper II and IV have the special property that different sites have different tasks. As seen in section 2.3, the different sites cannot be (and are not) positioned all over the surface, but are dispersed forming small nanoclusters that are hopefully well spread over the surface. It is easy to realize that reactions including both Pt and Ba sites depend on the proximity of the sites. To rigorously model these (nano-) phenomena on a macro scale is (at least with today's computer capacity) practically impossible and hence the need for yet another approximation: the mean field (MF) approximation. A MF model approximates all sites to be equal and equally distributed, *i.e.*

- Uniform particle size and shape
- Uniform coverage of active sites.
- Any "distance effect" (*e.g.* between Pt and Ba) must be compensated for by the kinetic parameters

This approximation is of course never true, but by letting the fitted kinetic parameters compensate for these defects, the MF approximation becomes very useful. Other methods exist like Monte Carlo simulations [Olsson 2003], but again detailed assumptions of the surface structure must be postulated and the uncertainty is just "moved" to yet another "scale". To conclude, for modelling of monoliths at atmospheric conditions, it seems difficult to find any better alternatives than the MF approximation. (See also section 6.2.)

3.6.2. Atomistic models

The lower limit of modelling relevant to heterogeneous catalysis is on the atomistic level. If one can describe *e.g.* how atoms move on a surface or how atoms react on a surface, this knowledge may be transferred to the macro-scale level. Presently, the dominating modelling technique is Density Functional Theory (DFT). These models take into account electron densities assuming that an atom's nucleus moves much more slowly than its electrons. DFT finds electron and nuclei positions that minimize the total energy. The theory and application of DFT is beyond the scope of this thesis, however it can serve as a beneficial technique to estimate various properties to be used in modelling on the macro-scale. These properties include:

- Binding energies, *i.e.* activation energies for desorption. (physisorption/chemisorption)
- Adsorption conformation, *i.e.* plausible geometrical position for an adsorbed species.
- Vibrational frequencies in order to identify adsorbed species (typically reaction intermediates)

Although these results may be very accurate; the reliability for a real system is uncertain. This is due to the many approximations done during the calculations and in particular assumptions about the support:

- crystal planes or perfectly defined clusters
- any distribution of crystal planes, surface size or cluster size distribution is neglected

However, the technique can be used to estimate boundary values for Microkinetic models which can be extremely useful. Furthermore it can serve as the basis for the kind of models presented in section 3.6.5.

Calculations on NSR catalysis have been performed by Broquist et al. predicting reaction paths [Broqvist 2004] as well as heats of adsorption [Broqvist 2002].

3.6.3. Microkinetic modelling

Microkinetic modelling has been much appreciated in recent years thanks to James A. Dumesic et al. who contributed with a textbook in the early 1990s [Dumesic 1991].

> *"A fundamental principle in microkinetic analysis is the use of kinetic parameters in the rate expressions that have physical meaning and, as much as possible, that can be estimated theoretically or experimentally. With reasonably good estimates of parameters such as …, this analysis can suggest which steps of the mechanism are likely to be kinetically significant and which surface species may be most abundant. This information is vital for predicting the manner in which the various steps in the mechanism may affect catalyst performance.*
>
> *Should the microkinetic analysis be successful in reproducing all available experimental data using values of kinetic parameters that are consistent with known theoretical and experimental estimates, then microkinetic analysis may become an important tool in catalytic reaction synthesis. … microkinetic analysis provides a framework for the quantitative interpretation, generalization, and extrapolation of experimental data and theoretical concepts for catalytic processes."*

Frame 2. Citation from introduction section in the textbook "The Microkinetics of Heterogeneous Catalysis [Dumesic 1991]

A microkinetic model consists of elementary steps, *i.e.* most stoichiometric coefficients are equal to one and all equilibrium reactions are modelled as two separate steps. Each reaction rate is expressed as:

$$r = k \prod_{\text{reactants}} c^{\alpha} \qquad \textbf{(27)}$$

Where c is a dimensionless concentration (*i.e.* mole fraction y for gas phase species or coverage θ for surface species), α is the stoichiometric coefficient and k is the rate constant described by an "Arrhenius expression":

$$k = Ae^{\frac{-Ea}{RT}} \qquad \textbf{(28)}$$

Where A is the pre-exponential factor and Ea is the activation energy. This expression was actually one of several possible formulations described by Van't Hoff [Van't Hoff 1884, 1896] but was refined and established by Arrhenius [Arrhenius 1889a, b, Partington 1964]. For temperatures far from absolute zero (which is the case for experiments relevant to this thesis), the exponent (-Ea/RT) will have a large influence on k. This means that a change in theoretical reaction rate can be induced either by a change in Ea or in A, *i.e.* we have correlation between these parameters. This is avoided by scaling, also referred to as centred pre-exponentials see section 4.3.

There exist also a number of techniques to theoretically estimate kinetic parameters. These calculations always assume some kind of ideality but serve as useful starting guesses. These methods are for example DFT (as described above), Bond-Order Conservation (BOC),

Transition State Theory and kinetic gas theory. For more details about theoretical parameter estimation methods, see [Dumesic 1991] and the appendix C.

The most attractive features of microkinetic modelling are (as cited above):

- It enables deeper analysis (identification of rate limiting steps, etc)
- It should be better for extrapolation (compared to other more kinetically lumped models)

Among the drawbacks are:

- A More complex mechanism
  - Larger system of differential equations to solve (increased computational cost), especially for transient (time dependent) simulations.
  - More correlation between parameters (difficult parameter fitting and model evaluations)
  - Risk of making inappropriate assumptions about mass transfer limitations (*i.e.* neglecting these effects due to computational limits)

These parameter fitting aspects will be further discussed in section 6.6.
Microkinetic modelling has been successfully described in the literature, see *e.g.* [Stegelmann 2004, Stoltze 2000]

3.6.4. Thermodynamic constraints

For equilibrium reactions the thermodynamic laws should be fulfilled at all times and the change in Gibbs free energy is given by:

$$\Delta G = \Delta H - T\Delta S = -RT\ln(K) \qquad \textbf{(29)}$$

If the net enthalpy change (ΔH_{net}, given by calculation from gas phase species) is constant (for all times and all states), the activation energies in the microkinetic mechanism must fulfil:

$$\Delta H^{0}_{net} = \sum_i \upsilon_i Ea_{i,\,forward} - \sum_i \upsilon_i Ea_{i,backward} \qquad \textbf{(30)}$$

This must also be fulfilled for all coverages and if one uses coverage dependent activation energies (Ea), then this must also be taken into account. (see *e.g.* [Park 1999]
Similarly for ΔS, the change in entropy must be constant for all temperatures:

$$\prod_i \left(\frac{A_{i,backward}}{A_{i,\,forward}} \right)^{\upsilon_i} = e^{\frac{\Delta G^0_{net} - \Delta H^0_{net}}{RT}}$$
$$\frac{\Delta S^{0}_{net}}{R} = \sum_i \upsilon_i \ln(A_{i,\,forward}) - \sum_i \upsilon_i \ln(A_{i,backward}) \qquad \textbf{(31)}$$

These thermodynamic constraints can be implemented as restrictions on the parameters, adjustment of some chosen parameters (*e.g.* [Olsson 1999]) or reformulation of the problem (modelling of equilibrium instead of separate reaction steps, *e.g.*[Mhadeshwar 2003]). Alternatively, the "Thermodynamic state variable modelling approach" can be applied as described in the next section.

3.6.5. Thermodynamic state variable modelling

In order to maintain thermodynamic consistency *c.f.* eqs. (30) & (31), one pair of parameters (A,Ea) needs to be adjusted during parameter fitting (by treating them as "slack" parameters) for each global reaction path. If the slack parameters are chosen carefully, this approach may work satisfactory. However, the introduction of a slack step also introduces stiffness in the parameter fitting, especially for experimental data with fast transients. Thus, the concept of Thermodynamic state variable modelling is an interesting alternative approach that avoids the necessity of slack parameters and has additional benefits.

Instead of having model parameters of Arrhenius type, thermodynamic state variables (H, S) are used as model parameters. The Ea and A in the Arrhenius expression can then be easily calculated for arriving at the conventional rate expressions, when solving the mass balances,

$$\begin{aligned} Ea_i &= H_i^{\#} - \sum_j \nu_{ij} H_j \\ T\ln(A_i) &= S_i^{\#} - \sum_j \nu_{ij} S_j \end{aligned} \qquad \textbf{(32)}$$

where superscript # denotes the transition state and the summation *j* is over the reactants in reaction *i*.
One drawback with the direct use of A and Ea as model parameters is that they are often considered to be independent of temperature even though they mostly have at least a slight temperature dependence. By using the present approach, the thermodynamic consistent temperature dependence of both H and S can be easily implemented by introducing temperature dependence for H and S. Another benefit with this modelling approach is that parameter bounds can be made physically sound, *e.g.* for entropy: $S > 0$ and $S_{ads} < S_{gas}$, moreover, these restrictions can be easily implemented. In order to obtain initial estimates for S and H, independent methods such as density functional theory (DFT) and calorimetry can be used (see also the Appendix). Similar to traditional parameter fitting, a set of parameters will be subject to fitting, including adsorbed states and/or transition states.

It should be realized that one important difficulty is to determine the initial values for H and S at transition states. However, BOC and Transition state theory (together with other techniques and published values) can be applied to retrieve the necessary transition state values. Note, the transition state values are easily retrievable from the Arrhenius parameters, H and S for the adsorbed species together with eq.(32).

The number of degrees of freedom (d.f.) compared with a traditional Arrhenius type of formulation imposing thermodynamic consistency will be the same, *i.e.* no gain in fewer parameters will be achieved. However, the reduced parameter stiffness, the proper description of parameter temperature dependence, the easier implementation of DFT estimates and better parameter bounds makes this method interesting.

This method was applied to a proposed mechanism for H_2-assisted NH_3-SCR over a Ag-Al_2O_3 catalyst. In Figure 13, an example of an energy diagram displays H and S for single adsorbates as well as transition states for the different reactions.

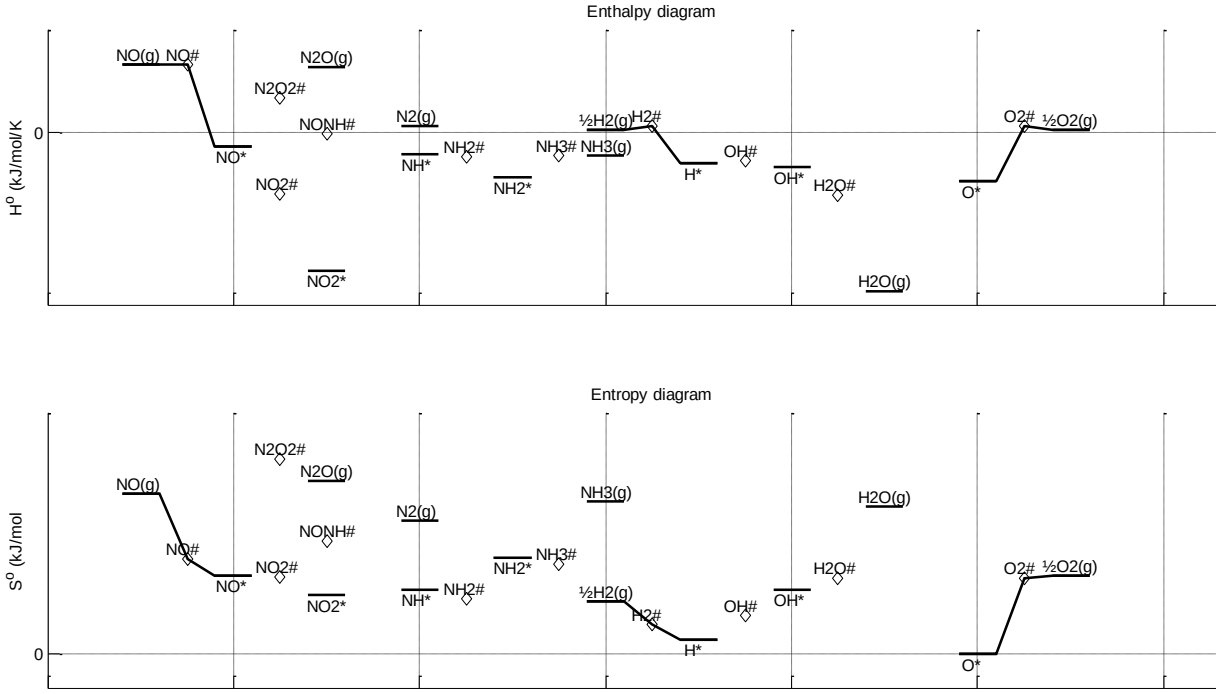

Figure 13. Example of an energy diagram using the present method. * indicates adsorbed specie, # indicates a transition state for a reaction.

3.6.6. Lumped kinetic models

Even though detailed (microkinetic) models prevail in this thesis, there are other kinetic models worth mentioning in this context. These lumped kinetic models are usually intended to express the rate of an overall reaction and not a set of elementary reactions.

Power law model

A power law model is typically set up as:

$$r = k \prod_{\text{reactants}} c^{\alpha} \qquad \textbf{(33)}$$

Which in essence is the same form as the microkinetic form, but with the difference that the exponents α can have any value (not only integers), k is still in an Arrhenius expression.

Langmuir-Hinshelwood model

Here one assumes that adsorption and desorption processes are much faster than the surface reaction and the adsorbed species will be in equilibrium with the gas phase. The reaction rate will be proportional to the surface concentrations and by analytically expressing these surface concentrations in terms of gas phase concentration one can arrive at:

$$r = \frac{-kK_A P_A K_B P_B}{(+K_A P_A)(+K_B P_B)} \qquad \textbf{(34)}$$

This equation is just one example for the reaction A + B => C where A and B is assumed to adsorb on separate sites. k is a reaction rate constant, K_A and K_B are adsorption equilibrium constants and P_A and P_B are the gas phase concentrations (expressed in partial pressure).
Other models such as Rideal or Eley-Rideal generate similar expressions and assume that the reaction occurs between one adsorbed species and one gas phase species.
These types of kinetic expressions are usually applied to express the rate of overall reactions and not to detailed kinetic models. For further reading about common kinetic models, see *e.g.* [Satterfield 1980]

4. PARAMETER FITTING AND ASSESSMENT

"When we gather information from the world,
we contribute to its entropy and hence its unknowability." - *Otto Rossle*

In order to get good estimates of the model parameters that are unknown, some kind of adjustment is necessary. In mathematical terms one defines an "objective function" and then one wants to manipulate the model parameters so that the objective function reaches some criteria. The most common objective function is the residual function:

$$f(\mathbf{x},\boldsymbol{\beta}) = y_{observed} - y_{model}(\mathbf{x},\boldsymbol{\beta}) \quad \textbf{(35)}$$

The criterion to be met is the minimization of the objective function and therefore the square of the residual is often used. In the following we will use β for model parameters, so that the objective function can be stated as:

$$\min_{\beta} f(\mathbf{x},\boldsymbol{\beta})^2 = (y_{observed} - y_{model}(\mathbf{x},\boldsymbol{\beta}))^2 \quad \textbf{(36)}$$

In the following sections different approaches to parameter fitting will be briefly described.

4.1. Linear least squares method

The least squares method was already reviewed in section 3.1.1. This method is the most fundamental method and will be referred to many times. The solution to the problem above, eq (36), is given by:

$$\mathbf{b} = (\mathbf{X}'\mathbf{X})^{-1}\mathbf{X}'\mathbf{Y} \quad \textbf{(37)}$$

The term "linear" arises from the fact that y is a linear function of b, *i.e.* $\partial^2 y/\partial b_i \partial b_j = 0$ for all *i* and *j*. Note that the roman letter **b** is used for parameters in linear models, where as the Greek letter β is used for nonlinear models.

4.2. Nonlinear least squares methods

Below is a very short version of nonlinear regression analysis from [Bates 1988].

For a nonlinear function y, the partial derivative of the function is still dependent on at least some parameter, *i.e.* $\partial^2 y/\partial \beta_i \partial \beta_j \neq 0$. This means that the parameter vector that minimizes the residual cannot be directly calculated as in eq (37) above. When optimizing in the least squares sense, the objective function is:

$$\min_{\boldsymbol{\beta}} S(\boldsymbol{\beta}) = \left\| y_{observed} - \boldsymbol{\eta}(\boldsymbol{\beta}) \right\|^2 = \left\| \mathbf{z}(\boldsymbol{\beta}) \right\|^2 \quad \textbf{(38)}$$

where $\eta(\beta) = y_{model}(x, \beta)$ with the dependence on x being dropped because we consider a specific set of observations. $z(\beta)$ is the residual corresponding to *f* in the linear case.

The solution is obtained in several steps:

1. Approximate the objective function $S(\theta)$ by a Taylor expansion:

$$S(\boldsymbol{\beta}) \approx S(\boldsymbol{\beta}^0) + \left.\frac{\partial S(\boldsymbol{\beta})}{\partial \boldsymbol{\beta}}\right|_{\boldsymbol{\beta}^0} (\boldsymbol{\beta} - \boldsymbol{\beta}^0) + (\boldsymbol{\beta} - \boldsymbol{\beta}^0)' \frac{1}{2} \left.\frac{\partial^2 S(\boldsymbol{\beta})}{\partial \boldsymbol{\beta} \partial \boldsymbol{\beta}'}\right|_{\theta^0} (\boldsymbol{\beta} - \boldsymbol{\beta}^0) =$$

$$= \begin{bmatrix} \left.\frac{\partial S(\boldsymbol{\beta})}{\partial \boldsymbol{\beta}}\right|_{\theta^0} = \boldsymbol{\omega} \\ \boldsymbol{\Omega} = \left.\frac{\partial^2 S(\boldsymbol{\beta})}{\partial \boldsymbol{\beta} \partial \boldsymbol{\beta}'}\right|_{\theta^0} \\ \boldsymbol{\beta} - \boldsymbol{\beta}^0 = \boldsymbol{\delta} \end{bmatrix} = S(\boldsymbol{\beta}^0) + \boldsymbol{\omega}'\boldsymbol{\delta} + \boldsymbol{\delta}' \frac{\boldsymbol{\Omega}}{2} \boldsymbol{\delta} \qquad \textbf{(39)}$$

2. The quadratic approximation will have a minima when the gradient is zero, *i.e.*:

$$\boldsymbol{\omega} + \boldsymbol{\Omega}(\boldsymbol{\beta} - \boldsymbol{\beta}^0) = 0 \qquad \textbf{(40)}$$

   and if Ω is positive definite $\delta = -\Omega^{-1}\omega$. When the linearization is exact, the optima will be reached with the step δ (called the Newton-Raphson step).

3. For the function $S(\beta)=(y-\eta)'(y-\eta)$, the gradient ω and Hessian Ω are given by:

$$\boldsymbol{\omega} = -2Jz$$
$$\boldsymbol{\Omega} = 2J'J - 2\frac{\partial J}{\partial \boldsymbol{\beta}} z \qquad \textbf{(41)}$$

When setting the second term of the Hessian to zero, we obtain the "Gauss-Newton" method. For further details, see [Bates 1988].

The above citations were given to illustrate what needs to be calculated during parameter fitting of nonlinear systems. If one has for example 10^4 experimental data points, the calculation of these data points constitutes one function call. If one then has p adjustable parameters, then the Jacobian takes about p function calls. The Hessian takes about p^2 function calls which becomes considerable if p is moderately large, since this must be performed for every iteration during the fitting procedure. See also section 6.8.

4.2.1. Quadratic Programming, Lsqnonlin

Quadratic programming is a procedure for carrying out nonlinear least squares optimization but with constraints on the parameters. For more information, see *e.g.* [Edgar 2001].
An example of one such is *Lsqnonlin* found in the *Matlab* optimization toolbox,. *Lsqnonlin* is a least squares optimizer for nonlinear problems. There are several options of algorithms and when bounds on the parameters are specified (*e.g.* activation energies greater than zero) the lsqnonlin function uses a "large scale" algorithm.

The large scale algorithm uses a trust region method and preconditioned gradients. The description of these algorithms can be found in the Matlab documentation, [Coleman 2001, Mary Ann Branch 1999, Thomas Coleman 1996]

4.2.2. Gradient Free fitting algorithms

One alternative way of minimizing the objective function is to use gradient free methods. These methods do not assume any gradient, but must evaluate more parameter settings during the fit. This introduces a trade-off between deviation from a trustworthy gradient and computational cost. For a parameter space that is limited to two levels, a factorial design will cover the parameter spaces and 2^p function evaluations would be enough to find the most optimal point (for 20 parameters, $2^{20} \approx 10^6$ function evaluations). If each parameter can have many values (*e.g.* discretized in 10 intervals), the number of function evaluations increases dramatically to 10^p (for 20 parameters, 10^{20} function evaluations).
Gradient free methods are not within the scope of this thesis but are still very interesting since the reliability of gradients is low for highly non-linear systems, especially with poor parameter estimates (parameter values far from optimum). Examples of a gradient free algorithms are simulated annealing [Aghalayam 2000, Eftaxias 2002, Kalivas 1992, Raimondeau 2003, S. Kirkpatrick 1983] and Genetic Algorithms [Routray 2005].

4.3. Parameter pre-treatment

As in every regression situation we assume independence and specifically independent variables. In Quadratic Programming for NSR systems, the variables are the model parameters and the objective of the parameter pre-treatment is to transform them to be as uncorrelated as possible. The concept is "taken" from DoE (section 2.1) where a classical scaling is the "UV-scaling" which means centring of the variables and scaling them to unit variance. In the case of parameter fitting this means:

$$\boldsymbol{\beta}_{scaled} = \frac{\boldsymbol{\beta}_{raw} - \boldsymbol{\beta}_{mean}}{std(\boldsymbol{\beta})} \qquad \textbf{(42)}$$

where β_{raw} is the unscaled current parameter value, β_{mean} does not necessarily mean the average, but rather the "setpoint" or "best guess" of the parameter value. Std(β) does not necessarily mean the spread of the parameter but rather a measure of the allowed range for the parameter value.
By applying this transformation to all parameters regardless of their physical meaning (*i.e.* treating pre-exponential and activation energies separately) we obtain all the parameters on the same "level" as well as on the same "scale".
The "allowed range" can be implemented in (at least) two ways:

1. to correspond to the actual allowed range, which implies that an extreme parameter value (on the border of allowed range) will have a scaled value of +/- 1.
2. to correspond to a defined response in the system. For example that the "allowed range" will correspond to a doubling of halving of the reaction rate. This will make the settings of the bounds much easier.

In order to get the pre-exponential and the activation energies to be as uncorrelated as possible, one performs "centring" of the pre-exponentials:

$$k = Ae^{\frac{-Ea}{RT}} = Ae^{\frac{-Ea}{R}\left(\frac{1}{T}+\frac{1}{T_{ref}}-\frac{1}{T_{ref}}\right)} = Ae^{\frac{-Ea}{RT_{ref}}} e^{\frac{-Ea}{R}\left(\frac{1}{T}-\frac{1}{T_{ref}}\right)} = k_{centered} e^{\frac{-Ea}{R}\left(\frac{1}{T}-\frac{1}{T_{ref}}\right)} \quad \textbf{(43)}$$

This "transformation" will obtain the centered pre-exponentials to capture the "amplification" and the Ea will capture the temperature dependence, since T_{ref} is chosen as the average temperature for the experimental data. This technique was, to my knowledge, first introduced by [Hawthorn 1974].

4.4. Model and model parameter evaluations

Once an acceptable fit has been obtained, it is important to evaluate the fit and the model performance. A number of analyses are available and the choice will depend on the objective and on ones level of ambition.

4.4.1. Residual analysis

Since the objective function of any "Least squares" is comprised of the residuals, it is of course vital that they are analysed. For linear models there are a number of standard analyses which need to be done:

1. How large is the residual? This can be done by an ANOVA (ANalysis Of VAriance) table.
    a. If the residual (quantified as the sums of squares, SS) is significantly larger than the SS of the model (compensated for degrees of freedom), than one cannot reject the hypothesis that the model parameters could have any values including zeroes.
    b. Lack of Fit (LoF) analysis: The residual is compared to an estimate of pure error (PE), *e.g.* from replicates. If the $SS_{residual}$ is significantly larger than the SS_{PE}, then there is a systematic contribution to the residual which was not captured by the model and the model was not "correct". This was assumed in the first place so if the model has LoF, then counter-measures must be taken.
2. Has the residual any structure? This can be assessed by various techniques:
    a. Normal probability plot: This plot can reveal if the residual has a normal distribution. This is always assumed to be the case, so if the residuals do not show this behaviour, counter-measures bust be taken.
    b. Plot of residual versus run order: If this plot shows systematic behaviour, then the residuals are not independent. The reasons for this behaviour should be found and counteractions taken.
    c. Plot of residuals versus variables: If this plot shows a systematic behaviour different causes may be contributing *e.g.* Lack of Fit, deviation from assumptions of constant variance, deviations from assumptions that x was exactly known.

One first analysis subsequent from a residual analysis may be a partitioning of the residual into smaller (and hopefully) independent sources. *E.g.* $\sigma^2_{tot} = \sigma^2_{model} + \sigma^2_{signal\ disturbance} + \sigma^2_{instrumental\ errors} + \sigma^2_{sample\ deterioration} + \sigma^2_{parameter\ fitting} + \ldots$. Then one may assess the causes of the residual and countermeasures may be taken. For more details about residual analysis, see any textbook about DoE, *e.g.* [Montgomery 2001].

All these analyses and potential countermeasures are possible for linear systems. When we have nonlinear systems and in particular time dependent observations, the whole situation becomes more complicated. However, it is very important to keep the linear situation in mind, in order to be able to sort among all different causes for non-ideal fit.

4.4.2. Parameter confidence intervals

The confidence interval of a model parameter in a linear model is given by:

$$\beta_i = \hat{\beta}_i \pm t_{\alpha/2,n-p}\sqrt{\hat{\sigma}^2 Q_{ii}} \qquad \textbf{(44)}$$

This formula tells us many things about what influences the uncertainty of the parameters:

- t-value: the probability level (α) always needs to be specified
- t-value: the degrees of freedom (n-p) are important
- σ^2: The level of noise is (of course) an important part.
- Q_{ii}: The correlation (from eq. 49) indicates the independence of observations.

For a nonlinear model, the analysis is the same, but the nonlinear model needs to be approximated by a linear one. This is done by some kind of Taylor expansion around a certain parameter point.

- This then indicates that the confidence intervals are valid ONLY at one specific set of parameter values.

As for the analysis of residuals, the assumptions are the same as in section 3.1.2. For example it is assumed that the model is correct and that the other variables (as well as all other fixed parameters) are known without errors. For more discussion on this subject, see section 6

4.4.3. Parameter sensitivity analysis

As described in [A. Varma] sensitivity analysis is (as indicated by the name) is a method of evaluating how sensitive a certain *dependent variable* (**y**) is for small perturbations in model *input parameters* (β). This is done by analyzing the derivative, either analytically or numerically, by using finite differences. There are different types of sensitivities but only two that are used in this thesis:

1. **local sensitivity:**

$$\mathbf{s}_{local}(\mathbf{y},\boldsymbol{\beta}) = \frac{\partial \mathbf{y}}{\partial \boldsymbol{\beta}} \qquad \textbf{(45)}$$

This is the local sensitivity matrix. There can be many parameters in the parameter vector β which will give the columns of S. The input parameters β are usually the kinetic parameters (pre-exponentials and activation energies) but can be ANY "constant" in the model structure such as:

- Number of active sites
- Effective diffusivity, mass transport coefficients
- ODE solver parameters

Also, there can be many observations of y (*e.g.* time dependent observations) which will give the rows of S. Moreover, there can be different responses in **y** which can give a third dimension of the Sensitivity array. Examples of y are:

- outlet concentrations
- average surface coverage
- reaction rates

The practical way to treat a three-way matrix (at least in this thesis) is by "slicing" the three-way array to a more easily handled two-way matrix.

2. **Objective sensitivity:**

$$\mathbf{s}_{objective}(\mathbf{f},\boldsymbol{\beta}) = \frac{\partial \mathbf{f}}{\partial \boldsymbol{\beta}} \tag{46}$$

This sensitivity is based on some objective function, **f** and can be one of the dependent variables but also any output from the model such as:

- Objective function during parameter fitting
- Conversion of a reactant at a specific time point
- Selectivity for a desired product at the reactor outlet

Since the different dependent variables and the input parameters have varying numerical range and since one wants to compare sensitivities, one sometimes uses a normalized sensitivity:

$$\mathbf{S}_{normalized}(\mathbf{y},\boldsymbol{\beta}) = \frac{\boldsymbol{\beta}}{\mathbf{y}}\frac{\partial \mathbf{y}}{\partial \boldsymbol{\beta}} = \frac{\partial \ln(\mathbf{y})}{\partial \ln(\boldsymbol{\beta})} = \frac{\boldsymbol{\beta}}{\mathbf{y}}\mathbf{s}_{local}(\mathbf{y},\boldsymbol{\beta}) \tag{47}$$

The sensitivity of the parameter fitting objective function (*e.g.* residual sums of squares) with respect to the fitted parameters is referred to as the Jacobian, **J**.

If one is using "manual" analysis of the Jacobian, it is convenient to time-average the sensitivity matrix and to use the correlation matrix instead:

$$\mathbf{C} = \frac{\mathbf{Q}}{\sqrt{diag(\mathbf{Q})' diag(\mathbf{Q})}} \tag{48}$$

Where

$$\mathbf{Q} = (\mathbf{J}'\mathbf{J})^{-1} \tag{49}$$

In this thesis sensitivity analysis is often used:

- In Paper II, the Jacobian is used for parameter estimation
- In paper III the gas phase sensitivities are used for experimental design
- In section 5.5 various sensitivities are used for the assessment of model parameters and model assumptions

Other examples of applications of Sensitivity Analysis (SA) include:

- Sensitivity analysis (SA) of **Q** has been performed for model reduction using PCA by Vajda [Vajda 1985]. SA of reaction rates (using eigenvalues from PCA) has been done by Turányi [Turányi 1989]
- Sensitivity analysis for model reduction has also been done by Jansson analysing the correlation matrix [Jansson 2002, Jansson 2004]
- Sensitivity analysis for model evaluation and model reduction has been used with success by the group of Vlachos [Aghalayam 2000, Mhadeshwar 2004, Mhadeshwar 2005a, b, Raimondeau 2003] but only for steady state experiments.
- Valid parameter ranges can be calculated using sensitivity analysis as demonstrated by [Song 2002] however not emphasizing parameter correlations.
- The incorporation of noise estimates is a rare topic in the literature. The reasons may be that other concerns are judged more important. Sound basics in statistics and DoE should mostly be sufficient see *e.g.* Meinrath [Meinrath 2000].

4.5. Design of Experiments for precise parameter estimation

General aspects of DoE were described in section 2.1(Design of Experiments (DoE)) and this section gives some comments on DoE for non-linear modelling. The DoE for nonlinear models was first developed by [Box 1959] and has further been developed since then, see [Walter 1990] for a review. Below is a list with some aspects considered in this thesis and especially in paper III. See also the Introduction section of paper III.

4.5.1. Batch sequential approach

Transient experiments are very valuable for kinetic modelling [Berger 2008] and parameter estimation, as illustrated in paper IV, thus motivating the use of many observations in the parameter fitting. Furthermore, due to practical reasons, a set of experiments (a "batch") is preferred.

4.5.2. Screening v.s. searching

Due to the many parameters and the high parameter correlation, a classical search for optimal design is computationally impractical. However, the parameter correlation enables a reduction in dimensionality by the use of an LV model, *e.g.* PCA. The use of a PCA model enables more efficient use of the experiments, since the number of components (*i.e.* the number of independent phenomena manifested in the data) gives the minimal number of experiments that span the effective parameter space. This number of experiments is fewer than the number of parameters which would be the number of required experiments if no correlation was assumed. Since the number of components is not known a priori (it depends on the experiments and also on the specific parameter values) a screening approach is preferred. The screening can be made as large as the computational capacity allows.

4.5.3. Design objective function

In the non-linear case, the model is linearised by the use of a sensitivity analysis, *e.g.* the Jacobian. Since the model is non-linear in the parameters, an orthogonal design (such as a factorial design) is often practically impossible to obtain. Instead, one needs to determine the

"goodness" of a plausible design and the different criteria uses the Jacobian, in this context denoted as X. See *e.g.* [Walter 1990]for a survey:

- D-criterion: maximize the parameter volume, *i.e.* the determinant of X'X
- E-criterion: maximize the smallest eigenvalue of X'X
- C-criterion: minimize the pairwise correlation [Pritchard 1978]
- AC-criteria: different variations which minimize parameter correlations [Franceschini 2008b]
- METER-criterion: minimise the expected total error [Bardow 2008]

In paper III the D-criterion was used since it is the most widely used criterion and since it was one of the options in the design software used (Modde 8.0 from Umetrics).

4.6. Comments on numerical aspects

When performing simulation of time-dependent, large reaction mechanism systems, there are some important aspects to consider:

- The system of ODEs is probably stiff due to the variability in dx/dt (some reactions are much faster than others). Even if a stiff solver was used (ode15s in MATLAB) throughout this thesis project, care needs to be taken in order to obtain reliable results.
- Furthermore, for parameter fitting using gradient methods, where the gradient is calculated by finite differences (as in lsqnonlin in MATLAB), the size of the step used to calculate the derivative is important. If it is too small, numerical noise in the ode-solver will deteriorate the gradient estimation and if it is too large it will include non-linearities.

A range of numerical parameters were evaluated for a kinetic model of NO oxidation over Pt-Al_2O_3 using the one set of transient experiments from paper III [Brühwiler 2007] and the main conclusions were:

1. The use of transient experiments resulted in 100 times smaller confidence intervals compared to steady state experiments, but with a increased computational cost of 30 times longer computations.
2. The gradient search method requires that the initial parameter values are close to the "true" values. If the initial values deviated more than 38% from the "true" values, the gradient search method failed. Unfortunately, this case study used only steady state experiments.
3. Tolerances in the ode solver should be checked, *e.g.* using the condition number of J'J as a measure. When the condition number is "stable", the ode solver is insensitive to the ode-parameters, which is desirable. In this study it was found that the absolute tolerance should be less than 1×10^{-6} and the relative tolerance should be less than 1×10^{-5}. However, the calculation time is also a practical parameter, see Figure 14.
4. In lsqnonlin, the calculation of the Jacobian using finite differences, is sensitive to the step size (dp). Even though scaled parameters were used (see eq.42), the default size of 1×10^{-8} gave a condition number of J'J much higher than $1\times10^{+18}$, which yields inaccurate results since the inverse of J'J is needed. In order to reach cond(J'J) values smaller than $1\times10^{+18}$, a dp>1×10^{-6} was needed. Furthermore, the size of the confidence intervals should be independent of the dp and moreover, the results should be independent of whether +dp or –dp is used. The range for these requirements were obtained for 1×10^{-4}<dp<1×10^{-2}, see Figure 15.

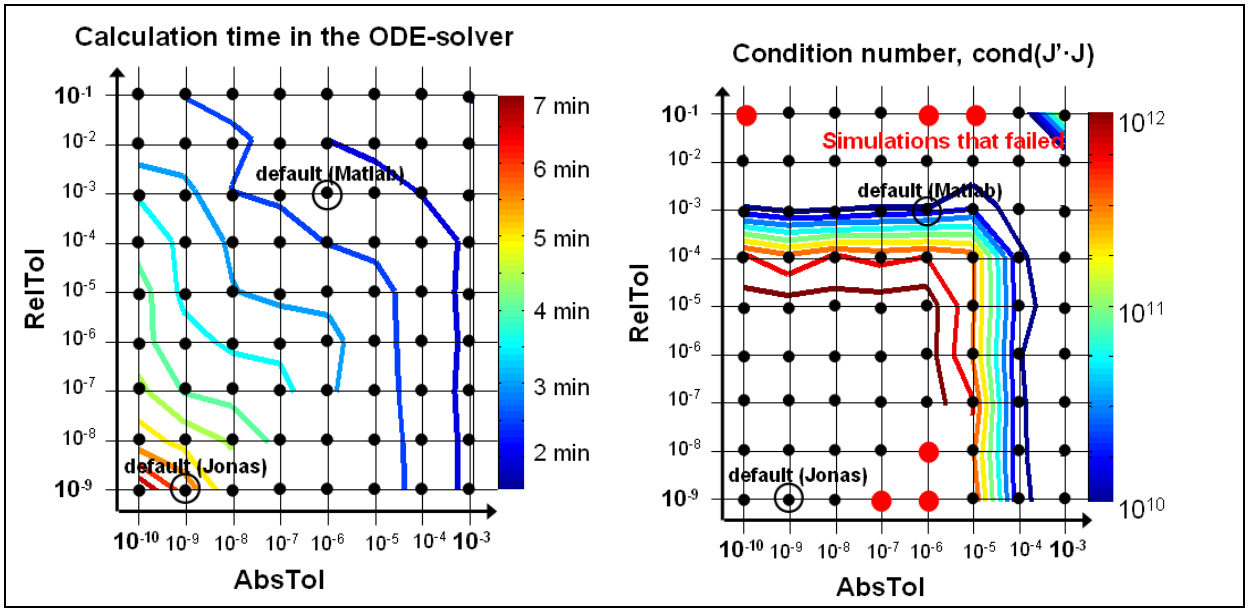

Figure 14 Calculation times and cond(J'J) for varying the tolerances in ode15s. RelTol is the relative tolerance and AbsTol is the Abolute tolerance. Note that the mole fractions are expressed as ppm, thus the relatively low values of the absolute tolerances.

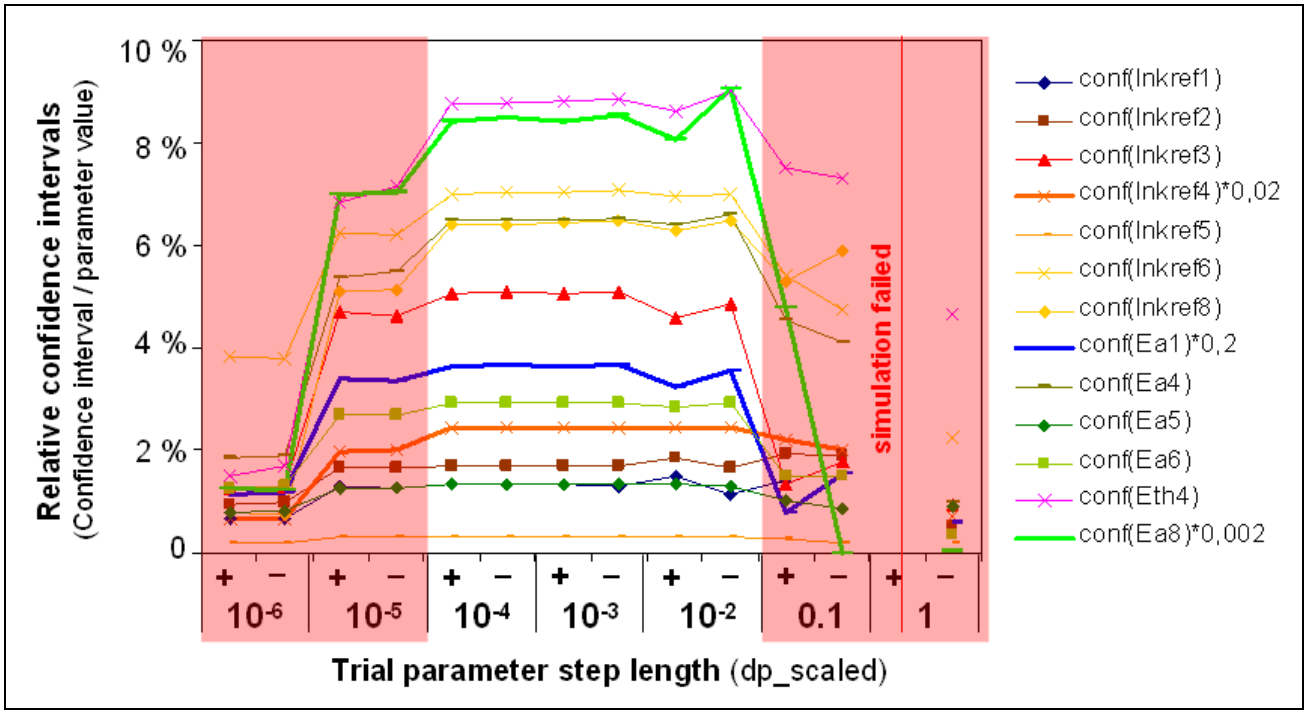

Figure 15. Confidence intervals for the 13 fitted parameters (using a set of transient experiments) as a function of the step size during calculation of the Jacobian using finite differences. For small dp the confidence intervals were small, but cond(J'J) was large and the confidence intervals were inconsistent with the ones obtained with a larger dp. For large dp values non-linearities were observed because the confidence intervals were sensitive to whether +dp or –dp was used for the finite differences.

5. MODEL APPLICATIONS

"One of the most difficult problems concerns the chemical analysis of mixtures containing an unknown number of unknown amounts of unknown components"
E.R. Malinowski (1992)

5.1. Paper I: Use of experimental design in development of a catalyst system

In a research programme funded by the Swedish National Energy Administration, a full scale NSR process was tested and developed using a Heavy Duty diesel engine (Scania 11 dm^3) in an engine rig. The system is depicted in the figure below:

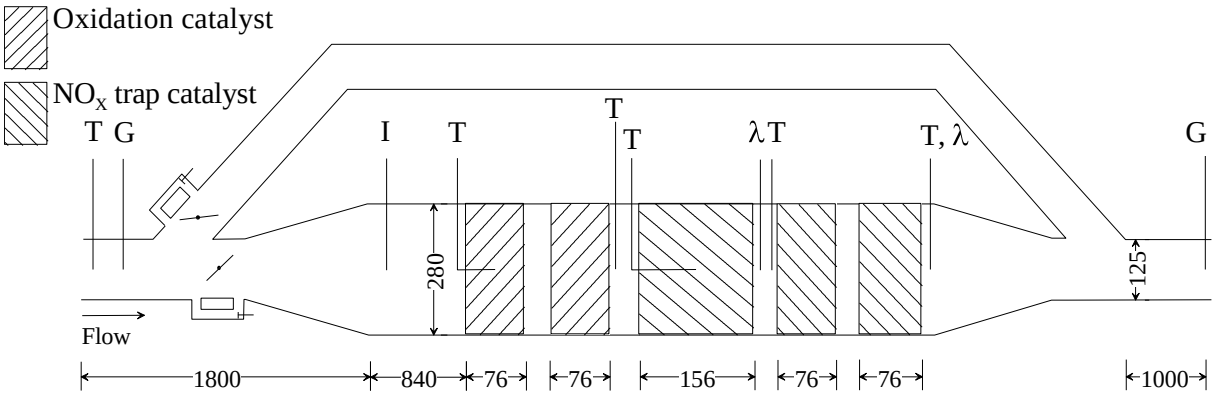

Figure 16. Catalyst setup. G = gas sampling point, T = thermocouple, λ = broad band λ-sensor, I = injector.

In this system NO is oxidized to NO_2 in two oxidation catalyst monoliths with a total volume of 9.4 dm^3. Downstream NO_2 is stored on 3 NO_X trap monoliths with total a volume of 18.9 dm^3. The catalysts were commercial and their exact composition unknown. However the oxidation catalyst contained Pt on Al_2O_3 and the NO_X trap contained Pt/BaO on Al_2O_3. The system has a bypass line operated by butterfly and EGR valves.
The project objective was to demonstrate NO_X reduction corresponding to Euro IV[22] on a European Transient Cycle (ETC).[23] In order to set up a control strategy, it was decided to optimize a number of representative load points[24] at stationary conditions. Typical Storage and reduction cycles for stationary runs (constant load and speed) are shown in Figure 17.

[22] Euro IV is the common name for legislation limits for vehicle emissions [Fontaine 2000]. For Heavy Duty Diesel engines this means a 60% reduction of NOx compared to previous limits (Euro III).
[23] ETC is an engine rig test protocol to demonstrate compliance with emission legislations. It has a duration of 30 minutes which simulates 10 minutes each of urban, rural and highway driving.
[24] A load point is a combination of the speed of the engine (rpm) and load applied on the break (Nm). This combination of two variables almost completely (apart from transient effects) determines the engine performance and thus the amount and composition of the emissions.

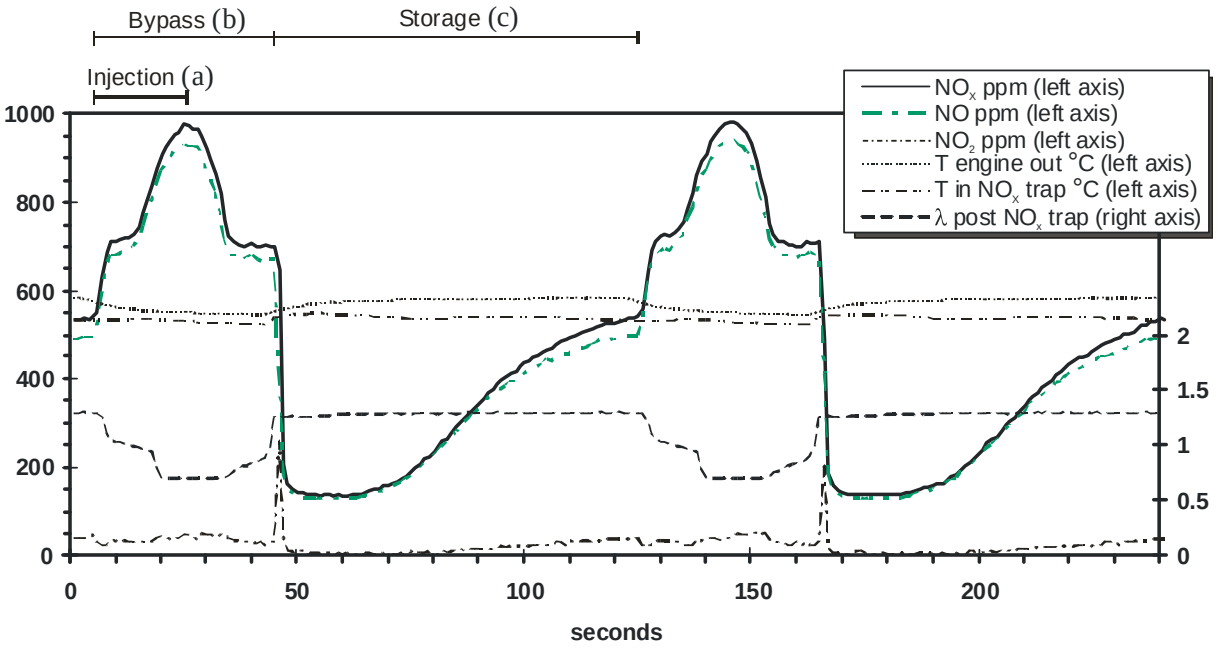

Figure 17. Time trend plot showing different signals from the system during two cycles. The gas sampling point was after the catalyst. (This experiment was N4, it=20s ir=938mg/s, bt=40s, ct=120s). The plot illustrates: a) the injection period (4-24 s, 124-144 s) where the injected reducing agent creates a breakthrough peak and the lambda value goes well below one, b) the bypass period where at the end the outlet NO_X levels suddenly decrease when the bypass line is closed, c) the storage period beginning with a baseline in NO_X levels at about 140 ppm indicating the maximum NO_X storage rate followed by a decrease in NO_X storage rate resulting in an increase in NO_X levels.

The objective of this study was to adjust the controllable injection parameters to optimize NOx reduction and at the same time minimize fuel penalty. The four controllable parameters included:

1. Cycle time (ct) [s]
2. Injection time (it) [s]
3. Injection rate (ir) [mg/s]
4. Bypass time (bt) [s]

The system was to be optimized using a linear model which also contained a cross product it*ir = injected amount. The optimization was to be repeated for different load points, so the use of Design of Experiments came naturally. Small screening designs capable of estimating main effects (plus the cross product) were used in order to investigate which combinations of parameters could achieve optimal NOx reduction with minimal fuel penalty. The models were fitted with PLS and coefficient plots were interpreted. Also surface response plots were used to illustrate which combination of parameters to use.

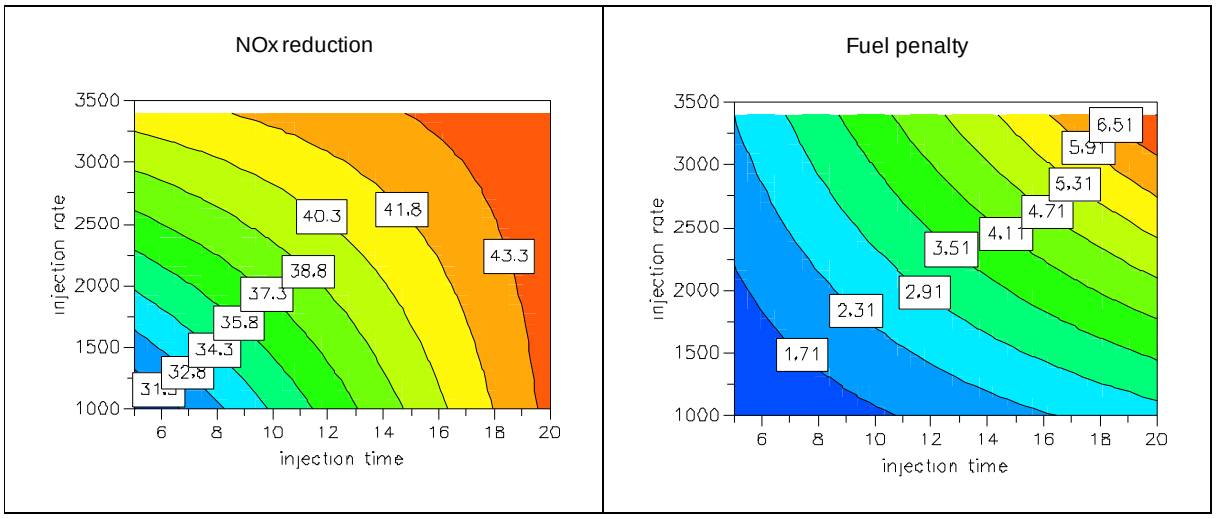

Figure 18. Response surface plots showing NO_X reduction and fuel penalty for various settings of injection time and injection rate. The cycle time is fixed at a low level (120s) and the bypass time is fixed at the centre level (20s)

In could be seen in Figure 18 that the highest NOx reduction was obtained at high injection times and high injection rates, but this led to a high fuel penalty. A low injection time and high injection rate were selected as optimal settings.

Similar designs were performed for several other load points. When inspecting the different optimal settings for different load points, it became clear that besides thermodynamic limitations (NO oxidation is prevented at high temperatures) and kinetic limitations (slow NOx storage for low temperatures) system limitations possibly due to the system design were identified.

One of the valuable conclusions from this study was the identification of the optimal injection parameter settings within the investigated space, for this rather complex process. Continued optimization was then applied expanding the parameter space even further. Studies and optimization of operating parameters for NSR systems have been published before [Kabin 2004, Theis 2002] but their methods did not contain any DoE. This does not mean that these results were wrong, but rather that the experiments probably could have been carried out more efficiently.

After this study the optimal injection settings were used as a map for all load points in an ETC. Additionally, the temperature was used to decide how the regeneration was to be performed. This resulted in a NO_X reduction of 60% together with a fuel penalty of 6.6%. [Papadakis 2007]

5.2. Paper II: New Approach for Microkinetic Mean-Field Modelling using Latent Variables

After inspiration from a PhD course in Microkinetic Modelling it became evident that an infinite number of parameter sets were possible to achieve a good fit for a simple system (in this case a temperature programmed reaction (TPR) curve for SO_2 oxidation on Pt). The plan was to demonstrate this on a larger system, *e.g.* an NSR system (a larger mechanism, multiple sites, and more transient conditions) and the goal was to show how different parameter settings gave different conclusions and thereby indicating the need for confirmation experiments. However, the first task was difficult enough even though it may seem possible to adjust a large number of parameters to a relatively small dataset.

The paper develops new methods for parameter fitting by introducing sensitivity analysis during the fitting procedure. Sensitivity analysis is commonly performed AFTER the fitting for the purpose of parameter evaluation, calculation of confidence intervals or model reduction. The sensitivity analysis is further refined compared to previous work by using LV regression methods *e.g.* PLS. Previous work (*e.g.* [Davis 2004, Vajda 1985]) uses PCA or similar analysis methods that do not include the objective function in the analysis. A somewhat similar method was also published by Luna-Ortiz [Luna-Ortiz 2005] which deals with a model reduction-based optimization scheme. They also used projection methods to capture the slow dynamics but they did not focus on the objective function itself.

The use of sensitivity analysis gives three important messages:

1. Awareness of the correlation among kinetic parameters for Microkinetic models.
2. Analysis of the correlation structure gives valuable information about the experimental rank and thus the number of parameters suitable for fitting.
3. A deeper analysis of the correlation structure also directs the choice of which parameters to choose when many parameters are subject to uncertainty.

The fist step in the method is to calculate the Jacobian using finite differences.

$$J \equiv \frac{\partial f}{\partial \theta} \qquad \textbf{(50)}$$

Then the Jacobian is regressed against the residual itself, so we get a (linear) model describing the relationship between J and Y:

$$\begin{aligned} \hat{\mathbf{Y}} &= \mathbf{J} \cdot \boldsymbol{\beta}_{\mathbf{PLS}} \\ \boldsymbol{\beta}_{\mathbf{PLS}} &= \mathbf{W} \cdot (\mathbf{P}' \cdot \mathbf{W})^{-1} \mathbf{C}' = \mathbf{W}^{*} \mathbf{C}' \end{aligned} \qquad \textbf{(51)}$$

Predictions are not performed, instead the regression matrix itself, $\mathbf{W}^{*}\mathbf{C}$ is used further. Two different alternatives are shown in the frames below:

Step 1. The number of significant PLS components were often around 10 (A=10). Thus about 10 parameters were chosen to be fitted.
Step 2. The parameters to fit were chosen so that all parameters spread reasonably well in all loading plots (w*c1/w*c2, w*c3/w*c4, and so on). The choice was always influenced by the reaction that they represented.

Frame 3. Method I how to select parameters by using an LV model.

Step 1. Calculate a PLS model by regressing the Jacobian against the residuals (commonly explaining 70-90% of the variance in Y using A=10 components)
Step 2. Initialize the parameter vector to fit **t** (of length Ax1). The values being zeros for reasons of scaling.
Step 3. Within the function call "extract" the original parameters using the loading matrix W^* [kxA]: θ [kx1] = W^*t and calculate the objective function as usual.

Frame 4. Method II how to select parameter combinations (loadings) to use for fitting.

The use of LV models in this process yields:

1. Fewer components than the case for *e.g.* PCA (*e.g.* as in [Vajda 1985])
2. A straightforward method to choose parameters (method I) or to fit in LV space (method II) which also could be implemented in the fitting code directly

After a number of iterations of fitting and using manual tuning to escape from local minima, the result was still not perfect. The reasons for this can be at least one of the following:

- The model was not correct, and there exists no set of parameters that can describe the experimental data
- The applied method using different kinds of gradients was not able to find the desired fit.

On the methodological side, one conclusion was that the traditional way of regarding parameter fitting for microkinetic models stated as:

"Calculate what you can and fit the rest"

Should be replaced with an alternative maxim stated as:

"Fit only the parameters necessary to span the effective parameter space"[25].

This may not seem revolutionary to some people, but from studying the literature, this insight is not visibly declared.

[25] In paper II this was stated as: "*Fit only parameters that span the experimental space"*, but this can accidentally be interpreted as the experimental conditions determining the parameter sensitivity, which is not the case. The parameter sensitivity is given by the model, the parameter values and the performed experiments in combination. The *effective parameter space* should therefore be a better notation for the orthogonal subspace of the parameter space, which evidently possessed high correlation in this study.

5.3. Paper III: Latent variable projections of sensitivity data for experimental screening and kinetic modeling

After paper II, different investigations were performed to analyse the reasons for the lack-of-fit Bengtsson, 2006 #924}[Lundström 2005]. One major factor was the lack of proper experimental design because the data in paper II was collected with objectives that did not include parameter estimation. In order to exploit the potential of LV models in kinetic modelling a method for experimental screening was developed. Since traditional methods are not well adapted to the combination of transient experiments, multiresponse data, many adjustable parameters and batch sequential approaches, a "brute force" method was chosen. The method consisted of the following steps:

1. Define the experimental space (flows, temperatures, concentrations)
2. Simulate these experiments and calculate the parameter sensitivity for every response.
3. Reduce the number of correlated columns to a few orthogonal ones by means of PCA. The resulting score matrix will now define the reduced parameter space (*i.e.* the effective parameter space).
4. Select a limited number of experiments necessary to span the effective parameter space, by means of a D-optimal design.
5. Perform these experiments, perform the parameter estimation (in this case using a gradient search method, lsqnonlin in MATLAB) and iterate from step 1 if necessary.

In this study, this iteration was performed twice using steady state experiments and subsequently transient experiments. The kinetic mechanism was NO oxidation on Pt consisting of 13 adjustable parameters. Published parameter values [Olsson 1999] with added noise were used to simulate experiments and the parameter estimation was initiated with different, independent parameter values. The results showed that very accurate fit could be obtained showing almost no lack of fit. On the other hand, the "true" parameter values were not obtained, thus indicating the consequences of parameter correlation.

This approach has several benefits:

- By using the "brute force" method, a search method for the optimal experiment was avoided. This should be beneficial since the many parameters, the many responses and the transient nature would probably be computationally expensive. On the other hand, the sensitivity analysis was also very computationally expensive.
- In traditional approaches, the Fisher information matrix is used as a measure of how valuable an experiment is:

$$\mathbf{M} = \sum_{r=1}^{m}\sum_{s=1}^{m}\sigma_{rs}\mathbf{J}_r{}'\mathbf{J}_s \qquad \textbf{(52)}$$

  Where m is the number of response variables and σ_{rs} is the element (r,s) of the inverse of the variance-covariance matrix of the experimental measurements and **J** is the Jacobian. This means that the information matrix is lumped both in responses as well as in time to produce a square matrix for further evaluation. By using the uncompressed sensitivity data, unfolding it, and compressing it this time by using a PCA model, no lumping is performed, but merely an approximation to fewer dimensions.

5.4. Study of NH_3-SCR over silver alumina

Since the pioneering work of Miyadera [Miyadera 1993], Silver alumina (Ag/Al_2O_3) has become increasingly interesting for HC-SCR due to its high activity in the presence of water and especially with addition of hydrogen, the low temperature activity is dramatically increased. There is a large number of published papers on NO_X reduction over silver-alumina, see *e.g.* [Breen 2006, He 2008], but the literature dealing with kinetic modelling of $Ag\text{-}Al_2O_3$ systems is sparse and limited to steady state experiments [Backman 2006, Mhadeshwar, Rönnholm 2007]. Beyond the difficulties of the complex reaction mechanism for SCR, silver alumina possesses even further challenges. One delicate problem with the modelling of this system is the strong interaction between the metal and its support [Hellman 2008] and another problem is the nature of the silver particles, being silver nano-particles, silver clusters, monodispersed silver atoms, or a combination of all [Breen 2007, Shimizu 2001] Through a scholarship from CenTACat (Queens University, Belfast, UK), a series of isotopic labeled experiments were performed. These results were presented at a conference (5th International Conference on Environmental Catalysis) 2008, but has not yet been documented as a journal article.

5.4.1. SSITKA of NH3-SCR over Ag/Al_2O_3

Various reaction mechanisms for the SCR over silver –alumina have been published, *e.g.* [Breen 2006, Yeom 2006] and one possible reaction intermediate is ammonia, NH_3. Since ammonia is used as the reductant formed from the commercial ad-blue concepts, silver-alumina has been suggested as an alternative to the potentially toxic vanadia-based catalysts [Richter 2004]. NH_3-SCR has very low activity compared to every other reducing agent (*e.g.* octane, propene, ethanol), but by adding hydrogen, the activity is boosted to the same level as any other reducing agent, see Figure 19.

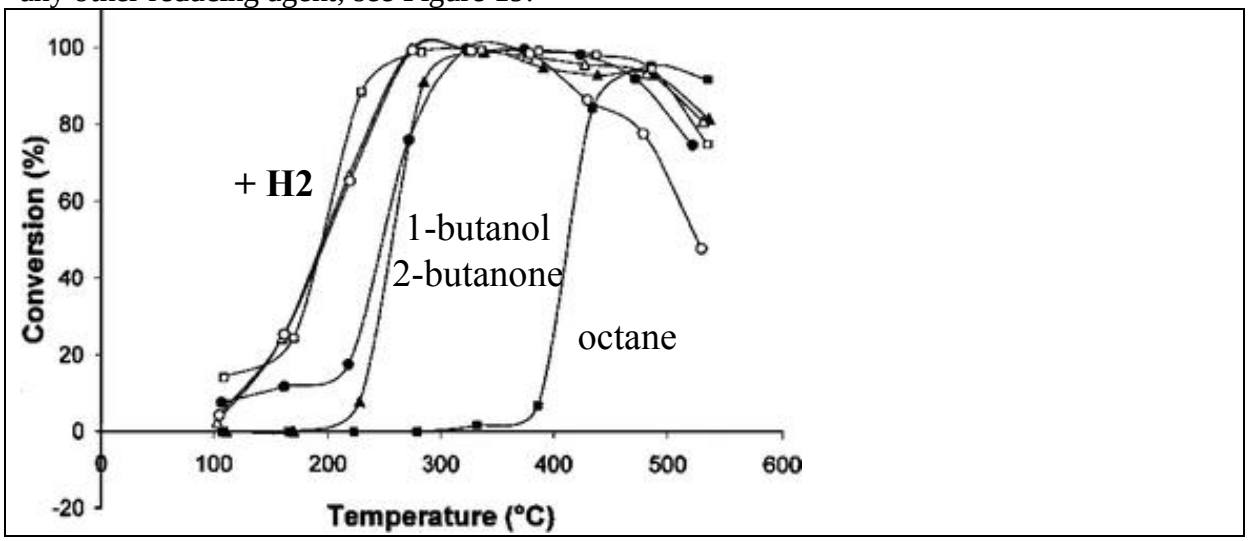

Figure 19. The NO_X conversion as a function of temperature for various reducing agents (filled symbols) and the boosting effect of hydrogen when used as a co-feed (open symbols). Figure from [Shimizu 2006]

Objective

In order to understand the HC-SCR over Ag/Al_2O_3, the increased understanding of the NH_3-SCR should be a valuable contribution to the HC-SCR. Furthermore, as NH_3 itself can be used as a reducing agent (and possibly with H_2 addition), the kinetic analysis during SCR conditions are important. The objective was to perform Steady State Isotopic Transient

Kinetic Analysis (SSITKA) experiments to elucidate the amounts of reaction intermediates on the catalyst during SCR conditions.

Experimental

SSITKA was performed under SCR conditions using both H_2/D_2 and $^{14}NO/^{15}NO$ switches. No water was used in the experiments, fixed levels of reactants were used: 1000 ppm NO, 1000 ppm NH_3, 1% H_2, 5% (or 10%) O_2. The catalyst was a 2% w/w Ag/Al_2O_3 (impregnated) sample. The reactor was a packed bed containing approximately 25 mg of catalyst sample with particle size 250-425µm. The bed diameter was 2.9 mm and the length was 5 mm. The temperature was controlled by a thermocouple and the reactor was heated by an oven. The reactor outlet stream was analysed with an MS from HIDEN Analytical (HPR20) via a capillary, positioned immediately downstream from the catalyst bed. To enable fast sampling, the switch was repeated several times detecting different fragments each time (together with the Kr as internal standard). This is the reason why some signals are missing in Figure 21 below.

Results and conclusions

Two representative experiments are displayed in Figure 20 and Figure 21.

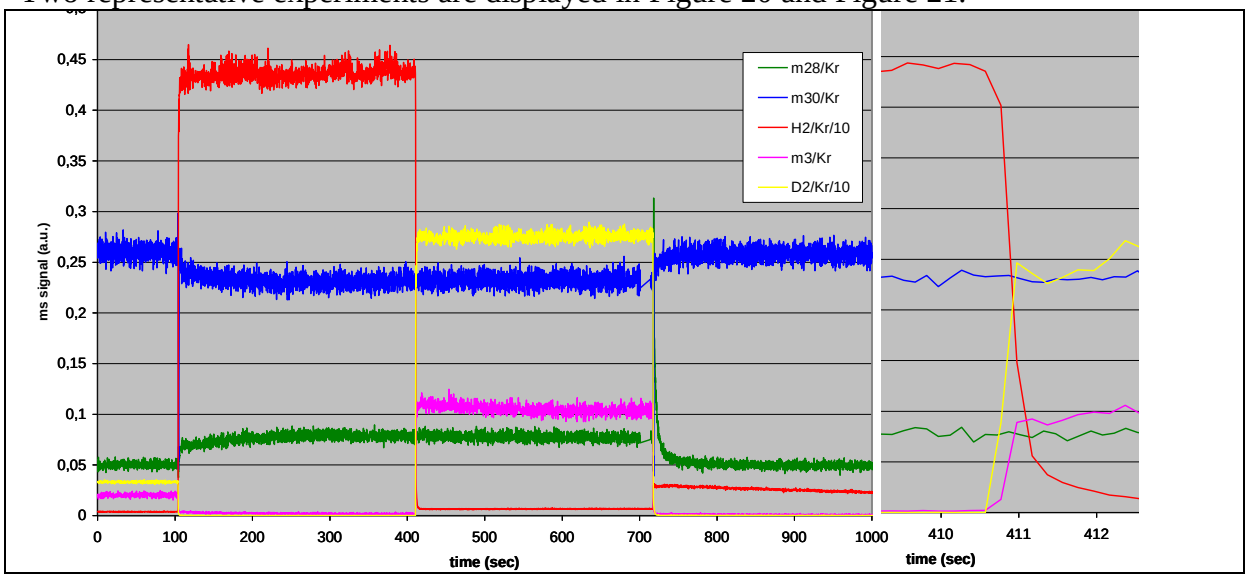

Figure 20. SSITKA experiments in a packed bed reactor. Step in H_2, switch to D_2 and step out at 170°C.

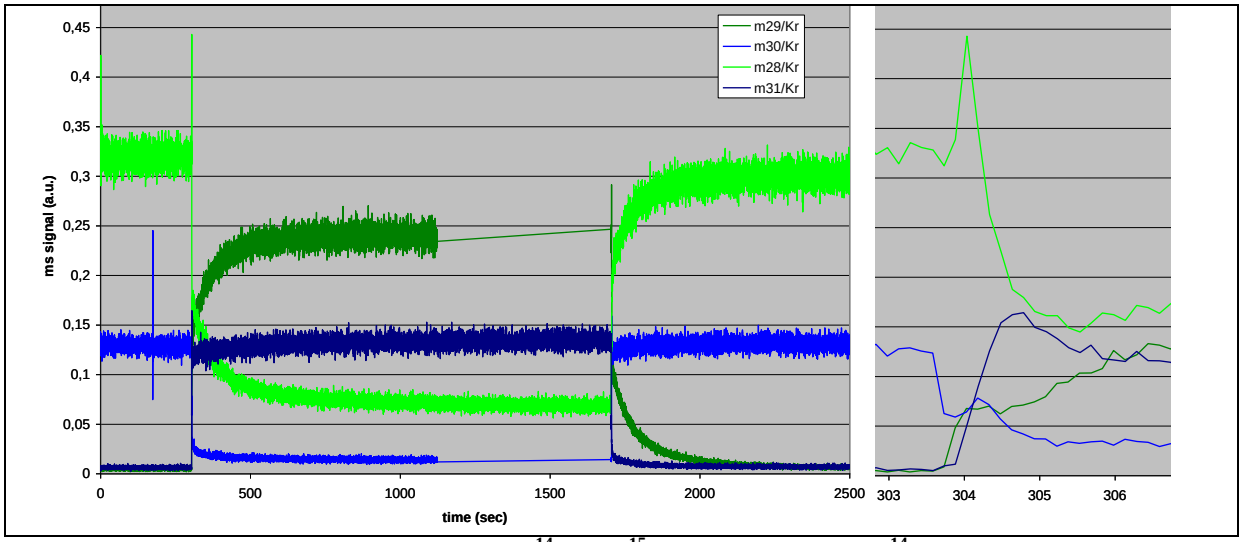

Figure 21. SSITKA experiment. Switch from ^{14}NO to ^{15}NO and then back to ^{14}NO at 199°C.

Various conclusions could be drawn from these experiments:

- H_2/D_2-switch:
  - The time response for the H_2/D_2 switch was fast (changing value in one sample, approx. 150ms), indicating that the accumulated amount of hydrogen on the surface was low and/or the adsorbed hydrogen are very mobile.
  - The production of HD (corresponding to MS signal m3) during D_2 feed (together with NO, NH_3 and O_2) indicates that dissociation of H_2 and NH_3 occurs.
- $^{14}NO/^{15}NO$-switch:
  - The time response for m30/m31 ($^{14}NO/^{15}NO$) was fast indicating there are low amounts of adsorbed NO.
  - The time response for m28/m29 ($^{14}N_2/^{14}N^{15}N$) was slower indicating there are relatively larger amounts of stored NO_X or intermediates that finally become converted to N_2, *i.e.* $^{14}N^{15}N$.
  - Small amounts of N_2O were formed (not shown), but only as $^{14}N^{15}NO$ and $^{15}N_2O$, indicating that production of N_2O may stem from dimerization of NO, since NH_3 can be converted to adsorbed NO (also indicated from the m30 signal during ^{15}NO feed).
  - Almost no production of NO_2 for this catalyst (not shown).

Unfortunately, various experimental problems occurred that made the quantification of the data impossible and further analysis very problematic. However, rough estimates from the $^{14}NO/^{15}NO$ switch gives some interesting findings:

- Assuming 100% dispersion gives a upper limit of the number of Ag sites to be 4.8µmoles[26]
- Approximating the conversion to be 63% and integrating the area of the difference between the m28 and m29 signal and the corresponding steady state level, gives that the amount of stored $^{14}NO_X$ at the switch is approximately 27µmoles[27], i.e. about 5 times more than the number of silver sites, thus indicating the role of the support. This will be further discussed in the next section.

5.4.2. Quantification of spectroscopic data

In order to further investigate the nature of reaction intermediates and the role of "spectators" (adsorbed species, not active in the NO_X reduction), Diffuse Reflectance InfraRed Fourier Transform Spectroscopy (DRIFTS) experiments (see section 2.2.3.2) in combination with SSITKA were also performed. Due to the potentially heavy overlap between spectators and reaction intermediates Multivariate Curve resolution (MCR) using Alternating Least Squares (ALS) was performed (see section 3.2.4).

Objective

The objective was to perform SSITKA experiments in combination with DRIFTS in order to obtain information about reaction intermediates prior to N_2 formation and to characterize these intermediates by the analysis of the IR spectra.

[26] Loading=2%, Dispersion=100%, Mm=107.9g/mole, m=25.7mg

[27] Total molar flow=1mmol/s, 1 adsorbed NO_X gives 1 $N_{2(g)}$.

Experimental

Step responses (including SSITKA) were performed using ^{14}NO and ^{15}NO. No water feed was used in the experiments. The following fixed levels of reactants were used: 1000 ppm NO, 1000 ppm NH_3, 1% H_2, 5% O_2. The catalyst was a 2% w/w Ag/Al_2O_3 (impregnated) sample. The reactor was a DRIFT cell containing approximately 12 mg of catalyst sample as fine particles (<100µm). The DRIFTS reactor was essentially identical to the one described in Figure 3, section 2.2. The IR instrument was a Bruker Vertex 70 with a DRIFTS cell from Spectra Tech. The MS was from HIDEN Analytical (HPR20) with a SEM detector and an ion counter module. Kr was used as internal standard and the MS calibration was performed as described in appendix A, using the sensitivity matrix in Table 3, expanded with the isotopes, but neglecting contributions from $^{15}N_2$, $^{15}N_2O$ and fragment m30 from $^{14}N^{15}NO$. In the figures below only N_2 and NO are displayed for clarity. Generally no NO_2 was observed and only small amounts of N_2O.

Prior to all experiments, the catalyst was pre-treated in oxygen at 450°C for 30 minutes, flushed with Argon and then taken to the relevant experimental temperature. The objective of the pre-treatment was to obtain the catalyst essentially free of adsorbed species. Four different experiments are presented here and used in the MCR evaluation:

1. NO-oxidation: 1000 ppm ^{14}NO+5% O_2 in Ar at 250°C
2. Pulsing of 1000 ppm ^{15}NO in a feed of 1000 ppm $^{14}NH_3$+1% H_2+5% O_2 in Ar at180°C
3. simultaneous pulsing of 1000 ppm^{15}NO + 1000 ppm$^{14}NH_3$ in a feed of 1% H_2+5% O_2 in Ar at 245°C
4. SSITKA of 1000 ppm $^{14}NO/^{15}NO$ switch in a feed of 1000 ppm NH_3+1% H_2+5% O_2 in Ar at 400°C

ALS analysis and results

The four spectral matrices had different sampling frequencies and contained 21, 56, 117 and 119 spectra respectively and were merged forming a 393 x 233 matrix (233 wave numbers from 1650 cm^{-1} to 1200 cm^{-1}).

After analysis of the eigenvalues of a PCA model of the spectral matrix, the effective rank (number of components) was set to 5 and ALS was performed using non negativity for both contributions and pure spectra, see section 3.2.4. Furthermore, for experiment 1, the contributions for component 4 and 5 were set to zero since they represent $^{15}NO_X$ species and no ^{15}NO was used in this experiment. The resulting pure spectra (**S**) for the data sets are shown in Figure 22 and the corresponding contributions (**C**) are shown in Figure 23 - Figure 26.

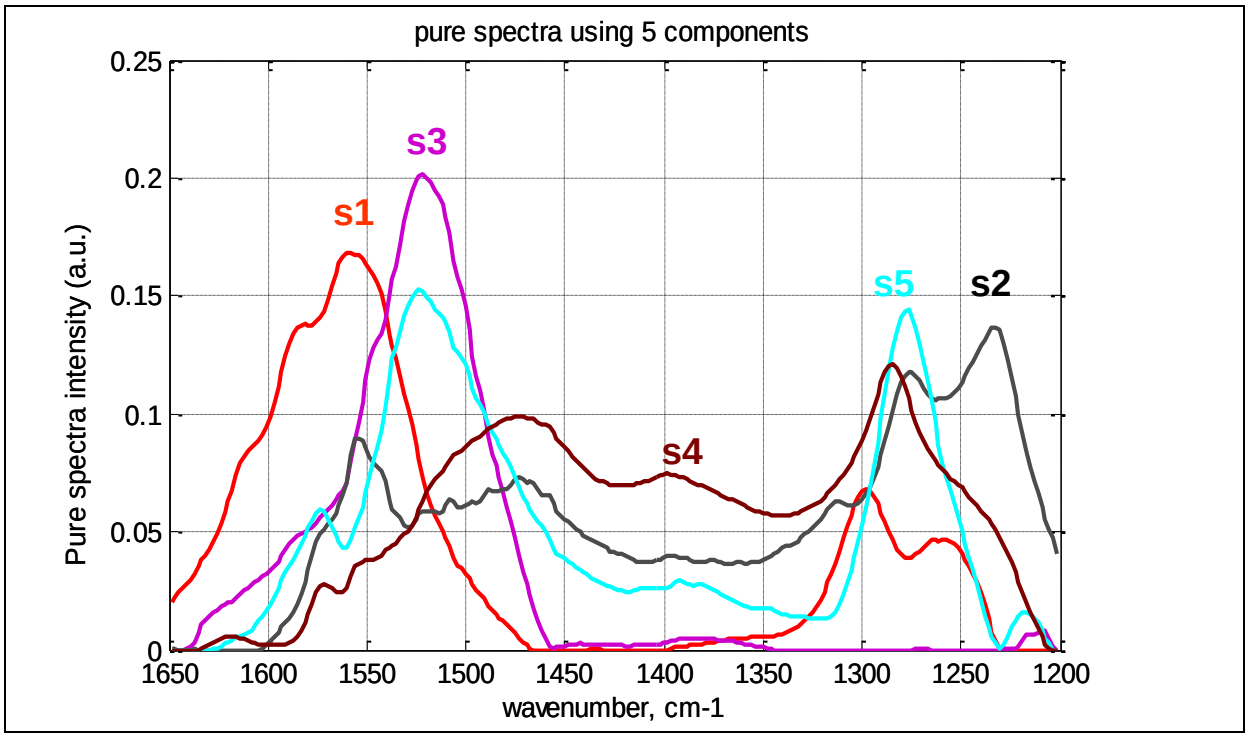

Figure 22. Pure spectra (S) from the ALS using 5 components. Spectra from all 4 experiments were used simultaneously in the analysis. Note the pure spectra have arbitrary units, since S is normalized to unity.

The relevant surface species may be interpreted from the peak positions in the different pure spectra and previous experience. However, due to the high temperatures and to the diversity of different sites at the atomic scale, peak assignment is not trivial [Desikusumastuti 2008]. Still, using the literature we know that adsorbed NO_X is visible in the spectral region displayed in Figure 22. Isotopic peak shifts can also be explained, *e.g.* for s1/s3. Also, since each pure spectrum is associated with a contribution profile, the peaks can be assigned to:

- species associated with ^{14}NO (s1-red, s2-black) and
- species associated with ^{15}NO (s3-purple at 400°C, s4-brown at 180°C and s5-turquoise at 245°C)

The assignments above and further analysis is also enabled by contribution plots. The contribution plots from experiment 1 to 4 are shown in Figure 23 to Figure 26 respectively.

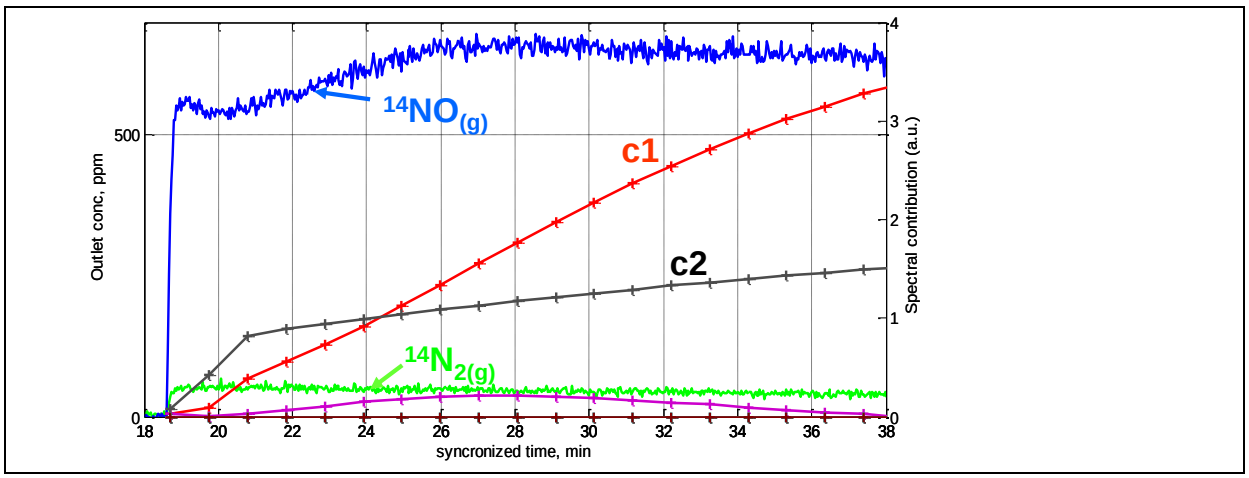

Figure 23. Experiment 1 (NO oxidation at 250°C). Outlet gas phase concentrations together with ALS contributions.

The step in NO feed (as ^{14}NO) shows a clear accumulation of surface species from the gas phase during the first 8 minutes. (The N_2 signal is unfortunately dominated by a leak of air into the ^{14}NO feed pipe.) The step is followed by spectral accumulation of component c1 and c2. Assuming that NO is first oxidized to nitrite and then to nitrate species, it is possible to interpret that c2 would be nitrite and c1 nitrate species. This could also be inferred from Figure 22 where larger the peaks in s1 and s2 correspond to literature values of nitrates and nitrites respectively [Meunier 2000] However, the peak at 1470cm^{-1} is quite broad, indicating a varying surrounding environment for this adsorbate. This broadening may indicate adsorbed NO_X on the alumina support which is contradicting the first interpretation. Together with the analysis of the other experiments, it is thus suggested that c1 should be $^{14}NO_X$ on Ag sites and c2 should be $^{14}NO_X$ on the support.

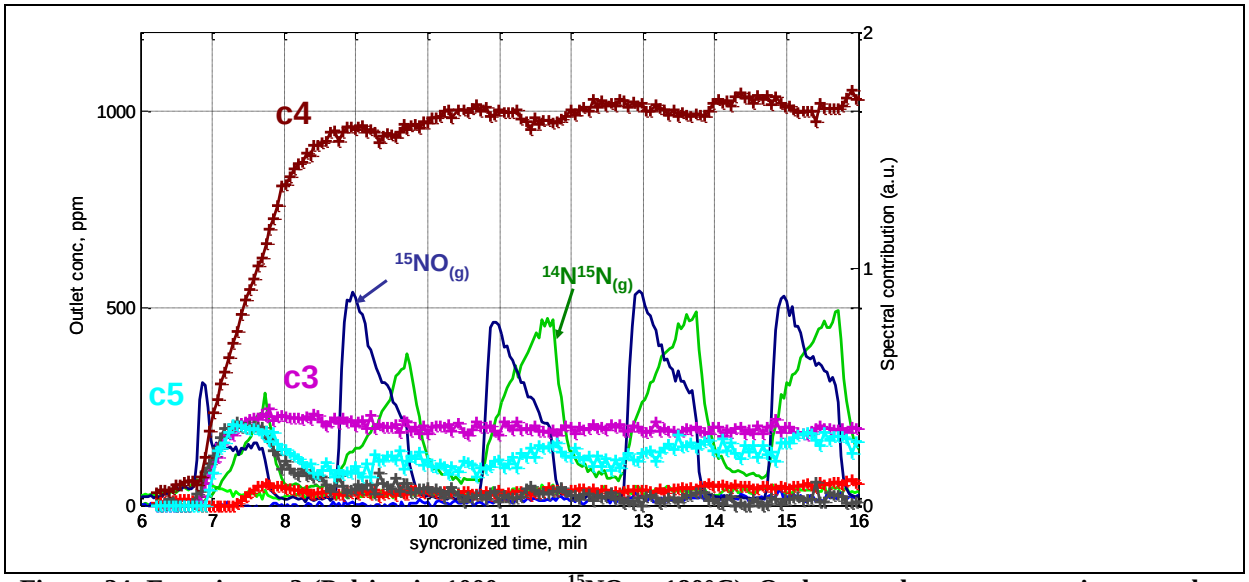

Figure 24. Experiment 2 (Pulsing in 1000 ppm ^{15}NO at 180°C). Outlet gas phase concentrations together with ALS contributions.

In experiment 2, the catalyst was first cleaned by the pretreatment, then NH_3, H_2 and O_2 was added to the stream. As soon as the first peak from ammonia became visible in the DRIFTS, the pulsing of ^{15}NO started (approx at 7 minutes). The plan was to observe reaction intermediates before the accumulation of spectators on the support had grown. This was not possible by visual inspection of the spectra. However, by ALS (which uses linear combinations of all wave numbers simultaneously) the different phenomena can be better separated. The $NO_{(g)}$ is rapidly adsorbed (indicated by the low outlet concentration of $NO_{(g)}$) and the production of N_2 (as $^{14}N^{15}N$) is increasing during the first three steps, reaching a reproducible level after 3 pulses. No signal of m30 (^{14}NO or $^{15}N_2$) is observed and only small amounts of $^{14}N_2$ (m28) indicating that small amounts of NH_3 oxidation occurs.
The formation of N_2 is preceded by accumulation of components c3, c4, c5. Here the interpretation of the peaks is clearer:

- c4 is a large signal, indicating there is a relatively large accumulation of its associated species through out the pulsing experiment. It has broad features at1470cm^{-1} and 1400cm^{-1}, which can be assigned to adsorbed $^{15}NO_X$ on the support (alumina). Note that NH_3 can form ad-NO_X ($^{14}NO_X$) visible as a small peak of c2, which also was visible in the ^{14}NO oxidation experiment 1. This small amount is probably the intermediate for the $^{14}N_2$ production.
- c3 is associated with a species present in much smaller quantities because it reaches a nearly constant level already after the first pulse. It is possibly related to a species on

the silver sites. It has one large peak at 1520 cm^{-1}. Its quite stable time profile suggests it may be associated with a stable species, such as nitrate ($^{15}NO_3^-$). It has been frequently suggested in the literature (*e.g.* paper IV) that these are responsible for poisoning the active sites.

- c5 is also associated with a species present in small quantities with two peaks (at 1525cm^{-1} and 1280cm^{-1}). This feature oscillates with the formation of N_2 around a nearly constant level after already the first pulse. It is thus the species that can be most related to the reaction intermediate, possibly a nitrite (NO_2^-) species.

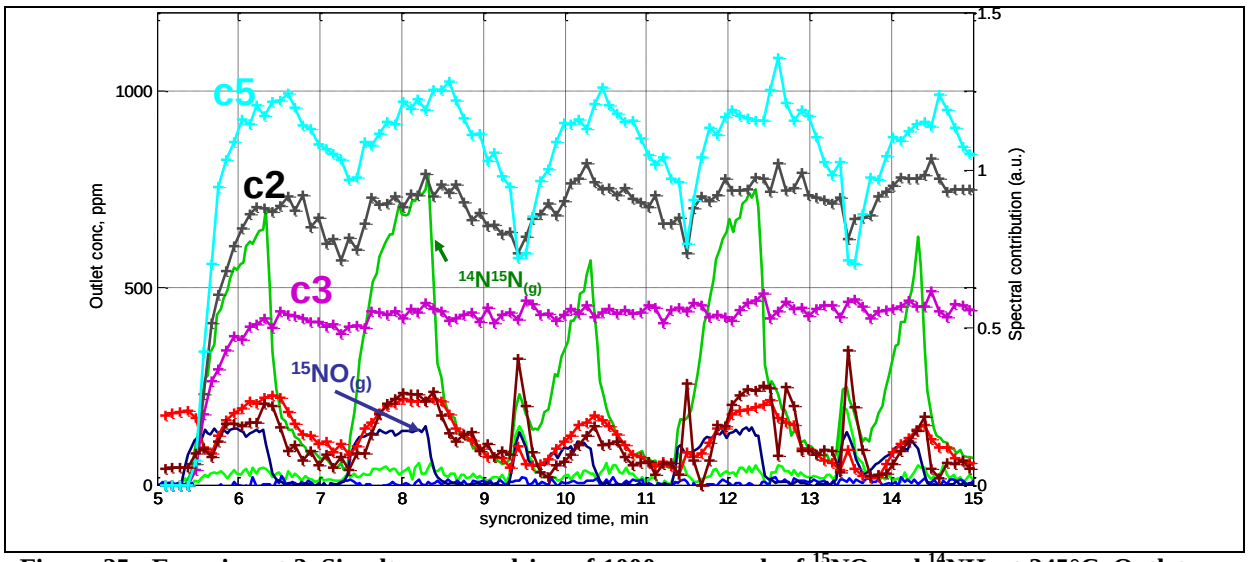

Figure 25. Experiment 3. Simultaneous pulsing of 1000 ppm each of ^{15}NO and $^{14}NH_3$ at 245°C. Outlet gas phase concentrations together with ALS contributions.

In experiment 3, ^{15}NO and $^{14}NH_3$ was co-fed as pulses in a stream of H_2 and O_2. The NO conversion is instantaneously quite high (approx 80%), the $^{14}N_2$ production (from NH_3 oxidation) is small and $^{15}N_2$ production (from ^{15}NO) is negligible. The formation of N_2 (as $^{14}N^{15}N$) is accompanied by all 5 components at different amplitudes, also those corresponding to $^{14}NO_X$. The following constitutes an interpretation of the spectral features and their relation to the reaction mechanism:

- c5 is associated with the dominating species and should therefore be associated with the dominating process, *i.e.* N_2 production (as $^{14}N^{15}N$) c5 is thus associated with the NO_X reduction reaction intermediate.
- c3 ($^{15}NO_X$) and c2 ($^{14}NO_X$) are the features that accumulate and then level out at nearly constant values. They potentially correspond to nitrates that act as "poisons".
- The c4 and c1 are associated with $^{15}NO_3$ and $^{14}NO_3$ on alumina and Ag sites respectively. They are slightly lagged compared to c5 (potential nitrite intermediate), which could indicate that they are nitrates produced as secondary products from the nitrites.
- There is also some negative correlation between c5 and c4 indicated by observations that when c4 increases, c5 correspondingly decreases. This indicates a deviation from a perfect design in the "spectral space". These variations are also correlated with imperfect switching (the $^{15}NO_{(g)}$ doesn't have a "square" shape) due to uneven pressures in the two feed lines.

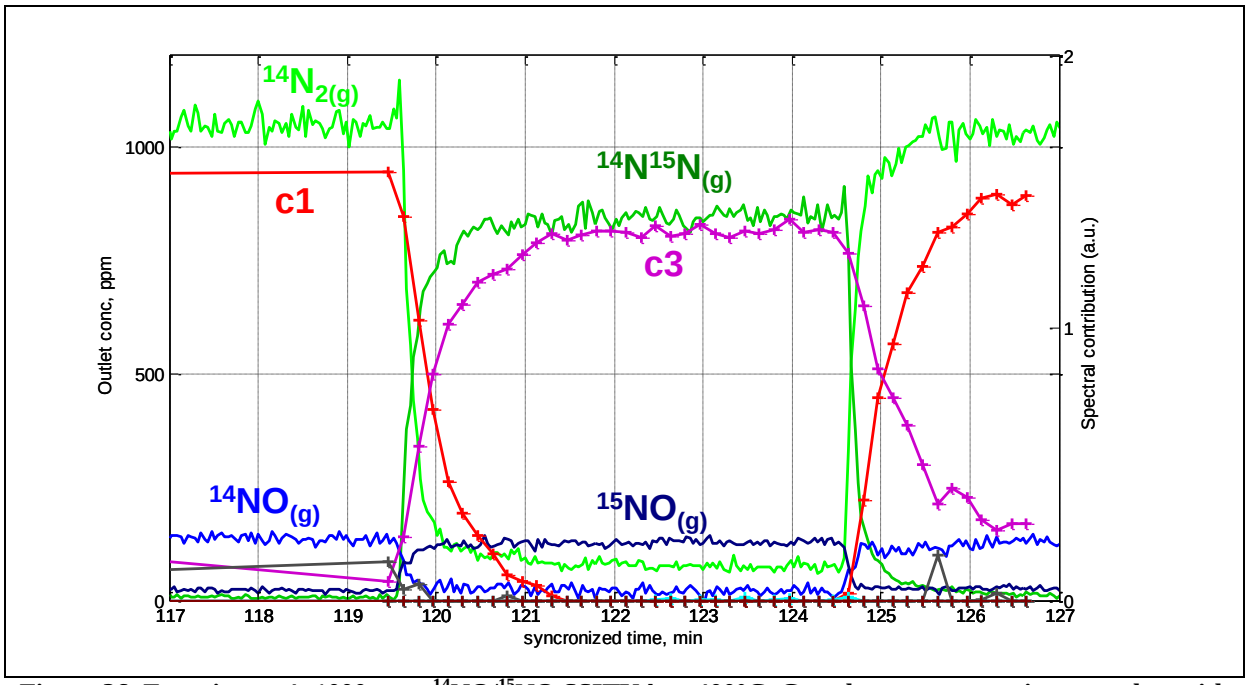

Figure 26. Experiment 4: 1000 ppm $^{14}NO/^{15}NO$ SSITKA at 400°C. Gas phase concentrations together with contributions from ALS.

In experiment 4, a true SSITKA experiment was performed. Due to practical circumstances, this was the only temperature that allowed MCR analysis. The NO conversion is high and the mismatch in N_2 levels ($^{14}N_2$ from ^{14}NO feed vs. $^{14}N^{15}N$ from ^{15}NO feed) are due to NH_3 oxidation as well as contaminants in the ^{14}NO feed. The fact that NH_3 oxidation occurs is indicated by the fact that the $^{14}N_2$ concentration does not reach zero during ^{15}NO feed. The NO levels (^{14}NO vs ^{15}NO) remain rather stable. Due to the high temperature and consequently low coverages and low spectral signals, in the MCR analysis the spectra was multiplied by a factor of 2 to make this experiment have more weight. The interpretations of the contributions are:

- Only c1 and c3 were visible, indicating they correspond to $^{14}NO_3$ and $^{15}NO_3$ on silver sites respectively. Their rate of change is almost as fast as the gas phase production, but still slightly lagging.
- The practical absence of support related species (c2-$^{14}NO_X$ and c4-$^{15}NO_X$) is expected at the elevated temperature of the experiment.
- The absence of c5, the potential intermediate is either due to:
    - The fast reaction making this adsorbate practically having zero coverage, or
    - The MCR deconvolution and imperfect experimental design in spectral space: The reaction intermediate may be confounded with other species (peak positions might be different at higher temperature). Alternatively, potential reaction intermediates may become visible in a later component (*e.g.* component 6 or higher.) However, the eigenvalue-analysis as well as the general conformity of this MCR analysis motivates the choice of 5 components for this data set.

Discussion and Conclusions from the combined MS and ALS analysis

The analysis of the spectral contributions together with the gas phase concentrations reveals a suggested spectral assignment. The corresponding "pure spectra" in Figure 22 are interpreted as follows:

- c1: $^{14}NO_3$-Ag (1560cm^{-1}, 1300 cm^{-1},1260 cm^{-1})

- c2: $^{14}NO_3$-alumina (1555 cm^{-1},1470 cm^{-1}(broad), 1275 cm^{-1},1230 cm^{-1})
- c3: $^{15}NO_3$-Ag (1530 cm^{-1})
- c4: $^{15}NO_3$-alumina (1470 cm^{-1}(broad), 1400 cm^{-1}(broad), 1285 cm^{-1})
- c5: $^{15}NO_X$ (nitrite)-Ag (1570 cm^{-1}, 1525 cm^{-1}, 1280 cm^{-1})

Again it should be stressed that the peak positions and the combinations of peaks, depend on the data set at hand. If the experiments would have been such that the spectral features were purely orthogonal, the analysis would have been unambiguous. However, due to the strong nonlinear system, the experimental errors and the set of experiments for this analysis, the confidence that can be applied to peaks belonging to specific adsorbents is reduced. However, this type of analysis is very useful, since it enables the subsequent discussion, analysis and continuing experiments that could confirm of reject the analysis presented here.

Unfortunately, due to experimental circumstances, spectra were not collected at a high frequency for the SSITKA corresponding to Figure 21. Furthermore, due to contamination of the NO feed (contaminated with air) the quantification of the MS signal became difficult. The list of potential and useful experiments could be made long, but the most important aspects are:

- Repeat similar experiments at different temperatures to investigate peak position dependence on temperature and coverage.
- Repeat all experiments shown here but at the same temperature in order to make the analysis more stringent.

However, the most important conclusion is that the methodology applied here is a viable route for enhanced mechanistic understanding and a practical way to integrate spectral quantification to the modelling toolkit, see also section 5.5 regarding the increase of parameter rank when adsorbates are included.

5.4.3. Paper IV: "Kinetic modeling of selective catalytic reduction of NO_X with octane over Ag-Al2O3"

In parallel to the studies described above, monolith experiments were performed using octane as reducing agent. A detailed kinetic model was developed that included the effect of hydrogen. This addition of hydrogen required the addition of heat balances, since a strong temperature rise was observed. An experimental design was developed and additionally, the transients were included. By selecting switches that included the transition of two variables simultaneously, a more information rich sensitivity should be acquired (compared to the alternative using only transitions of one variable at a time). The steady-state levels were analysed using an MLR model, see Figure 27.

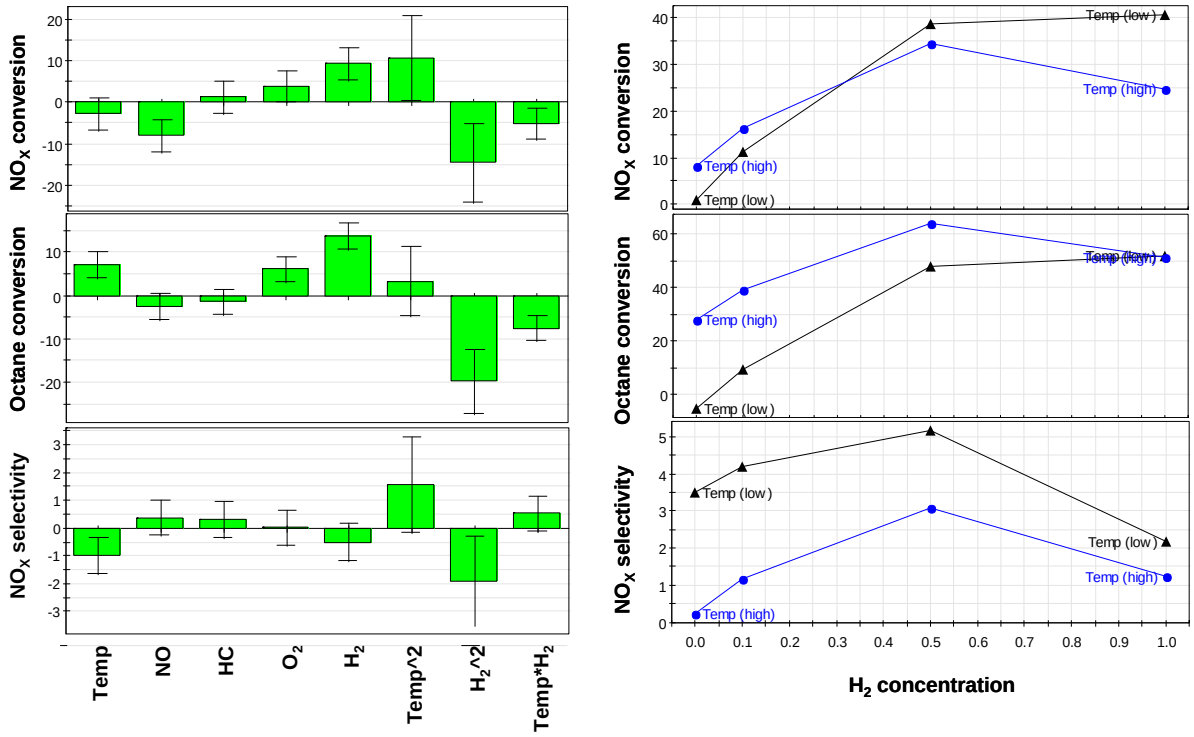

Figure 27. Left: Coefficient plot for the MLR model. Columns are coefficient values with bars indicating 95% confidence intervals. Right: Interaction plots for NO_X conversion, Octane conversion and NO_X conversion selectivity as a function hydrogen concentration at the two temperatures. The explained variance (R2) for the three responses was 0.89, 0.96 and 0.70, respectively.

The conclusions from the steady state data confirm the findings from the literature; see results section in paper IV. Some of these findings included:

- Consumption of NO_2 indicating that if NO is oxidized to $NO_{2(ads)}$, it is further reduced (ev. to form N_2) and does not desorb as NO_2. (not visible from Figure 27.)
- The addition of H_2 increases the NO_X conversion as well as the octane conversion. The "plateau" of the hydrogen effect where NO_X conversion levels out above 0.5% H_2 feed concentration as observed by others. This can be inferred from the coefficient plot (see left part of Figure 27) where H_2 has a positive main effect and a negative quadratic effect. A more clear illustration is made by the interaction plot (see right part of Figure 27).
- Temperature rise due to hydrogen oxidation could only partly explain the hydrogen effect.

The transient experiments were used for parameter fitting, and an acceptable fit was obtained. For further details, see paper IV.

5.5. Thorough assessment of the Model in paper IV

In order to evaluate the effect of different modelling assumptions and also to investigate the sensitivity of these assumptions, different model parameters are evaluated in this section.
As a case study, the model and experimental data of paper IV was chosen. The main reason is because it represents a common model type at KCK: time dependent, several experiments, detailed kinetics and "standard" model assumptions.

Objective

The objective is to illustrate the importance of model parameters as well as model assumptions on the simulation results, both in absolute and relative numbers. The intended outcomes are:

- To highlight the complexity of the task of parameter estimation.
- To give potential reasons for problems commonly encountered during parameter estimation efforts.
- To stress the erroneous assumption about the "model is correct" and the consequences for confidence intervals and other statistical analysis.

5.5.1. Scope of sensitivity analysis

The kinetic mechanism in paper IV is shown in table 1. Note that the reaction mechanism is detailed but not microkinetic, since it has quite a few global, irreversible reaction steps.
Furthermore, the reactor inlet dispersion effect was "modelled" by empty reactor experiments, the number of tanks in series was 15, a film model with a correlation for the Sherwood number from [Tronconi 1992] was used. The pore transport resistance was neglected.

The following parameters and assumptions were investigated:

- Kinetic parameters (22 preexponential factors, 22 activation energies)[28]
- Number of sites (* and #)
- Dispersion effects
    - Inlet conditions (tube dispersion effects)
    - Number of tanks in series (using realistically 25 or computationally fast 3)
- External mass transport resistance (Asymptotic Sherwood number (=3 or 4.4), component diffusivities (D_{AB}) calculated either by Fuller or Chapman-Enskog correlations)
- Temperature effects
    - Heat transfer model
        - bulk-surface: asymptotic Nusselt number (=3 or 4.4)
        - surface-quartz tube (sensitivity for lumped heat transport coefficient value (UA) as well as heat capacity of the quartz tube)
- Numerical effects: Ode-solver (relative and absolute tolerances)

In all, 62 different parameters were assessed. Of course, this list could have been made much longer including other effects such as internal mass transfer resistance, violation of constant

[28] In the mechanism there are 23 reactions, but since r9 is adjusted to the thermodynamics, these parameters are omitted in this study.

molar flow, sensor calibration failure or temperature sensor misplacement etc. But the assessment will be sufficient for the objectives.

	Reaction	Rate Expression
Reactions and rate expressions for adsorption/desorption on site 1 (*).		
1	$NO + * \rightarrow NO*$	$r_1 = k_1 P_{NO*} \theta_*$
2	$NO* \rightarrow NO + *$	$r_2 = k_2 \theta_{NO*}$
3	$O_2 + 2* \rightarrow 2O*$	$r_3 = k_3 P_{O2} \theta_*^2$
4	$2O* \rightarrow O_2 + 2*$	$r_4 = k_4 \theta_{O*}^2$
5	$NO_2 + * \rightarrow NO_2*$	$r_5 = k_5 P_{NO2*} \theta_*$
6[fEa]	$NO_2* \rightarrow NO_2 + *$	$r_6 = k_6 \theta_{NO2*}$
7	$CO + * \rightarrow CO*$	$r_7 = k_7 P_{CO} \theta_*$
8[fEa]	$CO* \rightarrow CO + *$	$r_8 = k_8 \theta_{CO*}$
Reactions and rate expressions for NOx adspecies on site 1 (*)		
9[th]	$NO* + O* \rightarrow NO_2* + *$	$r_9 = k_9 \theta_{NO*} \theta_{O*}$
10[fk, fEa]	$NO_2* + * \rightarrow NO* + O*$	$r_{10} = k_{10} \theta_{NO2*} \theta_*$
11[fk, fEa]	$NO_2* + O* \rightarrow NO_3* + *$	$r_{11} = k_{11} \theta_{NO2*} \theta_{O*}$
12[fk, fEa]	$H_2 + NO_3* \rightarrow H_2O + NO_2*$	$r_{12} = k_{12} \theta_{NO3*} P_{H2}$
Reactions and rate expressions for surface reactions on site 1 (*)		
13[fk, fEa]	$C_8H_{18} + O* + 7* \rightarrow 8CH_2* + H_2O$	$r_{13} = k_{13} P_{oct} \theta_{O*}^2 \theta_*$
14[fk, fEa]	$CH_2* + 2NO_2* \rightarrow N_2 + CO* + 2O* + H_2O$	$r_{14} = k_{14} \theta_{CH2*} \theta_{NO2*}$
15[fk, fEa]	$CH_2* + 2O* \rightarrow CO* + 2* + H_2O$	$r_{15} = k_{15} \theta_{CH2*} \theta_{O*}$
16[fk, fEa]	$CO* + O* \rightarrow CO_2 + 2*$	$r_{16} = k_{16} \theta_{CO*} \theta_{O*}$
Reactions and rate expressions for adsorption/desorption and oxidation reactions on site 2 (#)		
17	$O_2 + 2\# \leftrightarrow 2O\#$	$r_{17} = k_{17} P_{O2} \theta_\#^2$
18	$2O\# \rightarrow O_2 + 2\#$	$r_{18} = k_{18} \theta_{O\#}^2$
19	$NO_2 + \# \rightarrow NO_2\#$	$r_{19} = k_{19} P_{NO2} \theta_\#$
20[fEa]	$NO_2\# \rightarrow NO_2 + \#$	$r_{20} = k_{20} \theta_{NO2\#}$
21[fk, fEa]	$C_8H_{18} + 25\ O\# \rightarrow 8CO_2 + 25\# + 9H_2O$	$r_{21} = k_{21} P_{oct} \theta_{O\#}$
22[fk, fEa]	$C_8H_{18} + 25NO_2\# \rightarrow 8CO_2 + 25NO + 9H_2O + 25\#$	$r_{22} = k_{22} P_{oct} \theta_{NO2\#}$
23[fk, fEa]	$H_2 + O\# \rightarrow H_2O + \#$	$r_{23} = k_{23} \theta_{O\#} P_{H2}$

Table 1. Reaction mechanism in paper IV. Reaction number indicated by "f" was included in fitting and "th" was used for thermodynamic constraint ($NO_{(g)}+½O_{2(g)}\rightarrow NO_{2(g)}$).

5.5.2. Assessment, experimental

The assessment was a "straight forward" sensitivity analysis, this time using adjusted or normalized sensitivity similar to equation 47:

$$\mathbf{S}_{adj}(\mathbf{y},\boldsymbol{\beta},t) = \frac{3*conf(\boldsymbol{\beta})}{\mathbf{y}_{level}} \frac{\partial \mathbf{y}}{\partial \boldsymbol{\beta}} = \frac{\Delta \boldsymbol{\beta}}{\mathbf{y}_{level}} \mathbf{s}_{local}(\mathbf{y},\boldsymbol{\beta},t) \qquad (53)$$

The local sensitivity was adjusted by y_{level} which simply involved the multiplication of all mole fractions with 10^6 so temperatures (in Kelvin) and concentrations (in ppm) became comparable. The confidence intervals were calculated using eq. (44) and only considering parameters 1-56 since the last parameters are not adjustable in the same way as the other. The local sensitivity was also adjusted by three times the confidence intervals. This enables the sensitivities of different parameters to be compared, *e.g.* activation energy vs tanks-in-series.

The sensitivities were calculated compared to the reference case (paper IV) by the finite difference method. The parameters were changed as follows:

- The kinetic parameters as shown in Table 1: kref was changed 4.6% and Ea was changed 0.7kJ/mole.
- The number of sites (* and #) were changed by 1%.
- The asymptotic Sherwood number was changed by 1.4 from 3.0 (square channel) to 4.4 (corresponding to a circular channel).
- The lumped heat transfer coefficient to the quartz tube, UA was changed by 10% and the heat capacity of the monolith was also changed by 10%.
- The binary diffusivities originally using the Fuller correlation was changed to simulate the use of the Chapman-Enskog equation corresponding to a change of approx 5%.
- Also two different number of tanks-in-series were evaluated, ntank=25 (theoretically more correct) and ntank=3 (sometimes used in practice for numerical speed).
- The tolerances in the ode solver (ode15s in MATLAB) was also investigated as a comparison: Relative tolerance was changed from 10^{-5} to 10^{-3} and absolute tolerance was changed from 10^{-7} to 10^{-5}.
- The reactor inlet conditions in paper IV was based on empty reactor measurement data. This approach assumes that all dispersion effects occur upstream the reactor and no dispersion downstream (*e.g.* in the detectors). Three different scenarios were investigated: SA1: Sensitivity when no dispersion effect was assumed, SA2: Sensitivity when all dispersion effects occur downstream the reactor and no dispersion upstream, SA3: When half the dispersion was placed upstream and half the dispersion downstream.

This sensitivity is time dependent and the experimental data consisted of 5 transient experiments, resulting in 26.025 time points. For each time point there were 5 measured signals (Temp, NO, NO2, CO, CO2) and with the 62 parameters this gives a 3-way matrix with 8×106 numbers. In order to summarize this matrix, different figures of merit were calculated for every parameter and different responses. The following figures of merit were calculated (column headings in Table 2 in parenthesis)

- Confidence intervals
  - The confidence interval if All adjustable parameters were considered (conf_all)
  - The confidence intervals calculated in paper IV (conf_pIV)
- Standard deviation (deviation from zero, a root mean square value) of the adjusted sensitivity for all 5 responses.(S_{std}_x, x=T, NO, NO_2, CO, CO_2)
- For NO, further numbers were calculated:
  - The standard deviation of adjusted sensitivity at transients (S_{std}_Tr_NO)
  - The most extreme adjusted sensitivity ($S_{extreme}$_NO)
  - The average of the adjusted sensitivity, keeping the sign (S_{avg}_NO)
  - The most "similar" (correlated to S_{std}_NO) parameters (most correlated NO).
  - The 2nd most "similar" parameters (2nd most correlated_NO)

The results are presented in Table 2.

Parameter name	parameter value	conf_ all	Conf_ pIV	S_{std_T}	S_{std_NO}	S_{std_NO2}	S_{std_CO}	S_{std_CO2}	$S_{std\_Tr\_NO}$	$S_{extreme\_NO}$	S_{avg_NO}	Most correlated NO	2nd most correlated NO
ln(kref1)	13.57	1.5		4	20	5	13	122	48	433	6	0.948 (S_NO__k02)	0.664 (S_T___k02)
ln(kref2)	4.75	1.7		2	18	5	5	59	50	-485	-7	0.948 (S_NO__k01)	0.745 (S_NO__Ea01)
ln(kref3)	13.52	1.6		11	101	30	76	414	131	726	72	0.913 (S_NO__k14)	0.801 (S_CO__Ea08)
ln(kref4)	-1.55	0.6		3	38	21	17	107	58	-191	-18	0.923 (S_NO__Ea04)	0.861 (S_NO__Ea05)
ln(kref5)	13.34	0.8		13	118	13	58	501	159	796	6	0.990 (S_NO__k06)	0.860 (S_NO__Ea05)
ln(kref6)	5.88	0.4		9	68	15	36	341	86	-458	-13	0.991 (S_NO__Ea06)	0.990 (S_NO__k05)
ln(kref7)	13.58	5.5		14	38	7	687	856	47	-488	-2	0.999 (S_NO__k16)	0.997 (S_NO__k08)
ln(kref8)	9.34	5.4		14	39	7	703	878	48	504	3	0.997 (S_NO__k07)	0.996 (S_NO__Ea08)
ln(kref10)	12.34	1.0	0.10	5	22	22	28	179	37	241	2	0.747 (S_NO__k15)	0.682 (S_NO__Ea10)
ln(kref11)	7.96	0.3	0.07	11	73	14	32	392	71	506	48	0.979 (S_NO__k12)	0.897 (S_CO2_Ea17)
ln(kref12)	-0.02	0.2	0.09	12	66	10	42	397	68	-522	-40	0.979 (S_NO__DH2)	0.843 (S_CO2_Ea17)
ln(kref13)	14.06	0.6	0.07	20	132	20	90	744	135	-1033	-63	0.983 (S_NO__DH2)	0.888 (S_NO__Ea08)
ln(kref14)	5.57	0.3	0.06	8	72	9	35	318	97	-412	-52	0.913 (S_NO__k03)	0.778 (S_NO2_DO2)
ln(kref15)	2.29	0.3	0.28	5	39	7	15	172	38	315	21	0.972 (S_NO__k13)	0.879 (S_NO__Ea08)
ln(kref16)	9.29	8.7	0.05	22	60	11	1089	1362	75	-779	-4	0.999 (S_NO__k07)	0.997 (S_NO__Ea08)
ln(kref17)	13.52	5.8		30	77	85	54	1021	98	403	-43	0.998 (S_NO__k19)	0.997 (S_NO__Ea17)
ln(kref18)	-1.55	1.5		6	19	21	11	222	23	-73	12	0.992 (S_NO__k20)	0.959 (S_NO__Ea17)
ln(kref19)	13.34	2.9		30	78	85	55	1030	100	-394	45	0.998 (S_NO__k17)	0.994 (S_NO__Ea17)
ln(kref20)	5.73	4.7		40	119	133	66	1365	145	441	-71	0.999 (S_NO__k22)	0.992 (S_NO__k18)
ln(kref21)	-2.01	1.3	0.02	29	41	12	29	979	77	355	17	0.983 (S_NO__Ea21)	0.855 (S_CO__Ea19)
ln(kref22)	7.18	4.5	0.30	38	114	126	64	1302	138	-407	68	0.999 (S_NO__k20)	0.991 (S_NO__k18)
ln(kref23)	-0.39	1.3	0.04	56	146	23	46	475	177	-1266	32	0.981 (S_NO__N2)	0.863 (S_NO__k04)
Ea01	0.00	67.6		1	10	3	3	20	35	-347	-4	0.838 (S_NO__Ea02)	0.340 (S_CO__Ea02)
Ea02	120.00	80.1		1	10	2	2	26	41	417	2	0.866 (S_NO__k02)	0.838 (S_NO__Ea01)
Ea03	0.00	83.0		6	83	25	66	158	134	406	48	0.957 (S_NO__Ea14)	0.814 (S_CO__Ea13)
Ea04	150.00	40.9		3	68	23	15	65	98	-282	-35	0.948 (S_NO__Ea23)	0.931 (S_NO__Ea05)
Ea05	0.00	43.3		5	125	12	31	133	180	-469	-39	0.931 (S_NO__Ea04)	0.861 (S_NO__k04)
Ea06	114.60	2.3	0.49	11	81	17	39	411	97	551	20	0.991 (S_NO__k06)	0.982 (S_NO__k05)
Ea07	0.00	108.7		3	14	3	298	291	18	88	5	0.991 (S_NO__Ea16)	0.922 (S_NO__Ea05)
Ea08	98.13	24.7	1.44	12	33	6	579	743	41	-433	-4	0.997 (S_NO__k16)	0.996 (S_NO__k08)
Ea10	278.80	44.1	3.02	1	7	5	11	48	21	161	0	0.682 (S_NO__k10)	0.419 (S_NO2_DO2)

Table 2. Various figures of merit from the Sensitivity analysis of the parameters in paper IV.

Parameter name	parameter value	conf_ all	Conf_ pIV	S_{std_T}	S_{std_NO}	S_{std_NO2}	S_{std_CO}	S_{std_CO2}	$S_{std\_Tr\_NO}$	$S_{extreme\_NO}$	S_{avg_NO}	Most correlated NO	2nd most correlated NO
Ea11	182.80	23.8	2.10	4	72	12	22	155	90	417	42	0.965 (S_NO__Ea12)	0.943 (S_CO2_Ea18)
Ea12	44.49	9.3	2.73	3	26	2	8	58	31	-127	-13	0.965 (S_NO__Ea11)	0.884 (S_T___Ea20)
Ea13	207.70	51.8	1.70	13	108	23	90	318	124	436	-12	0.932 (S_NO__Ea15)	0.793 (S_NO__Ea05)
Ea14	12.68	9.1	1.95	1	38	2	4	33	60	-177	-23	0.957 (S_NO__Ea03)	0.852 (S_NO__k04)
Ea15	2.19	20.1	1.78	7	23	3	14	186	32	-141	7	0.932 (S_NO__Ea13)	0.746 (S_CO2_Ea05)
Ea16	212.10	109.0	2.64	3	14	3	300	293	19	84	5	0.991 (S_NO__Ea07)	0.922 (S_NO__Ea05)
Ea17	0.00	35.8		37	89	100	69	1273	117	-497	49	0.997 (S_NO__k17)	0.959 (S_NO__k18)
Ea18	150.00	72.2		4	23	21	7	132	25	97	13	0.996 (S_NO__Ea22)	0.993 (S_NO__Ea19)
Ea19	0.00	40.7		4	27	24	8	156	30	99	16	0.993 (S_NO__Ea18)	0.873 (S_NO2_Ea04)
Ea20	115.30	98.0	1.47	10	64	56	20	360	70	-230	-38	0.998 (S_NO__Ea22)	0.990 (S_NO__Ea19)
Ea21	71.67	1.7	0.75	1	1	0	1	34	2	9	1	0.983 (S_NO__k21)	0.872 (S_CO__Ea19)
Ea22	0.00	103.5	1.78	11	67	59	21	382	74	258	40	0.998 (S_NO__Ea20)	0.992 (S_NO__Ea19)
Ea23	9.32	3.7	1.26	3	10	1	2	11	11	36	5	0.948 (S_NO__Ea04)	0.923 (S_NO__Ea05)
N1	0.03	2E-03	9E-04	4	19	4	11	116	22	-141	-14	0.923 (S_NO__k11)	0.809 (S_CO2_Ea17)
N2	0.06	0.09		86	203	39	86	1429	268	-1390	69	0.981 (S_NO__k23)	0.909 (S_NO__k04)
Sha	3.00	3.0		4	21	4	9	132	21	-201	-11	0.987 (S_NO__DH2)	0.862 (S_NO2_DNO)
UA	0.01	4.8E-03		1	4	0	2	18	7	-50	0	0.975 (S_NO__nt25)	0.929 (S_NO__k05)
cppipe	754.00	21.9		1	3	0	1	11	7	-52	0	0.573 (S_NO__DCO2)	0.378 (S_NO__k08)
DNO	6,2E-05	1.0E-04		1	4	2	6	62	8	82	-1	0.732 (S_NO__k23)	0.654 (S_NO__k08)
DO2	6,2E-05	5.0E-04		1	3	1	1	10	4	61	0	0.610 (S_NO__Doct)	0.524 (S_NO__Ea08)
Doct	1,7E-05	1.4E-05		4	19	5	9	151	21	-208	-6	0.960 (S_NO__k13)	0.916 (S_NO__k08)
DH2	2,4E-05	7.4E-05		13	52	9	27	297	51	-450	-26	0.987 (S_NO__Sha)	0.864 (S_NO__Ea08)
DCO	6,1E-05	2.1E-04		0	1	0	8	10	3	25	0	0.546 (S_NO__k16)	0.542 (S_NO__Ea08)
DCO2	4,6E-05	5.2E-04		1	3	0	0	9	8	66	0	0.573 (S_NO__cppipe)	0.481 (S_NO2_DCO2)
DNO2	4,2E-05	5.9E-05		0	2	2	1	7	2	-10	0	0.815 (S_NO2_N1)	0.714 (S_NO2_DNO2)
nt25				0	11	1	8	65	15	128	2	0.975 (S_NO__UA)	0.910 (S_NO__k05)
nt03				0	17	3	5	69	20	-100	-7	0.848 (S_NO__nt25)	0.825 (S_T___Ea17)
RelAbsTol				0	0	0	0	0	0	5	0	0.583 (S_NO2_RelAbsTol)	0.273 (S_CO_RelAbsTol)
SA1				0	10	1	1	9	47	-482	0	0.556 (SA3_NO)	0.486 (SA1_CO)
SA2				0	2	1	0	3	9	96	0	0.532 (SA3_NO)	0.115 (SA1_CO)
SA3				0	2	1	0	2	8	-116	0	0.556 (SA1_NO)	0.532 (SA2_NO)

The sensitivity can also be assessed by means of LV models (as in paper II and III). As an example the two first components of a PCA model of the local sensitivity is displayed in Figure 28 (scores plot) and Figure 29 (loadings plot)

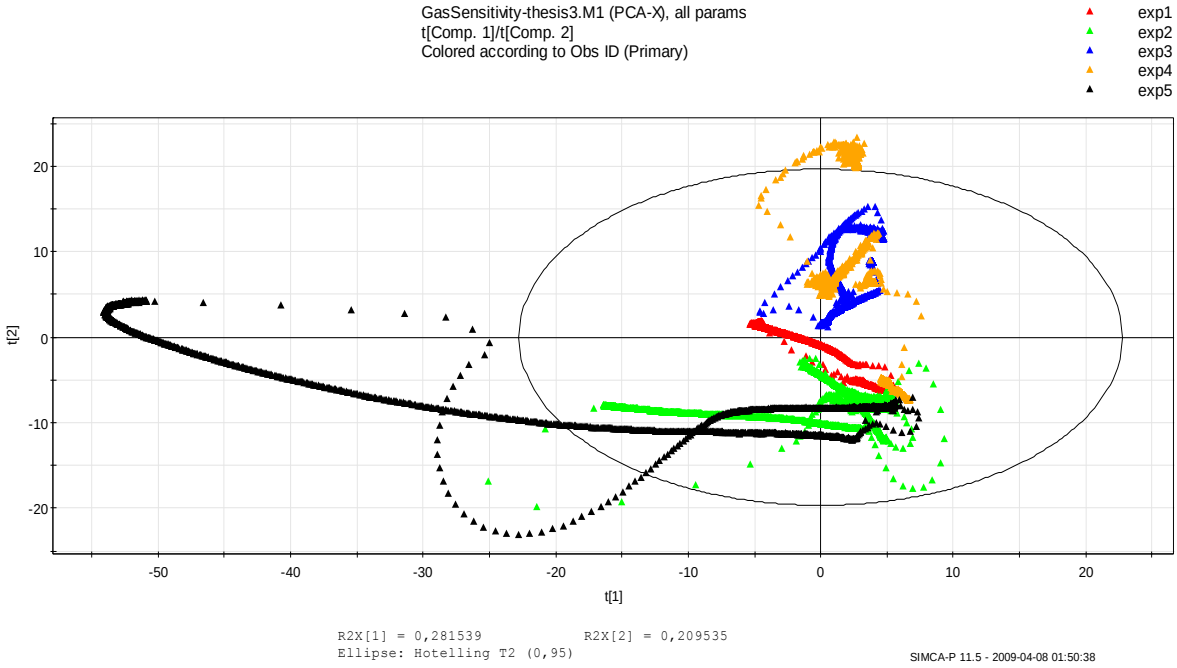

Figure 28. A scores scatter plot of the first 2 components of a PCA model with 25 components.

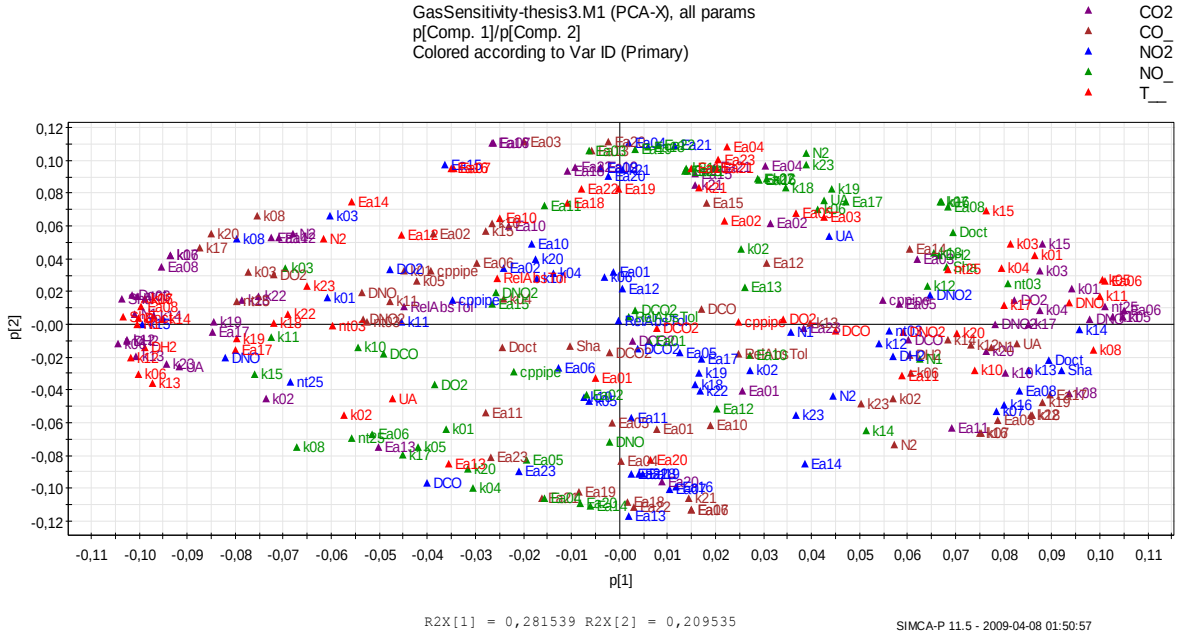

Figure 29 A loadings scatter plot of the first 2 components of a PCA model with 25 components.

5.5.3. Results and discussion

There are numerous analyses possible, all depending on the objective. Here are a few comments on some of the numbers in Table 2:

- The confidence intervals increased by one order of magnitude when assessing 56 parameters instead of 24 parameters. This is expected since the many parameters are highly correlated. At this point, a simple analysis of the Lack-of-Fit gives that the

average residual was 65 ppm, where as the visible noise in the detectors is of the order of one ppm (!), thus the lack of fit is huge and any further assessment of the confidence intervals should be avoided. However, the analysis of the relative sizes of the confidence intervals gives information about how sensitive a parameter is, *i.e.* if a parameter has a small confidence interval, it is accurately determined and this implies that the parameter is probably involved in a rate limiting step at some point during the experiments.

- The sensitivities for different responses have different standard deviations. S_{CO2} has on average 337 ppm where as S_{NO2} has only 19 ppm. This is due to the low levels of NO2 and the dominating process of CO_2 formation from several reactions in the mechanism.
- The different parameters have different sensitivities. The highest standard deviation on average was kref16 (CO oxidation). This is because CO* is formed from several reactions.
- The extreme sensitivities are quite high compared to averaged sensitivities. This indicates the importance of transients in parameter fitting.
- The highest correlations are naturally with the responses to the same signal (NO in this case) and also fast reversible reactions are correlated, *e.g.* r1/r2
- The sensitivity of the asymptotic Sherwood number as well as the sensitivities of binary diffusivities are quite high, especially for extreme sensitivities. This indicates that mass transfer limitation prevail, especially during the transients.
- The sensitivity for the ode solver was low. This indicates that the solver is stable and gives similar results even if the tolerances are changed to gain computational speed.
- The reactor dispersion effects are only comparable in size with the kinetic parameters for the most extreme cases. Thus the effect of adjusting dispersion effects during parameter fitting will probably be small if one uses standard residual sums of squares as the objective function. (The extreme point will have a small leverage because the majority of data points are not during the transients). However, to correctly capture transient spikes, the reactor dispersion effects should be taken into account.

The analysis of LV models can also be extensive, and only a few comments are given here:

- The adjacent points in the scores plot are similar since they are adjacent in time. Different experiments have different "excursions" in the scores plot. Experiment no 5 is clearly the most important experiment for the first component.
- The loading plot shows which parameters (and sensitivities) are similar (correlated). As an example, in the left end of the loading plot (first component) are the sensitivities for CO_2 and Temperature. This is also quite natural since CO_2 production is tightly connected with exotherms.
- The number of components in this PCA model was 25 (size of sensitivity matrix was 26025 x 307) indicating 25 linearly independent phenomena that is manifested in the sensitivity data. However, when performing a PLS of Sensitivity as X and the residual (the objective function) as Y, only 14 components is obtained. This means that 11 dimensions of sensitivity are not really connected to the residual, which is what we try to minimize. Thus, even if we could use 25 parameters to span the sensitivity space, only 14 parameters will be useful (assuming that the other parameter values can be considered as valid). This analysis can be very important when considering different fitting schemes, given that the computations often take many hours. The corresponding models using only the sensitivities for the 24 fitted parameters in paper IV, gave 18 components for a PCA model and 13 for a PLS model using the residuals as Y.

- Of course the methodology applied in paper II (parameter fitting) and paper III (experimental design) could be applied to this sensitivity matrix. However, this is beyond the scope of this assessment.

5.5.4. Analysis of additional surface coverage sensitivities

During the computations of all sensitivities, also the surface coverage sensitivities were stored. The sensitivities for temperature, measured gas phase species (NO, NO_2, CO, CO_2) and adsorbed NO_X (NO_2* and NO_3*) were analysed together[29]. Only the 23 kinetic parameters fitted in paper IV was included. This resulted in 23*7=161 sensitivities and 26025 observations as usual. A PCA model was made and the number of components was 24. A corresponding model excluding the sensitivities for the adsorbed species was only 18.
This means that if surface specie concentration data would be accessible, the parameter estimation would be enhanced by the additional 6 independent components. A suggested methodology for the quantification is given in section 5.4.2.

5.5.5. Conclusions

Many different parameters were assessed and analysed by means of summary numbers as well as LV models. Some sensitivities were quite small: reactor dispersion, ode solver tolerances and some binary diffusivities. This means that these parameters are not critical for the fit to experimental data. However, some model parameters that usually are not considered for fitting showed big sensitivities. These parameters were associated with mass transfer during transient (ex diffusivity for H_2, asymptotic Sh). This means that improvement for mass transfer should be considered in this case.

By analysing the sensitivity matrix by mean of a PCA model, the number of significant components could be used as a measure of how many parameters that is adequate to fit using the experiment and parameter values at hand. It was shown that 14 parameters could adequately be fitted, considerably less than the 24 parameters fitted in paper IV. However, if surface species would have been available, the number of components increased and the number of kinetic parameters suitable for fitting would increase.

[29] There are 10 different coverages in the mechanism, but some are never possible to quantify (empty sites and mono-atomic adsorbates) and e.g. CH_2* is a lumped expression that doesn't correspond to a defined quantity. The two included NO_X species represent a realistic scenario if surface coverage quantification would be performed.

6. DISCUSSION

"Only after completing the composition planned have we learned what the beginning should have been." - Blaise Pascal

During the modelling cycle, several issues can be encountered as shown in Figure 30.

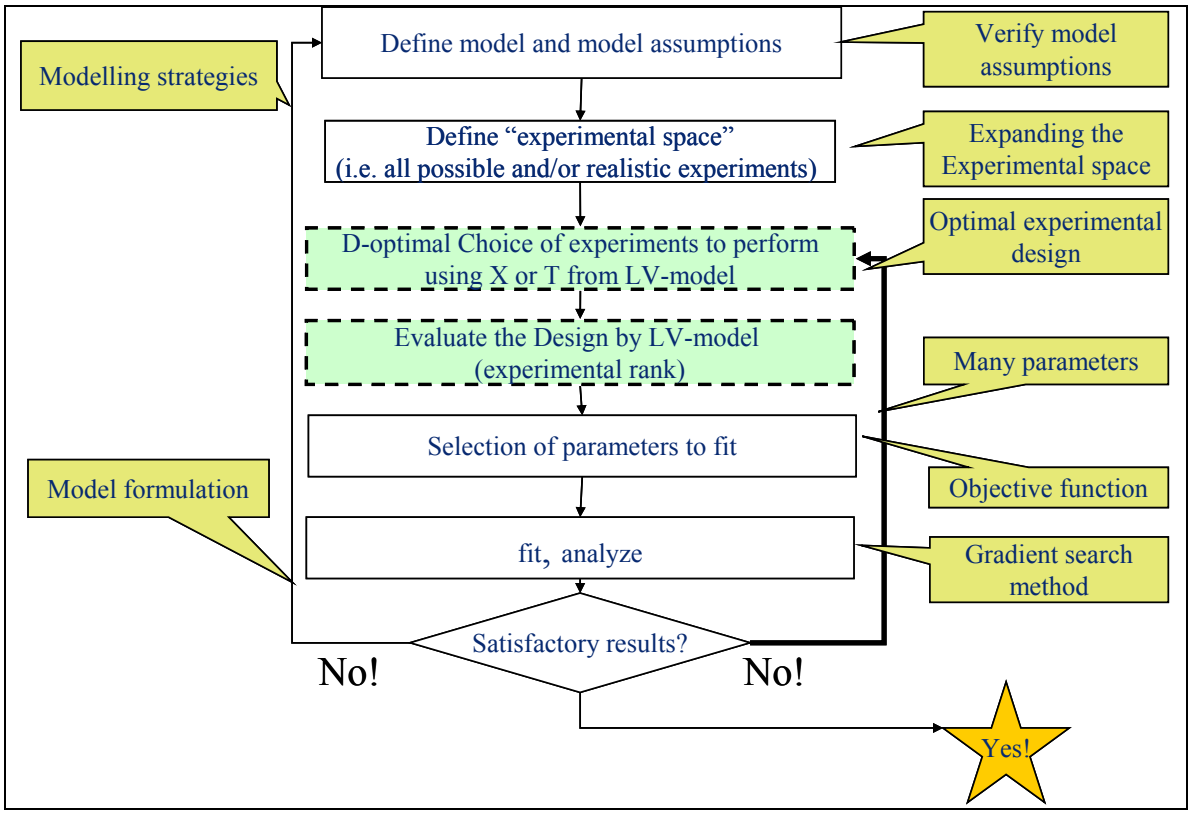

Figure 30. The modelling cycle and some of the tasks involved.

The figure is extended in scope compared to fig.1 in Paper III. Also, note that this illustration is not intended to be complete, it reflects the issues encountered during this PhD project. The aspects indicated will be more discussed in the subsequent paragraphs.

6.1. Different modelling strategies

The base modelling strategy during this PhD project has been the microkinetic approach [Dumesic 1991]. The microkinetic approach stems from the assumption that each individual reaction parameter in a large reaction mechanism can be estimated by using independent methods such as independent experiments or theory. The ingredients for successful modelling using microkinetics include:

- The pressure/material gap can be bridged by the use of ultra-high vacuum experimentation. However, this will not be possible if the metal particles/clusters interact with its support, which is the case for all systems studied in this thesis.[Bond 2008]
- The system is operated under steady state conditions, where most of the reactions never will be rate limiting. In this case, these kinetic parameters only need to be such

that they do not interfere with the rate limiting step, see *e.g.* [Mhadeshwar 2003]. In all systems targeted for emission control for vehicle applications, the system will very seldom be operated exclusively under steady state conditions, thus requiring the assessment of almost every step in the reaction mechanism.

Instead of using the bottom-up approach (microkinetic approach), one could envisage a top-down approach. One interesting framework for this approach is the MEXA (Model-based EXperimental Analysis) developed by the group of Marquardt [Marquardt 2008]. In this approach, the mechanism is developed from what is observable (*i.e.* measurements) and by iterative refinements, a plausible mechanism can be derived. However, the applications are often systems, in which the reaction intermediates are quantifiable in some way, *e.g.* batch reactor with in-line detectors. Applications to gas-solid heterogeneous catalytic reactors are still lacking. The challenge for the MEXA approach applied to NO_X reduction systems is probably the quantification of adsorbed reaction intermediates. The microkinetic approach however, offers some potential benefits including the possibility of extrapolation of kinetic parameter values to other systems. This aspect (as well as many other arguments) makes the microkinetic approach an attractive route to deeper understanding.

6.2. Model formulation: Mean field approximation

One potential problem is the mean field approximation itself. The benefit is that it enables the concept of "surface concentration" or "coverage", which is very convenient from a numerical perspective. One alternative would be more atomistic approaches *e.g.* Monte Carlo simulations [Olsson 2003] but at the price of computational time. When we have different types of sites, one can use different mechanisms on the different types of sites as in paper IV. One can also model the interplay between different sites as a "spill-over" reaction [Olsson 2002b, paper II] or as a diffusion process [Holmgren 1999]. Another way to mitigate the limitations of the mean field approximation is to introduce different neighbouring sites that can only react with each other [Sjövall 2009]. To conclude, the mean field approximation offers numerical benefits but has limitations when the catalytic surface is not a "field" (as for a crystal plane of Pt(111)). This limitation can be mitigated in several ways but has no "easy" universal solution. This phenomenon is another example of the famous "materials gap" in heterogeneous catalysis [Stoltze 1985] which hopefully can be bridged in the future.

6.3. Verifying model assumptions

During research aimed at increased understanding of heterogeneous catalysis, the experimental focus is often directed towards the "final application", *e.g.* NSR experiments similar to what will occur on a vehicle. The problem lies in the objective of this experiment which is not the same as the modelling objective to understand the phenomena using a mathematical model. Indeed, one can argue that if the application is NSR, then these are the experiments to be conducted. However, when drawing mechanistic conclusions (and thus increased understanding) using a model (being mathematical or conceptual), the basic assumptions will always need to be confirmed, or if necessary, the model needs to be adjusted accordingly. In section 5.5 the impact of model assumptions such as the Sherwood number and binary diffusivities were investigated. The indication that the actual numbers need to be accurately estimated may render some further investigations.

Other assessments of model assumption can be made by independent experiments, *i.e.* targeted experiments for different objectives, *e.g.*

- Varying the reactor design (different washcoat loadings, packed bed reactors, etc.) to induce different mass/heat transfer conditions
- Varying the heating rates during temperature ramped experiments (TPD, TPR [Anderson 2005, Kasuya 1995]) not only for accurate estimation of activation energies but also to assess assumptions about mass/heat transfer resistance, coverage dependent activation energies for desorption or the reaction mechanism itself, see *e.g.* [Deshpande 2005].

It is of course important that any independent experiment does not introduce any further "gap" (pressure-, temperature- or materials gap) that cannot properly be handled.

6.4. Expanding the experimental space

To achieve the objective of a plausible mechanism with confident parameter values, any information extraction method available should be considered. As long as the method contributes significantly compared to the price (and alternatives), it is worth investigating. In this thesis the general method has been gas phase analysis from the reactor operated under atmospheric conditions. Below is a list of alternatives in connection to this thesis and some comments about each of them:

Quantitative DRIFTS data

The quantification of DRIFTS data was attempted and a number of practical and numerical issues need to be addressed, see sections 2.2.3.2, 3.2.4 and 5.4.1. However, the impact on the increase of the parameter dimensionality as shown in section 5.5 clearly motivates further efforts in this direction.

Quantitative isotope experiments

The quantification of isotope experiments was performed in section 5.4.2 and the main issues were the lack of calibration gases (*e.g.* $^{15}N_2O$, $^{14}N^{15}N$) as well as selectivity issues. However, the strong qualitative conclusions that are possible indicate that significant contributions should be expected if isotope experiments in combination with quantification could be applied.

Other interesting techniques in this area are Temporal Analysis of Products (TAP) [Yablonskii 1998, Perez-Ramirez 2007], Spaci-MS [Choi 2005]. Some of these techniques also require substantial numerical efforts to merge with traditional data. Time will tell which technique will contribute the most.

6.5. On the choice of optimal experimental design

In paper III, the approach for the design of experiments for precise parameter estimation is a selection of candidate experiments from a huge number of possible ones (1792 transient experiments consisting of approx. 73.000 time points). This approach is adapted from the pharmaceutical industry [Olsson 2004, Olsson 2005, Wold 2004], where the search for candidate drugs is a formidable task. In both cases many parameters are reduced to a few latent variables, thus enabling a more efficient selection.

Within the research field of heterogeneous catalysis dealing with non-linear modelling and sequential experimental design, the prevalent approach is to *search* for the experiments to perform [Buzzi-Ferraris 2009, Franceschini 2008a, Walter 1990]. Even though this search is

performed in a well defined experimental space (concentrations, flows, temperatures, sampling position, sampling time etc), the evaluation of a candidate experiment will still be performed in the highly non-linear parameter space. This search will have the same "challenges/problems" as classical parameter fitting, since it needs to condense the sensitivity for many responses and many parameters into one number. Furthermore, as with any other gradient method, it may find local optima. To conclude, this search approach will thus be not only complicated but also time consuming.
The proposed approach in paper III however, will also be very time consuming because it involves simulating "all possible" experiments in order to assess which ones are most valuable. Furthermore, this needs to be done after each sequential cycle, since the parameter sensitivity is dependent on the parameters themselves [Box 1965a].
The optimal approach is thus a difficult choice. Generally, reviewing the literature and considering the general absence of experimental design methodology, the most important message is to at least do experimental design.

6.6. Fitting large sets of parameters

In paper II, III, IV a large number of parameters are subject to fitting. The large number itself can be handled by use of Latent variable (LV) methods as shown in paper II. But even if the number of parameters is large, the fit is still not excellent, *i.e.* there are systematic residuals (Lack of fit) unless excessive experimental design can be performed as in paper III.
Many chemical reaction engineers often state that you should not fit more parameters than two [Fogler 2000a]. The reasons stem from different systems as well as different objectives. Traditional chemical engineering systems are often operated under steady state, thus making the rate limiting steps a function of inlet conditions only (varying reactant concentrations, temperature and pressure). Furthermore, the objective is often to get a good fit between experimental and simulated data. In these situations the different sub-parts such as reaction mechanisms are already known and reliable from previous laboratory experiments thus making the gap between small scale (lab) and full scale (plant) manageable.
In modern modelling of heterogeneous catalysis for emission control, the situation is different:

- The model subparts, such as the reaction mechanism, are not known beforehand.
- The gap between small scale (atomistic studies, either by theory or high-vacuum experiments) and full scale (monolith reactor) is much wider (the so-called pressure/materials gap [Imbihl 2007, Perez-Ramirez 2007, Stoltze 1985]).
- The objective is not only to get an acceptable fit, but to try to catch the true mechanism and the corresponding parameter values.
- The systems are very transient in concentrations, flows, temperatures as well as the substantial effect of accumulation on the catalytic surface. This will make the parameter space (*i.e.* the number of parameters that adequately can be fitted) much greater than two as shown *e.g.* in paper III.

The quite difficult task is therefore to master the combination of all these aspects and consequently, in this perspective, the approach to fit many parameters, instead of a few, is motivated.
In this thesis, efforts have been made in the fitting procedure as well in the experimental design. Another successful approach is to increase the complexity of the mechanism step by step *e.g.* [Olsson 2002a]. However, fixing parameters (assuming them to be correct) can make the other fitted parameters erroneous due to unfortunate assumptions. *E.g.*, in [Wickman

2007] it was shown that the kinetic parameters for NO_X storage were highly influenced by mass transfer resistance. Future work should be directed towards the combinations of the methods mentioned in this section. A relatively rapid search for the weakest parts of the model should be identified and subsequent efforts should be conducted thereafter.

6.7. Parameter fitting using residual sums of squares as objective function

The standard formulation of the objective function is the residual sums of squares. It has shown to be useful for many years in many different areas but it has some assumptions:

- It assumes the model to be correct (as usual)
- It assumes that the residual only originate from the experiments, *i.e.* the model structure and the experimental input are without errors.

Since the model structure of a NOx reduction catalyst probably has "room for improvements" as well as experimental input may be inaccurate (and these factors have consequences on the parameter estimation as shown in section 5.5), other alternatives should be considered:

Adding terms to the residual sums of squares

One simple way is to expand the residual sums of squares with other deviations, *e.g.* deviation from thermodynamic consistency was shown to be effective in [Bengtsson 2006, Mhadeshwar 2003]

Residual in the time direction

Another simple (though more numerically demanding) approach would be to define the residual with respect to time (errors in x) instead of exclusively concentration (errors in y) as traditionally done. This corresponds to a Latent Variable approach [Pearson 1901], where the residual should be defined in the direction of the mismatch (not necessarily in concentration but in time instead). This approach could be efficient for transient experiments, preferable used in combination with traditional (concentration based) residuals.

Weight schemes

There are different ways to enhance some residuals in favour of others by means of weight functions and schemes. Weight functions can be applied according to

- Gas phase species (measurement weight)
- Different experiments, different time points (*e.g.* transients)
- Sensitivity, determined from sensitivity analysis either of the Jacobian or some other sensitivity. In the extreme case only the most informative experimental observations (*e.g.* selected as in paper III) are used in the objective function. At that point it becomes appropriate to discuss degrees of freedom and confidence intervals (assuming the residual to be small).

Shape functions

The depressing "fact" that manual tuning still is better performing than any traditional method, calls for new ideas. What is catching the human eye? What combination of displays (concentrations, ΔG, rates, coverage, etc) is directing the decision for a parameter adjustment? Different shape functions need to be systematically investigated and compared in order to make progress in this area.

6.8. Parameter fitting using gradient methods

The parameter fitting method used in the papers of this thesis was a gradient search method (lsqnonlin in MATLAB). Gradient methods are known for not being a guarantee to find global optima. This becomes even more pronounced if the experimental data does not provoke the parameter sensitivities, *e.g.* consider finding an optimum in 3D by only searching in 2D. One major reason for not finding global optima is because gradient methods assume the parameter values to be in the "vincinity" of the optimal (true) values. In this case, the objective function will be smooth and the gradient will find the optima.
When the parameter values are far from the optima (still assuming the model to be correct), second order effects will be more pronounced, *e.g.* parameter interactions will be important. Unfortunately, lsqnonlin assumes the optimal parameters are nearby since the calculations for extracting the Jacobian consist of a COST (Consider Only one Single variable at a Time) approach. A more appropriate computation scheme would be to perform a fractional factorial design (or a Placket Burman design) in the parameters. This would be beneficial in several aspects:

- More precise estimation of the main effect, since all simulations are used to estimate the main effects.
- The possibility to estimate parameter interactions (*i.e.* explicit calculation of the Hessian), if any, and to calculate a search step more relevant to this phenomenon.
- The possibility to estimate non-linearities by the use of centerpoints [Brühwiler 2007]

Alternatives to gradient based search methods should be investigated. In a side project to this thesis work, simulated annealing has been tried [Bengtsson 2006], but it deserves a more comparative assessment using a better experimental data set. Also related methods such as the Genetic algorithm seem to gain in popularity and deserve further investigation.

7. CONCLUSIONS

Different aspects of parameter estimation have been studied and presented. In this process, the use of Experimental design and Latent Variable (LV) models has proven useful. The experimental design is a valuable "work horse" to maximize the information content from a minimum number of experiments. The concept of LV models results in a reduction of dimensions, which is a useful feature when dealing with many model parameters and many possible candidate experiments. This reduction of dimensions enables an assessment of the parameter correlation structure and may also enable more efficient computations due to the reduced dimensionality.

In the process of developing a detailed understanding of a catalytic reactor's mechanisms for emission control, the aspects presented in this thesis are very important and the contributions from the published papers are of significance. However, there are still many remaining challenges. The most important challenge would be to speed-up the modelling cycle and the ability to master all cycle steps in such a detail that the "weakest link in the chain" is as strong as possible.

The findings and conclusions in this thesis are not only applicable to NO_X reduction for emission control. In almost every reacting system operating at full scale, it is of utmost importance to master the aspects discussed in this thesis. Consequently, this knowledge may be used broadly and thus enhancing the process towards a sustainable future [Markides 2009].

8. NOMENCLATURE

Abbreviations

Ag/Al_2O_3	Silver alumina using impregnation method
$Ag\text{-}Al_2O_3$	Silver alumina using sol-gel method
ALS	Alternating Least Squares
CFD	Computational Fluid Dynamics
ETC	European Transient test Cycle
DFT	Density Functional Theory
DoE	Design of Experiments
DRIFTS	Diffuse Reflectance InfraRed Fourier Transform Spectroscopy
GC	Gas Chromatography
HC	HydroCarbon
KCK	Competence Centre for Catalysis (Kompetenscentrum Katalys)
LV	Latent Variable
LNT	Lean NO_X Trap
MCR	Multivariate Curve Resolution
MF	Mean Field (-approximation)
MFC	Mass flow controller
MLR	Multivariable Linear Regression
MS	Mass Spectrometer
MVDA	MultiVariate Data Analysis
NSR	NO_X Storage and Reduction
PCA	Principal Component Analysis
PLS	Partial Least Squares, alt. Projections onto Latent Structures
SCR	Selective Catalytic reduction (of NO_X)
SSITKA	Steady-State Isotopic Transient Kinetic Analysis
TPD	Temperature Programmed Desorption
TPR	Temperature Programmed Reaction

General

x, **x**, **X**	general variable (scalar, vector, matrix)
∇	Gradient operator (d/dx, d/dy, d/dz)
‘(prim)	transpose of a matrix

Variables, constants and parameters

A	Pre-exponential factor in Arrhenius expression [various units]
a, A	Cross-sectional area [m^2]
b, **b**	Linear regression coefficient (vector of coefficients)
c	Gas phase concentration [mol/m^3]
c_p, C_p	Specific heat capacity [J/kg/K, J/mole/K]
C	Correlation matrix (uniquely determined from the experiments)
C	Contribution matrix for an ALS model
C, c	Y-loading matrix (vector) for a PLS (LV) model
d_h	Characteristic length, hydraulic diameter [m]
D	Bulk diffusivity [m^2/s]
D_{eff}	Effective diffusivity (*e.g.* in washcoat) [m^2/s]
D	Spectral data matrix
e	residual for a linear model
E_A	Activation energy in Arrhenius expression [J/mol]

F_{tot}	total molar flow [mole/s]
g	Gravity constant [m/s^2]
(ΔG) G	(change of) Gibbs free energy [J/mol]
h	Heat transfer coefficient [W/m^2/K]
(ΔH) H, ΔH_r	(change of) Enthalpy, heat of reaction [J/mol]
J	Jacobian matrix
J*	molar flux from diffusion [mol/m2/s]
j*	Mass flux from diffusion [kg/m2/s]
K	Equilibrium constant
k_{ref}	rate constant at a reference temperature [various units]
k	Rate constant [various units depending on the rate equation]
k_c	Mass transfer coefficient [m/s]
L	characteristic length [m]
m	mass [kg]
n, N	Number of observations [-], Number of active sites [1/kg$_{cat}$]
N_A	Total molar flux (diffusion and convection) [mol/m2/s]
Nu	Nusselt number [-]
P	Pressure [Pa]
P, **p**	Loading matrix (vector) in LV model
q, Q	Volumetric flow [m3/s], Heat flux [J/s]
r	Reaction rate [mol/s, mol/s/kgcat]
R	Universal gas constant [8.314 J/mol/K]
R	Rotation matrix during ALS analysis
(ΔS) S	(change of) entropy [J/mol/K]
s, (**S**)	Sensitivity (matrix)
S	Pure spectra matrix for an ALS model
S	Objective function (eq(38,39)
Sh	Sherwood number [-]
T, **t**	Score matrix (vector) in LV model
T, T_s, T_g, T_p	Temperature, temperature of surface, of gas, of pipe (quartz tube) [K]
U, u	Fluid velocity [m/s]
V	Volume [m3]
W	X-loading matrix for a PLS (LV) model
y	Gas phase mole fraction [-]
z(β)	Residual for a non linear model

Greek letters

β (**β**)	General model parameter (vector)
θ	Surface concentration (fraction of total number of available sites) [-]
θ	Parameter vector (non-linear case)
$\eta(\beta)$	estimate of a response variable using a nonlinear model
η	effectiveness factor for internal mass transport
λ	Thermal conductivity [W/m/K]
ν	Kinematic viscosity [m2/s]
ν	Stoichiometric coefficient [-]
ρ	Fluid density [kg/m3]
σ^2	estimated variance
Ω	Hessian matrix (2nd derivative of the objective function
τ	Mean residence time [s]

9. ACKNOWLEDGEMENTS

I would like to thank my supervisors Derek Creaser and Bengt Andersson for interesting and fruitful discussions and for letting me run this project with great liberty.

For the undergraduate projects which contributed to the depth of this thesis I would especially like to thank Andreas Lundström, Björn Wickman, Anders Bengtsson, Andrea Brühweiler and Anja Mûller.

I would like to thank Prof. Robbie Burch, Dr John Breen and the staff at Centacat (Queens University of Belfast) for nice research collaboration and the EC Contract 025995 for funding.

I would like to thank Magnus Skoglundh for encouraging discussions and KCK (Competence Centre for Catalysis) for being such a nice "melting pot" for catalysis research, *e.g.* the Ag-alumina constellation. Thank you Hanna, Hannes, Anders, Henrik, Stephanie and Derek for very nice and interdisciplinary discussions.

Klaus Papadakis, Ingemar Odenbrand and the steering committee of the project "NO_X storage and reduction for heavy duty diesel vehicles" are acknowledged for interesting discussions and collaboration.

I would also like to thank all colleagues at Chemical Reaction Engineering for a relaxed atmosphere and tolerant attitude. My room mates Carolin Olsson and Mattias Svensson Modén: thank you for pleasant discussions about everything from theory to practice, from soft matters to hard facts. Special thanks to the supporting personnel Linda, Agneta and Marianne: Without you the department would cease to live!

Also I owe a debt of gratitude to a number of persons for practical assistance: Lars Lindström and Heine Riedel for laboratory gas mixtures, Björm Wickman for labview programming and Andreas Lundström for various technical assistance

I would like to thank Dr Mats Josefson and the Pharmaceutical R&D at AstraZeneca Mölndal for introducing me to chemometrics and academic research as well as interesting meeting during my PhD project.

The Swedish research council and the Swedish National Energy Administration are gratefully acknowledged for financial support.

Finally but not least I would like to thank my family and especially my wife Marlén and our two lovely sons, Jacob and Viktor, who makes me realize that my work is not the most important thing in the world.

10. REFERENCES

A. Varma, et al., Introduction to sensitivity analysis, in Parametric Sensitivity in Chemical Systems: p. 9-25.

Abbott, E.A., Flatland, A romance of many dimensions. 1884.

Aghalayam, P., et al., Reactors, Kinetics, and Catalysis; Construction and optimization of complex surface-reaction mechanisms. AIChE Journal, 46 (2000) p. 2017 - 2029.

Anderson, J.A., et al. Inter-relationship between carbonate, nitrate and sulphates in NOx storage and Reduction (NSR) catalysts. in NAM19. 2005.

Arrhenius, S., Paper 2: On The Reaction velocity of inversion of cane sugar by acids, in Selected Readings in Chemical Kinetics, M.H. Back and K.J. Laidler, Editors. 1889a, Pergamon: p. 31-35.

Arrhenius, S., Über die Reaktionsgeschwindigkeit bei der Inversion von Rohrzucker durch Säuren. Zeitschrift für Physikalische Chemie, 4 (1889b) p. 226-248.

Backman, H., et al., Kinetic considerations of H2 assisted hydrocarbon selective catalytic reduction of NO over Ag/Al2O3: II. Kinetic modelling. Applied Catalysis A: General, 304 (2006) p. 86-92.

Bardow, A., Optimal experimental design of ill-posed problems: The METER approach. Computers & Chemical Engineering, 32 (2008) p. 115-124.

Barrett, E.P., et al., The Determination of Pore Volume and Area Distributions in Porous Substances. I. Computations from Nitrogen Isotherms, 73 1 (1951). p. 373-380.

Barsan, M.M. and Thyrion, F.C., Kinetic study of oxidative dehydrogenation of propane over Ni-Co molybdate catalyst. Catalysis Today, 81 (2003) p. 159-170.

Bates, D.M. and Watts, D.G., Nonlinear regression analysis and its applications, ed. Wiley. 1988, Wiley.

Bengtsson, A.E., Parameter fitting of a kinetic model using Simulated Annealing. Department of Chemical and Biological Engineering. Masters of Science thesis (2006), Chalmers University of technology.

Berger, R.J., et al., Dynamic methods for catalytic kinetics. Applied Catalysis A: General, 342 (2008) p. 3-28.

Bird, R.B., et al., Transport phenomena. 2nd ed, ed. Wiley. 2002, Wiley International.

Bond, G.C., The Use of Kinetics in Evaluating Mechanisms in Heterogeneous Catalysis. Catalysis Reviews, 50 (2008) p. 532 - 567.

Box, G.E.P. and Hunter, W.G., The Experimental Study of Physical Mechanisms. Technometrics, 7 (1965a) p. 23-40.

Box, G.E.P. and Hunter, W.G. Sequential Design of Experiments for Nonlinear Models. in Proceedings of the IBM Scientific Computing Symposium on Statistics October 21-23 1963. 1965b: IBM Data processing division, White Plains, New York.

Box, G.E.P., et al., Some Problems Associated with the Analysis of Multiresponse Data. Technometrics, 15 (1973) p. 33-51.

Box, G.E.P. and Lucas, H.L., Design of Experiments in Non-Linear Situations. Biometrika, 46 (1959) p. 77-90.

Box, M.J., Some Experiences with a Nonlinear Experimental Design Criterion. Technometrics, 12 (1970) p. 569-589.

Breen, J.P. and Burch, R., A review of the effect of the addition of hydrogen in the selective catalytic reduction of NOx with hydrocarbons on silver catalysts. Topics in Catalysis, V39 (2006) p. 53-58.

Breen, J.P., et al., A fast transient kinetic study of the effect of H2 on the selective catalytic reduction of NOx with octane using isotopically labelled 15NO. Journal of Catalysis, 246 (2007) p. 1-9.
Bricker, M.L., et al., Strategies and applications of combinatorial methods and high throughput screening to the discovery of non-noble metal catalyst. Applied Surface Science, 223 (2004) p. 109-117.
Broqvist, P., et al., NOx storage on BaO: theory and experiment. Catalysis Today, 96 (2004) p. 71-78.
Broqvist, P., et al., NOx storage on BaO(100) surface from first principles: a two channel scenario. Journal of Physical Chemistry B, 106 (2002) p. 137-145.
Brunauer, S., et al., Adsorption of Gases in Multimolecular Layers, 60 2 (1938). p. 309-319.
Brühwiler, A., Nonlinear parameter fitting using Matlab. Chemical and Biological Engineering. Master thesis (2007), Chalmers University of technology.
Burnham, A.J., et al., Latent variable multivariate regression modeling. Chemometrics and Intelligent Laboratory Systems, 48 (1999) p. 167-180.
Burnham, A.J., et al., Frameworks for latent variable multivariate regression. Journal of Chemometrics, 10 (1996) p. 31-45.
Buzzi-Ferraris, G. and Manenti, F., Kinetic models analysis. Chemical Engineering Science, 64 (2009) p. 1061-1074.
Choi, J.-S., et al., Spatially resolved in situ measurements of transient species breakthrough during cyclic, low-temperature regeneration of a monolithic Pt/K/Al2O3 NOx storage-reduction catalyst. Applied Catalysis A: General, 293 (2005) p. 24-40.
Coleman, T.F. and Verma, A., A Preconditioned Conjugate Gradient Approach to Linear Equality Constrained Minimization. Computational Optimization and Applications, 20 (2001) p. 61-72.
Dante, R.C., et al., Fractional factorial design of experiments for PEM fuel cell performances improvement. International Journal of Hydrogen Energy, 28 (2002) p. 343-348.
Davis, S.G., et al., A new approach to response surface development for detailed gas-phase and surface reaction kinetic model optimization. International Journal of Chemical Kinetics, 36 (2004) p. 94-106.
Dawson, E.A. and Barnes, P.A., A new approach to the statistical optimisation of catalyst preparation. Applied Catalysis A: General, 90 (1992) p. 217-231.
Deshpande, K.B. and Zimmerman, W.B., Experimental study of mass transfer limited reaction--Part I: Use of fibre optic spectrometry to infer asymmetric mass transfer coefficients. Chemical Engineering Science, 60 (2005) p. 2879-2893.
Desikusumastuti, A., et al., Identifying surface species by vibrational spectroscopy: Bridging vs monodentate nitrates. Journal of Catalysis, 255 (2008) p. 127-133.
Dumesic, J.A., et al., The Microkinetics of Heterogeneous Catalysis, ed. A.C. Society. 1991, American Chemical Society.
Edgar, T.F., et al., Optimization of Chemical processes. 2001.
Eftaxias, A., et al., Nonlinear kinetic parameter estimation using simulated annealing. Computers & Chemical Engineering, 26 (2002) p. 1725-1733.
Eriksson, L., et al., Multi- and Megavariate Data analysis, Priciples and Applications. 1st ed. 2001, Umetrics AB.
Fogler, H.S., Chapter 14, Models for nonideal reactors, in Elements of Chemical Reaction Engineering, N.R. Amundson, Editor. 2000a, Prentice Hall PTR: p. 946-1004.
Fogler, H.S., Elements of Chemical Reaction Engineering. 3rd edition ed. Prentice Hall International Series in the Physical and Chemical Engineering Sciences, ed. N.R. Amundson. 2000b, Prentice Hall PTR.

Fontaine, N. and Hassi, S., Directive 1999/96/EC of the European Parliament and of the Council, in Official Journal of the European Communities, 44 (2000), European Parliament.
Franceschini, G. and Macchietto, S., Model-based design of experiments for parameter precision: State of the art. Chemical Engineering Science, 63 (2008a) p. 4846-4872.
Franceschini, G. and Macchietto, S., Novel anticorrelation criteria for model-based experiment design: Theory and formulations. AIChE Journal, 54 (2008b) p. 1009-1024.
Gorte, R.J., Temperature-programmed desorption for the characterization of oxide catalysts. Catalysis Today, 28 (1996) p. 405-414.
Guthenke, A., et al., Development and application of a model for a NOx storage and reduction catalyst. Chemical Engineering Science, 62 (2007) p. 5357-5363.
Hansen, A., et al., Microkinetic modeling as a tool in catalyst discovery. Topics in Catalysis, 45 (2007) p. 219-222.
Hansen, J., Defusing the Global Warming Time Bomb. Scientific American, March (2004) p. 42-49.
Hawthorn, R.D., Afterburner Catalysts-effects of Heat and Mass Transfer Between Gas and Catalytic Surface. AIChE Symposium Series, 70 (1974) p. 428-438.
He, H., et al., Review of Ag/Al2O3-Reductant System in the Selective Catalytic Reduction of NO x. Catalysis Surveys from Asia, 12 (2008) p. 38-55.
Hellman, A. and Grönbeck, H., Activation of Al2O3 by a Long-Ranged Chemical Bond Mechanism. Physical Review Letters, 100 (2008) p. 116801-4.
HIDEN, Soft Ionisation for Analysis of Complex Gas/Vapour Mixtures, Gas Analysis Application Note 250 H.A. LTD, Editor (2007), HIDEN ANALYTICAL LTD: Warrington. p. 5.
Holmgren, A., et al., A Model of Oxygen Transport in Pt/Ceria Catalysts from Isotope Exchange. Journal of Catalysis, 182 (1999) p. 441-448.
Hosten, L.H. and Emig, G., Sequential experimental design procedures for precise parameter estimation in ordinary differential equations. Chemical Engineering Science, 30 (1975) p. 1357-1364.
Hunter, W.G. and Mezaki, R., An Experimental design strategy for distinguishing among rival mechanistic models. An Application to the catalytic hydrogenation of propylene. Canadian Journal of Chemical Engineering, 45 (1967) p. 247-249.
Imbihl, R., et al., Bridging the pressure and material gap in heterogeneous catalysis. Physical Chemistry Chemical Physics, 9 (2007) p. 3459-3459.
Issanchou, S., et al., Sequential experimental design strategy for rapid kinetic modeling of chemical synthesis. Aiche Journal, 51 (2005) p. 1773-1781.
Jansson, J., Studies of Catalytic Low-Temperature CO Oxidation over Cobalt Oxide and Related Transition Metal Oxides. Department of Chemical Reaction Engineering. Doctoral dissertation (2002), Chalmers University of Technology.
Jansson, J. and Andresson, B., Statistical Considerations in the Non-linear regression of a Microkinetic Reaction Model to Experimental data from a Low-temperature active carbon monoxide oxidation catalyst, in manuscript, (2004).
Kabin, K.S., et al., NOX storage and reduction on a Pt/BaO/alumina monolithic storage catalyst. Catalysis Today, 96 (2004) p. 79-89.
Kalivas, J.H., Optimization using variations of simulated annealing. Chemometrics and Intelligent Laboratory Systems, 15 (1992) p. 1-12.
Kannisto, H., Silver Alumina Catalysts for Lean NOx reduction. Department of Chemical and Biological Engineering(2009a), Chalmers university of technology.
Kannisto, H., et al., Ag-Al2O3 catalysts for lean NOx reduction--Influence of preparation method and reductant. Journal of Molecular Catalysis A: Chemical, 302 (2009b) p. 86-96.

Kapteijn, F. and Moulijn, J.A., Laboratory Leactors, in Handbook of heterogeneous catalysis, G. Ertl, J. Weitkamp, and H. Knözinger, Editors. 1997: p. 1359-1398.
Kasuya, F., et al., The thermal DeNOx process: Influence of partial pressures and temperature. Chemical Engineering Science, 50 (1995) p. 1455-1466.
Kirsten, G. and Maier, W.F., Strategies for the discovery of new catalysts with combinatorial chemistry. Applied Surface Science, 223 (2004) p. 87-101.
Koci, P., et al., Modelling of micro/nano-scale concentration and temperature gradients in porous supported catalysts. Chemical Engineering Science, 62 (2007) p. 5380-5385.
Lewi, P.J., From data to knowledge to more data. Where is the portal to progress? Chemometrics and Intelligent Laboratory Systems, 73 (2004) p. 167-168.
Luna-Ortiz, E. and Theodoropoulos, C., An input/output model reduction-based optimization scheme for large-scale systems. Multiscale Modeling & Simulation, 4 (2005) p. 691-708.
Lundstedt, T., et al., Experimental design and optimization. Chemometrics and Intelligent Laboratory Systems, 42 (1998) p. 3-40.
Lundström, A. and Wickman, B., Simulation of Heterogeneous catalysis using the Finite Element Method: Analysis of transients using detailed kinetic- and transport models. Department of Chemical and Biological Engineering. undergraduate thesis report (2005), Chemical Reaction Engineering.
Markides, K., Vision, goals and strategies 2008 - 2015 with outlook towards 2020, 2009 2009-03-10 (2009), Chalmers university of technology: Gothenburg. p. http://www.chalmers.se/insidan/EN/about-chalmers/vision-goals-strategies.
Marquardt, W., Special Issue: model-based experimental analysis: From Experimental Data to Mechanistic Models of Kinetic Phenomena in Reactive Systems. Chemical Engineering Science, 63 (2008) p. 4637-4639.
Martens, H. and Naes, T., Multivariate Calibration, ed. Wiley. 1989, Wiley.
Mary Ann Branch, T.F.C., Yuying Li, A Subspace, Interior, and Conjugate Gradient Method for Large-Scale Bound-Constrained Minimization Problems. SIAM Journal on Scientific Computing, 21 (1999) p. 1-23.
McGraw-Hill, Chemical properties handbook, Table: Critical Properties and Acentric Factor; Inorganic Compounds, (2009).
Meinrath, G., et al., Assessment of uncertainty in parameter evaluation and prediction. Talanta, 51 (2000) p. 231-246.
Meunier, F.C., et al., Mechanistic differences in the selective reduction of NO by propene over cobalt- and silver-promoted alumina catalysts: kinetic and in situ DRIFTS study. Catalysis Today, 59 (2000) p. 287-304.
Mhadeshwar, A.B., et al., The role of adsorbate-adsorbate interactions in the rate controlling step and the most abundant reaction intermediate of NH3 decomposition on Ru. Catalysis Letters, 96 (2004) p. 13-22.
Mhadeshwar, A.B., et al., Thermodynamic Consistency in Microkinetic Development of Surface Reaction Mechanisms. J. Phys. Chem. B., 107 (2003) p. 12721 -12733.
Mhadeshwar, A.B., et al., Microkinetic modeling for hydrocarbon (HC)-based selective catalytic reduction (SCR) of NOx on a silver-based catalyst. Applied Catalysis B: Environmental, In Press, Accepted Manuscript (2009) p.
Mhadeshwar, A.B. and Vlachos, D.G., Hierarchical, multiscale surface reaction mechanism development: CO and H2 oxidation, water-gas shift, and preferential oxidation of CO on Rh. Journal of Catalysis, 234 (2005a) p. 48-63.
Mhadeshwar, A.B. and Vlachos, D.G., Is the water-gas shift reaction on Pt simple? Computer-aided microkinetic model reduction, lumped rate expression, and rate-determining step. Catalysis Today, 105 (2005b) p. 162-172.

Miyadera, T., Alumina-supported silver catalysts for the selective reduction of nitric oxide with propene and oxygen-containing organic compounds. Applied Catalysis B: Environmental, 2 (1993) p. 199-205.
MKS Instruments, I., MKS Type MG2000™ Software Manual, 134985-P1, Rev B, 09/06, Software Version 06.30 (2006).
Montgomery, D.C., Design and Analysis of Experiments. 5 ed. 2001, Wiley.
Müller, A., Modelling and quantification of DRIFTS data for kinetic studies. Department of Chemical and Biological Engineering. Diploma thesis (2008), Chalmers University of technology.
Olsson, I.-M., et al., D-optimal onion designs in statistical molecular design. Chemometrics and Intelligent Laboratory Systems, 73 (2004) p. 37-46.
Olsson, I.-M., et al., Controlling coverage of D-optimal onion designs and selections. Journal of Chemometrics, 18 (2005) p. 548-557.
Olsson, L., Fundamental studies of catalytic nitrogen oxide removal: micro kinetic modelling, Monte Carlo simulations and flow reactor experiments. department of Chemical Reaction Engineering(2002a), Chalmers University of Technology.
Olsson, L., et al., Mean field modelling of NOx storage on Pt/BaO/Al2O3. Catalysis Today, 73 (2002b) p. 263-270.
Olsson, L., et al., A Kinetic Study of Oxygen Adsorption/Desorption and NO Oxidation over Pt/Al2O3 Catalysts. J. Phys. Chem. B., 103 (1999) p. 10433-10439.
Olsson, L., et al., Role of steps in the NO-CO reaction on the (1 1 1) surface of noble metals. Surface Science, 529 (2003) p. 338-348.
Papadakis, K., et al., Development of a dosing strategy for a heavy-duty diesel exhaust cleaning system based on NOX storage and reduction technology by Design of Experiments. Applied Catalysis B: Environmental, 70 (2007) p. 215-225.
Park, Y.K., et al., A Generalized Approach for Predicting Coverage-Dependent Reaction Parameters of Complex Surface Reactions: Application to H2 Oxidation over Platinum. J. Phys. Chem. A, 103 (1999) p. 8101 -8107.
Partington, J.R., Chapter XX Solutions, in A History of Chemistry. 1964, Macmillan & Co Ltd: p. 637-662.
Pearson, K., On Lines and Planes of Closest Fit to Systems of Points in Space. Philosophical Magazine, 6 (1901) p. 559-572.
Perez-Ramirez, J. and Kondratenko, E.V., Evolution, achievements, and perspectives of the TAP technique. Catalysis Today, 121 (2007) p. 160-169.
Poling, B.E., et al., Diffusion coefficients, in The properties of gases and liquids 2001, McGraw-Hill.
Pritchard, D.J. and Bacon, D.W., Prospects for reducing correlations among parameter estimates in kinetic models. Chemical Engineering Science, 33 (1978) p. 1539-1543.
Raimondeau, S., et al., Parameter Optimization of Molecular Models: Application to Surface Kinetics. Ind. Eng. Chem. Res., 42 (2003) p. 1174-1183.
Reactions in Heterogeneous systems. 1999, Chemical Reaction Engineering, Chalmers University of technology.
Richter, M., et al., Unusual Activity Enhancement of NO Conversion over Ag/Al2O3 by Using a Mixed NH3/H2 Reductant Under Lean Conditions. Catalysis Letters, V94 (2004) p. 115-118.
Routray, K. and Deo, G., Kinetic parameter estimation for a multiresponse nonlinear reaction model. AiIChE Journal, 51 (2005) p. 1733-1746.
Rönnholm, M., et al., ANN modeling applied to NO x reduction with octane in a new microreactor. Topics in Catalysis, 42-43 (2007) p. 195-198.

S. Kirkpatrick, C.D.G., Jr., M.P. Vecchi, Optimization by Simulated Annealing. Science, 220 (1983) p. 671-780.
Satterfield, C.N., Heterogeneous Catalysis in Practice. 1 ed. McGraw-Hill Chemical engineering series. 1980, McGraw-Hill Book Company.
Shannon, S.L. and Goodwin, J.G., Characterization of Catalytic Surfaces by Isotopic-Transient Kinetics during Steady-State Reaction. Chem. Rev., 95 (1995) p. 677-695.
Shimizu, K.-i. and Satsuma, A., Selective catalytic reduction of NO over supported silver catalysts-practical and mechanistic aspects. Physical Chemistry Chemical Physics, 8 (2006) p. 2677-2695.
Shimizu, K.-i., et al., Silver-alumina catalysts for selective reduction of NO by higher hydrocarbons: structure of active sites and reaction mechanism. Applied Catalysis B: Environmental, 30 (2001) p. 151-162.
Sjövall, H., et al., Detailed Kinetic Modeling of NH3 and H2O Adsorption, and NH3 Oxidation over Cu-ZSM-5, 113 4 (2009). p. 1393-1405.
Song, J., et al., Valid parameter range analyses for chemical reaction kinetic models. Chemical Engineering Science, 57 (2002) p. 4475-4491.
Stegelmann, C., et al., Microkinetic modeling of ethylene oxidation over silver. Journal of Catalysis, 221 (2004) p. 630-649.
Stoltze, P., Microkinetic simulation of catalytic reactions. Progress in Surface Science, 65 (2000) p. 65-150.
Stoltze, P. and Norskov, J.K., Bridging the Pressure Gap between Ultrahigh-Vacuum Surface Physics and High-Pressure Catalysis. Physical Review Letters, 55 (1985) p. 2502-2505.
Tagliabue, M., et al., Multivariate approach to zeolite synthesis. Catalysis Today, 81 (2003) p. 405-412.
Theis, J.I., et al., Phenomenological studies on the storage and regeneration process of NOx storage catalysts for gasoline lean burn applications, in SAE Technical Paper Series, SP-1676 2002-01-0057 (2002).
Thomas Coleman, Y.L., An Interior Trust Region Approach for Nonlinear Minimization Subject to Bounds. SIAM J Optimization, 6 (1996) p. 418-445.
Tronconi, E. and Forzatti, P., Adequacy of lumped parameter models for SCR reactors with monolith structure. AIChE Journal, 38 (1992) p. 201-210.
Turányi, T., et al., Reaction Rate Analysis of Complex Kinetic Systems. International Journal of Chemical Kinetics, 21 (1989) p. 83-99.
Umetri, Introduction to Design of Experiments. 1988, Umetri AB.
Vajda, S., et al., Principal Component Analysis of Kinetic Models. International Journal of Chemical Kinetics, 17 (1985) p. 55-81.
Walter, E. and Pronzato, L., Qualitative and quantitative experiment design for phenomenological models--A survey. Automatica, 26 (1990) p. 195-213.
Van't Hoff, J.H., Études de Dynamique Chimique. 1884.
Van't Hoff, J.H., zur Chemischen Dynamik, ed. D.E. Cohen. 1896, Fredrik Muller & co.
Wickman, B., et al., Modeling mass transport with microkinetics in monolithic NO x storage and reduction catalyst. Topics in Catalysis, 42-43 (2007) p. 123-127.
Wold, S., et al., The utility of multivariate design in PLS modeling. Journal of Chemometrics, 18 (2004) p. 156-165.
Yablonskii, G.S., et al., Moment-based analysis of transient response catalytic studies (TAP experiment). Industrial & Engineering Chemistry Research, 37 (1998) p. 2193-2202.
Yeom, Y.H., et al., A study of the mechanism for NOx reduction with ethanol on gamma-alumina supported silver. Journal of Catalysis, 238 (2006) p. 100-110.
Zamostny, P. and Belohlav, Z., Identification of kinetic models of heterogeneously catalyzed reactions. Applied Catalysis A: General, 225 (2002) p. 291-299.

11. APPENDICIES

A. Mass spectroscopy

Aspects of MS quantification

Below is a list of important aspects when it comes to quantification of MS data.

1. Capillary inlet. The capillary (at KCK) is a small glass tube (~1mm diameter, 4cm long) with a "melted" end, creating a very small opening and thus creating the pressure drop (from 1 bar to 1×10^{-6}bar).
2. If the opening is too small (by design or by clogging of by-products) the pressure drop will increase and the flow into the ionization chamber will decrease. This will make the signal weaker (more noise) and also make the effect of the inevitable leaks on the vacuum side more important. Furthermore it will increase the response time for transient experiments.
3. If the opening is too big, the pressure drop will decrease and the flow into the ionization chamber will increase. This will cause secondary effects, *i.e.* ions interacting with each other and thus changing the sensitivity but more importantly also changing the selectivity.
4. The counter-measure is to check the pressure in the ionization chamber and to use an internal standard as reference, see below.
5. To summarize: the ionization chamber pressure (governed mainly by the capillary) affects the response level (sensitivity) and the noise level as well as the sensitivity and finally also the response time.
6. Ionization chamber setup: The number of produced ions/fragments depends on the amount and energy of the incoming electrons, see Figure 31, but also the amount and composition of the incoming gas mixture and also on the combination of both electrons and gas mixture.

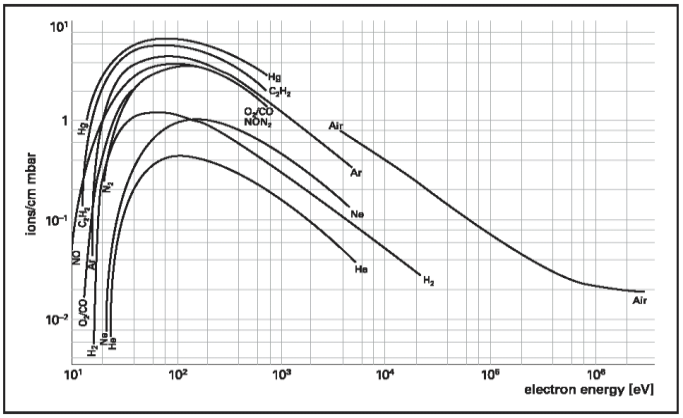

Figure 31 Ionization produced by electron impact, as a function of the electron energy.

If the energy is too low (below the ionisation limit) there will be no formation of ions. If the energy is too high, the signal will drop and more importantly: secondary effects will occur (molecules will either fragmentize more or produce double charged ions) obviously complicating any calibration. A high sensitivity is generally wanted and the most commonly energy of approximately 70eV is selected. The selectivity can be modelled by a proper experimental design, taking the interaction effect into account, see for example section 5.4.2. An alternative technique is the "soft ionization method" [HIDEN 2007] where it is possible to quantify *e.g.* NH_3 (m/e=17) in the presence of water which produces a significant fragment at m/e=17. The "trick" is to lower the electron energy, the secondary effects will be smaller (selectivity will increase) and a trade-off between selectivity and sensitivity is possible. Another way to increase the selectivity is to purchase an MS that works with other ionisation elements (*i.e.* not electrons) but larger charged elements such as Kr, Xe or Hg.

7. Quadropole setup: The main task for the quadropole is the separation between masses (resolution, mass selectivity) which, of course, comes at the price of sensitivity. If the resolution is too high the signal drops and if the resolution is

to low, the signal will be influenced by adjacent masses (see Figure 32).

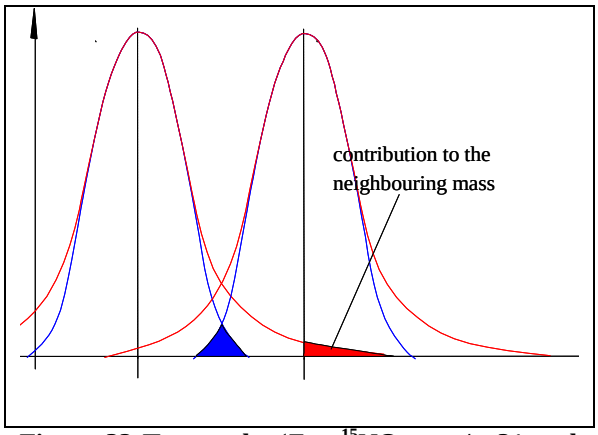

Figure 32 Two peaks (*E.g.* ^{15}NO at m/e=31 and $^{16}O_2$ at m/e=32) and the peak overlap if the resolution is not high enough or if the concentrations of $^{16}O_2$ is high and the concentration of ^{15}NO is low.)

8. The counter-measure is to investigate if the resolution can be increased and if not, if the peak overlap can be modelled, *i.e.* by including the interference in the calibration.
9. SEM setup: The SEM detector is (as indicated by the name: Secondary Electron Multiplier) a multiplier of the electrons that was released by the fragments that passed through the quadropole, see Figure 33

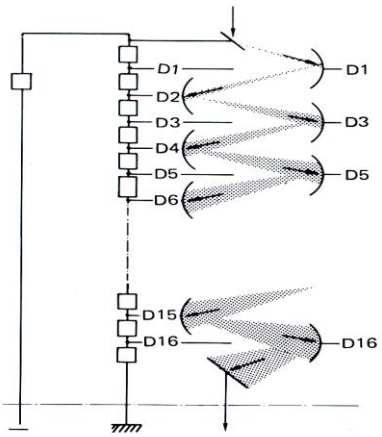

Figure 33 The SEM detector. The first few electrons emitted from the incoming fragment is multiplied many times and the signal increases.

The signal (in counts) should of course be as high as possible, but if the signal becomes too high, the electronics will not have the time to relax and thus the signal of the subsequent mass (in the scan) will be influenced.

MS calibration

The following steps should be a good starting point for quantitative analysis of MS data.

Data acquisition:

1. A reference mass should be collected at all times in order to capture drift in the SEM detector, preferably an ion with a signal level similar to the other analytes *e.g.* Kr @m82, (If Ar is used as a carrier gas, Ar@m40 should not be used since it has such a high signal that the SEM may have problems with signal decay times. Furthermore, the Ar concentration will vary with the other concentrations (since it is used as a "filler") and potential errors in the other concentrations will have an impact on the predictions)
2. Make a proper design in the concentration intervals that are of interest. Note if distinct levels are to be used (*e.g.* O_2 at either 5% or 0%) it is probably better to make two separate calibrations.
3. Since there are always leaks in the system, every mass will have a zero-level, *i.e.* at 0 ppm inlet concentration the SEM will still obtain a low signal. Record all masses with only the diluent gas (*e.g.* Ar) in the system.

Data pre-treatment:

4. adjust all MS signals to the Kr level (either dynamically or as a constant)
5. Subtract the zero baseline for each individual mass
6. If m31 is used (*e.g.* ^{15}NO) in combination with high levels of O_2, make sure to correct for the peak overlap (see Figure 32)
7. Make a calibration of the sensitivities and make the inverse calibration using least squares:

$$\mathbf{I} = \mathbf{CS}$$
$$\mathbf{C} = \mathbf{I}\beta = \mathbf{IS'inv(SS')} \quad \textbf{(54)}$$

Where **I** is the MS signals, **C** is the concentrations and **S** the sensitivity matrix. Note that the inversion of **S'S** is sensitive to small errors since correlation can exist, *e.g.* NO_2 has fragments m30 and m46. Below is an example of a NO_X sensitivity matrix:

	m28	**m30**	**m44**	**m46**
$^{14}N_2$	2.9	0	0	0
^{14}NO	0	3.3	0	0
$^{14}N_2O$	1	0	2.5	0
$^{14}NO_2$	0	1	0	0.3195

Table 3. example of an MS sensitivity matrix

8. If isotopes are used, then expand the matrix with the corresponding species and masses. Due to the confounding between $^{15}N_2$ and ^{14}NO, $^{15}N_2O$ and $^{14}NO_2$, special care should be taken if these species are to be quantified. Note that the experiment can indicate the species that are not likely to occur and hence some sensitivities can be neglected.
9. Make sure to check the predictions by calculating the mass balances and if necessary, adjust the sensitivity coefficients.

B. Linear modelling

More details on ALS

ALS was introduced in 3.2.4, and here are some additional details. By performing spectral decomposition, information about adsorbate concentration may be obtained:

$$\mathbf{D} \approx \hat{\mathbf{D}} = \mathbf{TP'} = \mathbf{TRR'P'} = \mathbf{CS'} \quad (55)$$

Where D is the spectral matrix of size NxK (N observations, K wavenumbers), T and P are the scores and loadings matrices from a PCA analysis. R is a rotation matrix, C is the contribution matrix, corresponding to concentrations and S is the matrix of pure spectra. The implementation of the MRC (Multivariate Curve Resolution) methodology is described here (using PLS toolbox v 4.1 in MATLAB):

1) Make an estimate (approximation) of D by means of PCA (Principal Component Analysis). This will determine the dimensionality (A) of the reduced space, *i.e.* the number of components present in the data.
2) "Sort" the corresponding scores so that they appear in a sequence by EFA (Evolving Factor Analysis) and use these corresponding scores as initial estimates for the subsequent ALS.
3) Perform ALS (Alternating Least Squares) that rotates the latent variables using a rotation matrix R subject to non-negativity constraints on both C and S.

The resulting decomposition is now an approximation of D that is composed of one matrix C, that corresponds to concentrations and one matrix S that corresponds to the pure spectra.

This decomposition is often non-ambiguous, but even a crude quantification of the adsorbate concentrations would be very beneficial. A simulation output is normally the gas phase concentrations from the rear of the reactor, whereas most of the reactions actually take place at the very entrance. This is the motivation why the introduction of surface concentration estimates is of great importance.

C. Relations and correlations for transport and kinetic aspects of modelling

In this section some model expressions are given with reference from the preceding sections.

3.5 Determination of Diffusivity, D_A

The binary diffusivity of species A in B (D_{AB}) can be calculated in various ways (B is omitted since the same diluent gas is used for all analytes, Ar in this case)
The most common way is the use of the Fuller correlation (from [Poling 2001])

$$D_{AB} = \frac{0.00143T^{1.75}}{PM_{AB}^{½}\left[\Sigma_{v\,A}^{1/3} + \Sigma_{v\,B}^{1/3}\right]^2} \quad (11\text{-}4.4)$$

Where D_{AB}=binary diffusivity [cm^2/s], P=pressure [bar], $M_{AB}=2/(1/M_A+1/M_B)$, T=temperature [K] and Σ_v is the diffusion volume, either as a molecule or as a sum of atom contributions in the molecule, see p11.11 in [Poling 2001].

The diffusivity can also be calculated from Chapman and Enskog theory [Poling 2001]

$$D_{AB} = \frac{0.00266T^{1.5}}{PM_{AB}^{½}\sigma_{AB}^2\Omega_D} \quad (11\text{-}3.2)$$

Where P=pressure [bar], σ_{AB} is the characteristic length and Ω_D is a diffusion collision integral (note that the integral is a function of temperature and the global temperature dependence of D_{AB} was $T^{1.75}$ in this thesis). These can be found in [Bird 2002] eq 17.3-12, E.2-2, 17.3-14,15, 1.4-11b and the molecular properties can *e.g.* be found and downloaded from [McGraw-Hill 2009]. Note that units may differ *e.g.* for pressure.

3.5.1 Determination of number of tanks in series

The following is adapted from [Fogler 2000b]. The number of tanks-in-series, n, necessary to model a real tube reactor is

$$n = \frac{\tau^2}{\sigma^2} \quad (14\text{-}12)$$

Where τ is the mean residence time and σ^2 is the variance of an impulse response. The mean residence and variance can be measured (if the surrounding pipes and detectors are properly modelled as well, see section 3.4) but can also be calculated using the reactor-Peclet number Pe_r:

$$Pe_r = \frac{UL}{D_a} \quad (14\text{-}19)$$

Where U is the superficial velocity (m/s), L is the reactor (monolith) length [m] and D_a is the axial dispersion coefficient [m^2/s].
The axial dispersion coefficient is given from a correlation:

$$D_a = D_{AB} + \frac{u^2 d_t^2}{192 D_{AB}} \quad (p965)$$

This correlation indicates that when the fluid velocity is low, the dispersion is equal to the binary diffusivity. For an open-open system using the reactor-Peclet number (also known as the Bodenstein number, Bo), the following relation applies:

$$\frac{\sigma^2}{\tau^2} = \frac{2}{Pe_r} + \frac{8}{Pe_r^2} \quad (14\text{-}46)$$

Eq (14-46) together with eq (14-12) gives n. n can also be calculated from another relation:

$$n = \frac{Bo}{2} + 1 \quad (14\text{-}50)$$

which gives about the same results.

3.5.2 Determination of kc

The mass transport coefficient k_c is given from the definition of the Sherwood number (eq. from [Fogler 2000b]:

$$Sh = \frac{k_c d_p}{D_{AB}} \qquad (11\text{-}38)$$

Where d_p is the characteristic length (channel diameter), D_{AB} is the binary diffusivity and Sh is taken from correlations. In this thesis the Sherwood number is obtained from [Tronconi 1992] who reported using the following correlation:

$$Sh = Sh_a + 6.874\left(1000z^*\right)^{-0.488}\exp\left(-57.2z^*\right)$$

Where Sh_a is the asymptotic Sherwood number, being 3 for square channels and 4.4 for circular channels. z* is the dimensionless axial position:

$$z^* = \frac{zD_{AB}}{ud_t^2} = \frac{z}{d_t}\frac{1}{\mathrm{Re}\,Sc}$$

3.5.3 Determination of an effectiveness factor for internal mass transport resistance

The Knudsen diffusivity is given in [Bird 2002]

$$D_{Kn} = \frac{8a}{3}\sqrt{\frac{RT}{2\pi M_A}} \qquad (24.6\text{-}1)$$

The effective diffusivity (D_{eff}) is given in [Fogler 2000b]

$$D_{eff} = \frac{D_{kn}\phi_p\sigma_c}{\tilde{\tau}} \qquad (12\text{-}1)$$

Where ϕ_p is the porosity, σ_c is the constriction factor and τ is the tortuosity, which can be approximated by:

$$D_{eff} \approx D_{kn}\frac{0.4*0.8}{3} \approx \frac{D_{kn}}{10} \qquad \text{(p816)}$$

Furthermore, the Thiele modulus for a plate is given by [*Reactions in Heterogeneous systems* 1999]

$$\phi = L\sqrt{\frac{n+1}{2}\frac{k_v c_{As}^{n-1}}{D_{eff}}} \qquad (2.184)$$

And the effectiveness factor is given by:

$$\eta = \frac{1}{\phi} \qquad (2.182)$$

Note that the Knudsen diffusivity applies when the pore diameter is about 2-50 nm. In the case for Ag-Al_2O_3 used in paper IV, the average pore diameter was 3nm, i.e. on the limit for Knudsen diffusion. Furthermore, to complicate the situation further, the pores in the washcoat are not only from the powder, but the pores also stems from spaces between particles, as shown in Figure 5, section 2.3. There it can be seen that particles of about 1µm is sintered to form the washcoat.

3.6.3 Expressions for kinetic parameters

These equations can also be derived from [Dumesic 1991], however the units are often not macroscopic so the equations have been re-written (equations from [Olsson 2002a]).

Preexponential factors for adsorption are obtained from Collision theory:

$$A_{ads} = \frac{N_A RT}{\sqrt{2\pi MRT}} A_s N_{cat} S(0) \qquad (5.1.5)$$

Where N_A is the Avogadros number, T is the temperature [K], M is the molecular weight, A_s is the surface area of one site [m^2/site], N_{cat} is the moles of active sites per kg catalyst and S(0) is the sticking coefficient at zero coverage.

Pre-exponential factors for surface reactions can be calculated from transition state theory, see Figure 34.

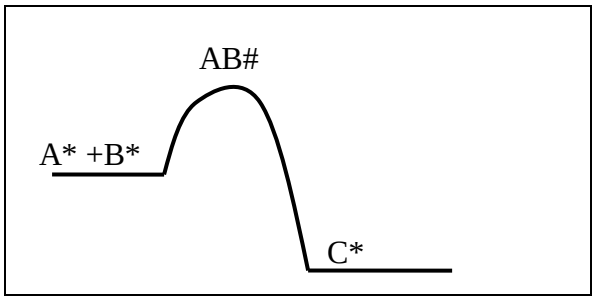

Figure 34. Schematic view of a surface reaction, AB# is the transition state, corresponding to a reaction intermediate in thermodynamic equilibrium with the reactants and the product.

The pre-exponential is given in [Dumesic 1991]

$$A_{AB} = \frac{k_B T}{h} \frac{Q_{AB}^{\#}}{Q_A^{\#} Q_B^{\#}} \qquad (29)$$

Where k_B is the Boltzmann constant (1.38×10^{-23} J/K), h is Plancks constant (6.626×10^{-34} J·s), T is the temperature [K] and $Q^{\#}$ are the partition functions. Each partition function has contributions from molecular translation, vibration and rotation:

$$Q_i^{\#} = q_{it} q_{ir} q_{iv} \qquad (22)$$

The translation contribution is given by:

$$q_{it} = \frac{(2\pi m_i k_B T)^{3/2}}{h^3}, (3D)$$
$$q_{it} = \frac{(2\pi m_i k_B T)}{h^2} A_s, (2D) \qquad (23)$$

depending on if the molecule moves in three dimensions or on a surface (in two dimensions) and m_i is the molecular mass [a.u.]. If the molecule can be assumed to be "fixed" or localized, q_{it} becomes unity. The rotational contribution is given by:

$$q_{ir} = \frac{8\pi^2 I_i k_B T}{\sigma_r h^2}, (linear)$$
$$q_{ir} = \frac{8\pi^2 \sqrt{8\pi^3 I_{ix} I_{iy} I_{iz}} (k_B T)^{3/2}}{\sigma_r h^3}, (nonlinear)$$

where I_i are the moments of inertia, σ_r is the rotational symmetry number. The vibrational contributions are:

$$q_{iv} = \prod_j \frac{1}{1 - \exp\left(-\frac{h\upsilon_{ij}}{k_B T}\right)} \qquad (26)$$

Where ν_{ij} are the frequencies of the normal vibrational modes. Note that these vibrational modes are one of the outputs from DFT calculations described in section 3.6.5 concerning HS modelling. Note that $k_B T/h = 10^{13}$ s^{-1} at 200°C.

For the pre-exponential factor for desorption, the ratio of the partition functions are $Q_A^{\#}/Q_A^* = 1$, thus giving the value of 10^{13} s^{-1}.

For estimation of activation energies, there exists several methods, eg. Bond order conservation. However, this method has only been sporadically used in this thesis and the reader is referred to the literature [Dumesic 1991, Mhadeshwar 2003] for details. For activation energies for desorption, DTF calculations or microcalorimetry experiments may be used since the activation energy correspond to the heat of adsorption (if the adsorption is non-activated)

D. MATLAB implementation

The simulation code written in Matlab was first developed by Björn Westerberg and then refined by Louise Olsson. The code had however become less general since many *ad hoc* solutions had been implemented as time went by. In order to improve the performance and increase the user-understanding of the code a number of changes were made:

- File structure: The different m-files were revised and variable definitions were relocated in order to increase the transparency of the code.
- Flexible thermodynamic constraints were added.
- A new ODE function was applied that also could take into account gas phase accumulation. Also heat balances were added in paper IV.
- Scaling of fitted parameters was added.
- Code was included to shift data in order to compensate for instrumental delay and detector rise time.
- Use of a mass matrix (M) was included in order to neglect accumulation if desired:

$$\mathbf{M}\frac{dx}{dt} = f(x,t) \qquad (56)$$

- Alternative ways to fit parameters were included (see paper II).

The structure of all m-files is displayed in Figure 35:

The objective of this work was to make the code tractable for other PhD students at KCK and thus enable common discussions and improved research results.

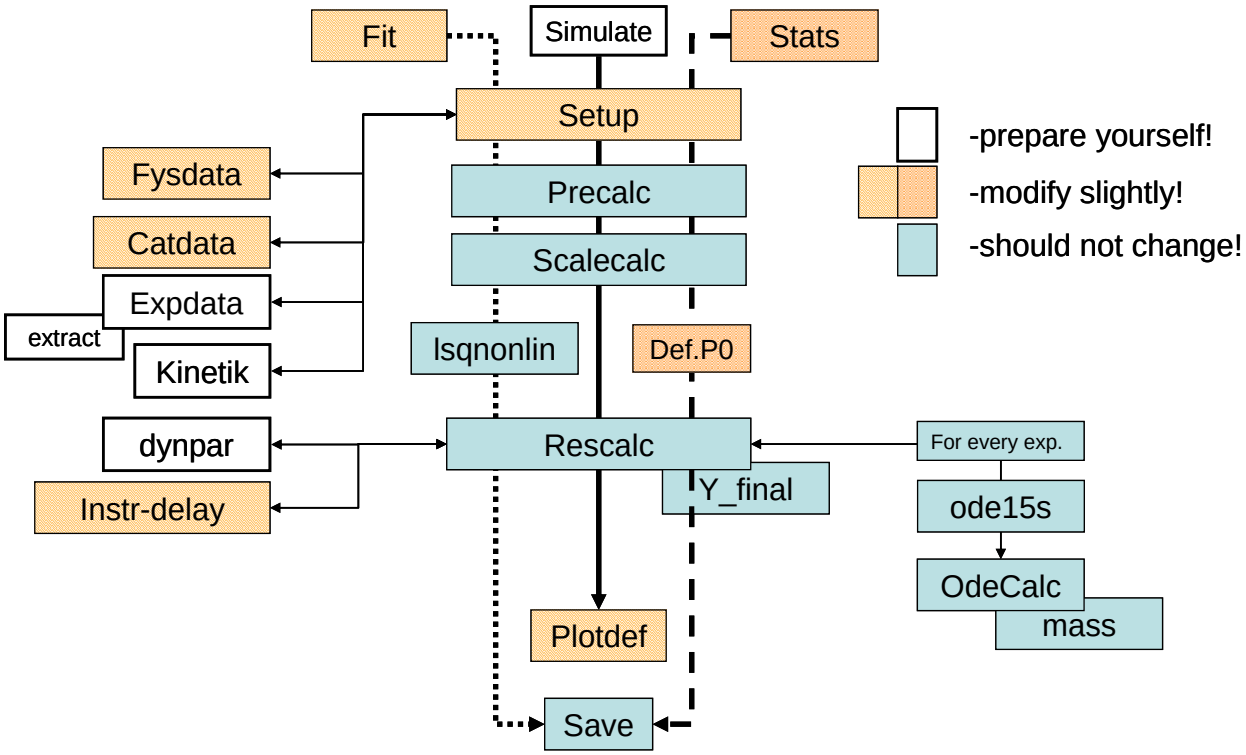

Figure 35. Code structure as used in this thesis. Each box corresponds to a Matlab m-file. The Setup file gathers physical data, monolith data, experimental data, and the kinetic mechanism. The rescalc file calculates the outlet concentrations and the residual. Three objectives are possible: 1) to run a simulation and plot the results (solid arrow), 2) to fit parameters to experimental data (dotted arrow) or 3) to evaluate a set of parameters for various purposes.